NVO-335

NVO-335
UC 702

A RADIATION BRIEFER'S GUIDE TO THE PIKE MODEL

NATIONAL OCEANIC AND ATMOSPHERIC ADMINISTRATION
WEATHER SERVICE NUCLEAR SUPPORT OFFICE
LAS VEGAS, NEVADA

MARCH 1990

PREPARED FOR THE U.S. DEPARTMENT OF ENERGY
NEVADA OPERATIONS OFFICE
UNDER CONTRACT DE-AI08-87NV10566

DISCLAIMER

Available from the National Technical Information Service (NTIS), U.S. Department of Commerce, Springfield, Virginia 22161

Price: Printed Copy A08

Microfiche A01

Codes are used for pricing all publications. The code is determined by the number of pages in the publication. Information pertaining to the pricing codes can be found in the current issues of the following publications, which are generally available in most libraries: *Energy Research Abstracts* (ERA); *Government Reports Announcements* and *Index* (GRA and I); *Scientific and Technical Abstract Reports* (STAR); and publication NTIS-PR-360 available from NTIS at the above address.

DOE/NV--335

DE90 009575

A RADIATION BRIEFER'S GUIDE TO THE PIKE MODEL

Charles R. Steadman, Jr.

National Oceanic and Atmospheric Administration
Weather Service Nuclear Support Office
P.O. Box 94227
Las Vegas, Nevada 89193-4227

March 1990

Prepared For

U.S. Department of Energy
Nevada Operations Office
Contract No. DE-AI08-87NV10566

TABLE OF CONTENTS

CONTENTS - CONTINUED

CONTENTS - CONTINUED

LIST OF FIGURES

LIST OF TABLES

ABSTRACT

Gamma-radiation-exposure estimates to populations living immediately downwind from the Nevada Test Site have been required for many years by the U.S. Department of Energy (DOE) before each containment-designed nuclear detonation. A highly unlikely "worst-case" scenario is utilized which assumes that there will be an accidental massive venting of radioactive debris into the atmosphere shortly after detonation. The Weather Service Nuclear Support Office (WSNSO) has supplied DOE with such estimates for the last 25 years using the WSNSO Fallout Scaling Technique (FOST), which employs a worst-case analog event that actually occurred in the past. The "PIKE Model" is the application of the FOST using the PIKE nuclear event as the analog.

This report, which is primarily intended for WSNSO meteorologists who derive radiation estimates (radiation briefers), gives a brief history of the "model," presents the mathematical, radiological, and meteorological concepts upon which it is based, states its limitations, explains its apparent advantages over more sophisticated models, and details how it is used operationally.

CHAPTER 1

FALLOUT MODELS

For 25 years, the Weather Service Nuclear Support Office (WSNSO)[1] has extensively utilized the PIKE Model for predicting potential exposures from radioactive fallout to populations living downwind from the Nevada Test Site (NTS). These estimates have been made in association with detonations of nuclear devices which have been buried deeply under the earth's surface. These underground nuclear events are said to be "containment-designed" since they are devised in such a manner to minimize the possibility that nuclear debris will be released into the atmosphere. The PIKE Model is one of the primary guides upon which public safety decisions are presently made in association with nuclear detonations at the NTS.

INTRODUCTION

The PIKE Model is currently utilized by meteorologists assigned to the Radiation Estimates and Research Branch (RERB) of the WSNSO. Prior to the detonation of a containment-designed nuclear device, the conservative assumption is made by the U.S. Department of Energy (DOE) that, as a result of the detonation, a massive release of radioactive debris into the atmosphere will occur. Furthermore, it is assumed that much of this debris (fallout) will be deposited upon the immediate-downwind locations surrounding the NTS. Based upon this assumption, one of the RERB meteorologists, referred to as the "radiation briefer," uses the PIKE Model to calculate exposures that downwind populations would receive should this improbable accident scenario actually occur. These estimates are presented prior to the detonation to the DOE Test Controller, who has the responsibility to ensure the safety of downwind populations. Based upon these estimates, the Test Controller can delay a detonation if significant exposures are forecast in areas where populations can not be swiftly sheltered or evacuated.

Should there actually be a massive release of radioactive debris following an underground detonation, the radiation briefer can use the PIKE Model along with post-detonation data and observations to make preliminary estimates of exposures to downwind populations. These estimates would aid the Test Controller in making evacuation decisions.

The Radiation Briefer's Guide to the PIKE Model was specifically written for new members of the RERB so that they may more easily assimilate the basic concepts of the PIKE Model and be able to apply it correctly to the appropriate

---

[1] The WSNSO, which is a unit of the U.S. Department of Commerce, was originally the Weather Bureau Field Research Station. It was first organized to support activities at the Nevada Test Site in the mid 1950s. WSNSO has undergone several name changes since that time.

situations. The guide gives a concise history of the model and presents the mathematical, radiological, and meteorological concepts upon which the PIKE Model are based. This guide also states the PIKE Model's limitations, explains its functional advantages over more sophisticated models, and details how it is used operationally.

FALLOUT-SCALING TECHNIQUE

What is commonly referred to as the PIKE Model is actually a special application of the WSNSO Fallout-Scaling Technique (FOST). The FOST can be used to predict the radiation exposures along the path of maximum debris deposition (centerline) in association with either "cratering" events or containment-designed events. The FOST was specifically developed in the mid-1960s for estimating exposures in association with cratering events (Reference 1.1). These were events in which nuclear devices were purposely buried at shallow depths so as to produce relatively large craters on the earth's surface. As detailed in Reference 1.1, the FOST was proven reliable for predicting exposures in association with such cratering events. Based upon the success of the FOST with cratering events, the FOST was adapted for use with containment-designed detonations.

In using the FOST for cratering or containment-designed applications, one must rely upon an analog nuclear event (a well-documented past nuclear event which produced fallout). Ideally, this analog is chosen for its similarity to the event for which exposure predictions are being made.

For 25 years the analog event that has been recommended by the DOE and the two national laboratories[2] conducting the underground tests has been the PIKE[3] event. Thus, before each underground nuclear detonation, it is assumed that there will be a massive venting of radioactive materials into the atmosphere in a similar manner as was observed with the PIKE event. The radiation briefer then uses the PIKE analog in the FOST to derive the forecast exposure estimates.

IDEAL FALLOUT MODEL

Theoretically, if the exact distribution of particles within a radioactive cloud is known when the cloud has stabilized, and if the wind field over the area affected by the cloud is known during the period of particle fallout, then it would be possible to derive the surface distribution of the radioactive particles (fallout pattern) accurately. (In essence, such a theoretical model would first determine the impaction point of each particle and then calculate the cumulative radioactive energies of the deposited particles.) If such a fallout pattern was

---

[2]These laboratories are the Los Alamos National Laboratory (LANL) based in Los Alamos, New Mexico, and the Lawrence Livermore National Laboratory (LLNL) based in Livermore, California.

[3] PIKE was detonated on Friday, March 13, 1964.

derived, then radiation exposures to individuals in any part of the pattern could be determined.

Thus, if:

> (1) the participating national laboratory conducting a nuclear detonation could provide an accurate prediction of the initial[4] aerial distribution of particles according to their sizes and to the quantity of radioactivity embedded in or on them, and
>
> (2) the WSNSO could provide an accurate prediction of the wind field within and surrounding the cloud as it progressed downwind,

then accurate predictions of the resulting fallout pattern and the exposures to the population could be made. Unfortunately, as will be discussed below, there are some great obstacles to this ideal approach.

PARTICLE-SIZE AND ACTIVITY DISTRIBUTIONS

The first obstacle to the ideal approach is one of defining the radiological source term. This source term is the quantity of particles in the debris cloud, the physical characteristics (shape, size, etc.) of these particles, the types of radioactive material contained on and within these particles, and the distribution of these particles as a function of their initial height above the earth's surface.

Derivation of the source term is presently insurmountable without first making a few simplifying assumptions, which will be discussed in Chapter 2. It will be shown that once these assumptions are made, the radiological parameters that are needed to input into the ideal fallout model are the particle-size and radioactivity distributions as a function of height in the cloud at the time of stabilization.

While the source-term problem is not as complex with these simplifying assumptions, it is still complicated to solve because it is quite difficult to determine the initial aerial particle-size and activity distributions for nuclear debris clouds.

The best opportunity of documenting these distributions was during the atmospheric-testing days of the 1950s and 1960s. During this period, many above-ground nuclear events were systematically detonated. Fortunately, there were cloud-sampling aircraft available for data collection. Unfortunately, the aerial data gathered in association with any of these events are quite disappointing if one is interested in a knowing the initial aerial particle-size and activity distributions.

---

[4]Initial refers to the time when the debris cloud stopped its dynamic growth.

When a massive amount of nuclear debris was released into the atmosphere in the past, sampling aircraft could not penetrate the cloud at early times. The aircraft and crew would have been swiftly contaminated by the highly-energized debris. At some later time after the detonation, the debris cloud became safe enough to penetrate due to radioactive decay and atmospheric dispersion. However, by that time:

(1) a substantial amount of debris had either descended a considerable distance from its initial position or had already struck the earth's surface, and

(2) the volume of the cloud had become so large that the small fleet of sampling aircraft could no longer make enough simultaneous observations to provide a "snapshot" of the particle-size and activity distributions.

In short, due to large technical limitations existing in the 1950s and 1960s, a massive debris cloud was never documented well enough so that a comprehensive aerial particle-size and activity distribution could be derived. The data were so sparse that the "best" attempts at describing such distributions were limited to composites made of bits and pieces of data from dissimilar detonations. Such composite models were never seriously considered to be acceptable solutions to describing the particle distributions resulting from individual nuclear events.

The same sampling problems encountered during the atmospheric-testing days were also present during the sampling of debris clouds associated with ventings in the early days of containment-designed testing. Furthermore, sampling was even more difficult in association with such ventings since (1) the crews were operating in more of a "crisis" mode because the venting was unexpected and (2) there was usually much less visible debris to delineate the cloud.

Thus, at this writing, there has not been an accurate, comprehensive documentation of a nuclear cloud's particle-size and activity distributions. Furthermore, with a lack of such empirical data, it would be difficult to formulate a method by which an upcoming nuclear event's particle-size and activity distributions could be predicted.

Even if there were comprehensive particle-size and activity distribution data for many past nuclear detonations, it would still be quite difficult to predict the distributions in association with an upcoming underground nuclear detonation because venting mechanisms can not be predicted.

In advance of each containment-designed nuclear detonation, many precautions were made by DOE to ensure (1) that the nuclear device was buried at a sufficient depth, (2) that the drill hole leading from the surface to the device was properly sealed, (3) that the ground surrounding the device was geologically stable, (4) that the mechanisms that had caused previous ventings would not be allowed to reoccur, and (5) that any potential problems that could result in association with unfamiliar devices, techniques, geological areas, etc., would be thoroughly evaluated before the detonation.

In the early days of containment-designed testing, all these precautions had been taken. Yet, despite these efforts, there were still accidental ventings. As experience in containment-designed nuclear testing grew, the number of ventings drastically decreased during the 1960s. Massive ventings at the NTS have not occurred since 1970.[5] It is possible that a venting will never occur again. However, if one should occur, it is certain that the venting mechanism causing it will have been unpredictable.

In summary, although it is now highly unlikely that a massive venting will ever occur, the DOE Test Controller must be convinced before each detonation that the downwind populations would not be in danger and that the proper actions could be taken to protect public health and safety if there should be a massive venting. The Test Controller requests exposure estimates based upon a credible massive-venting scenario. Up to the present time, no one has been able to furnish such estimates using an ideal fallout model due to the radiological source term problem as discussed above.[6]

WIND-FIELD PREDICTIONS

In a discussion of fallout predictions in his 1957 paper (Reference 1.2), Stopinski stated:

> *The wind problem has been considered, by some workers at least, as being more serious than* [the problem of the particle-size and activity distributions]. *Even under the best of conditions, it is impossible to state precisely the structure of the wind field over a large area through a considerable depth of the atmosphere because of the sampling techniques which are necessarily used. Since it is virtually impossible to describe a wind field exactly by direct observation, then it is obviously even more difficult to predict that wind field continuously for periods of up to 24 hours or more. Such a prediction would be necessary for precise fallout predictions.*

Today, it is still impossible to ***precisely*** state the initial structure of the wind field. The cost of establishing a dense network of atmospheric sampling equipment capable of approximating the wind field would be prohibitive.

---

[5]The last prompt-massive venting that occurred at the NTS was in association with the BANEBERRY event detonated on December 18, 1970.

[6]At about the same time that the FOST was first utilized, other organizations were experimenting with mathematical models which would predict exposures for cratering detonations. In these models, the particle-size and activity distributions were estimated using some extremely simple assumptions. If the resultant estimates from such models did not match the observed fallout patterns, then the particle-size and activity distribution assumptions were repeatedly changed until there was a resemblance between the predicted and observed. Obviously, this method had limited operational predictive applications.

However, while the particle-size-and-activity-distribution problem is still firmly entrenched as it was over 30 years ago, the "wind problem" as viewed by Stopinski has been mitigated somewhat.

Since 1957, technological advances have allowed the establishment of advanced networks of ground and upper-air remote weather sensors. By no means do these give a *precise* description of the atmosphere but they do give a fair approximation. In addition, computer technology has made remarkable advances since 1957. As a result, atmospheric transport models on the larger mainframe computers can now successfully approximate particle movements within small-scale circulations and over complex terrain. It is contended that such models, which have a good diagnostic record, will eventually evolve into accurate prognostic models and will even be run on microcomputers. Such a trend is favorable for the solution of the wind-field component of the fallout prediction problem.

However, if the atmosphere can be precisely described and predicted in the future, the problem of the lack of particle-size and activity distributions still clouds the horizon.

THE "PIKE" SOLUTION

As far back as the mid 1950s, various organizations were developing computer programs loosely based upon what has been referred to in this report as an ideal fallout model. They were never used operationally due to the lack of computers in the field in those days, and to the lack of the necessary radiological source term.

In the mid 1960s, the FOST provided a "temporary" path around this problem. As will be seen in the following chapters, exposure estimates can be made assuming that the venting being predicted will have similar initial aerial particle-size and activity distributions as a past venting (analog venting). The predicted venting is ***scaled*** to the analog venting. Obviously, if the predicted venting is to have similar distributions as the analog, the detonation being predicted should have characteristics similar to the detonation upon which the analog was based.

When the FOST was first used in association with cratering detonations, there were few analog events from which to chose. However, at that time in the mid-1960s, many scientists envisioned the construction of large canals and bays with nuclear cratering detonations (Plowshare Program). It appeared that there would be many cratering tests at the NTS prior to the actual use of such devices at the construction locations. If this had been the case, a catalog of cratering analogs would have evolved. One could then chose the analog associated with the detonation most representative of the future detonation for which exposure predictions were needed. Unfortunately, both for the compilation of a cratering-analog catalog and for the ideal utilization of the FOST, very few cratering events were actually detonated.[7]

The selection of the most appropriate analog event for the FOST in association with containment-designed events has always been and remains a problem. The major problem, as with the cratering detonations, is a lack of suitable analogs. If many underground events had ejected massive debris into the atmosphere, there would now be a comprehensive catalog of venting analogs from which to choose. But underground events are designed to be totally contained beneath the earth's surface and a great majority have been. Furthermore, of those containment-designed events that have vented radioactive material into the atmosphere, a large portion have slowly leaked small amounts of gases which produced very small exposures outside the boundaries of the NTS. These events were ***seepages*** not ventings and can not be used as analogs, as will be explained below.

Before each containment-designed nuclear detonation, the DOE Test Controller needs to assess the consequences should ***massive*** amounts of debris be quickly released into the atmosphere as a result of an accidental venting. Such a ***prompt-massive*** venting would produce the greatest amount of fallout in the populated areas around the NTS. The Test Controller is also interested in a "worst case" accidental release. Such a ***maximum-prompt-massive*** venting would provide him with the most conservative estimates upon which to assess the threat to downwind populations.

However, if the Test Controller utilized a maximum-prompt-massive-venting analog based upon a detonation in which the venting mechanism was one that is never expected to occur again, the estimates could be considered unrealistic. For example, two of the maximum-prompt-massive-venting analogs were derived from the PLATTE and DES MOINES events, both of which were conducted in 1962 in horizontal tunnels in solid rock (tunnel events). These ventings occurred at the beginning of the containment-design-detonation era, when accidental ventings were relatively frequent. Experience gained from these early accidents has made the occurrence of similar venting mechanisms a remote possibility. Thus, these two analogs are not considered credible today and are not employed. Consequently, it may be said that the Test Controller is interested in the ***maximum-credible-prompt-massive-venting*** accident scenario.

In summary:

(1) there have been very few prompt-massive ventings at the NTS upon which to derive analogs,

(2) in ideal circumstances, the analog event's detonation characteristics (e.g., the type of soil or rock and the type of nuclear device) should be similar to the upcoming event's detonation characteristics, and

[7] There was only a total of nine cratering events detonated at the NTS, the last of which was conducted on December 8, 1968.

(3) the analog utilized should be associated with a maximum-credible prompt massive venting.

The combination of fact (1) with requirements (2) and (3) severely limits what can be used as an analog event for a containment-designed detonation. This problem will be explored in more detail in Chapter 4.

The first use of the FOST for predicting fallout exposures was in April 1964, about a month after the PIKE event. Since PIKE was the maximum-credible-prompt-massive-venting at that time, it was used as the analog for all the other vertical-shaft underground detonations. After the PLATTE and DES MOINES analogs were declared "not credible," the PIKE analog was, by default, also used for tunnel events. Because the PIKE analog has remained the maximum (most conservative) analog since the mid 1960s, it has been used exclusively in the FOST, except for cratering detonations.

Furthermore, since an appropriate ideal mathematical fallout model has not been accepted to date, the "temporary" PIKE solution still remains in effect.

CHAPTER 2

FALLOUT CONCEPTS

The FOST may be better understood if some basic concepts about fallout are first grasped. This chapter discusses fallout, the trajectories of particles, the fallout hodograph, and the fallout sector.

FALLOUT

As a result of a nuclear detonation near or under the earth's surface, relatively large amounts of radioactive particulate matter are created. If the nuclear explosion is not fully contained, those radioactive particles escaping containment form a debris cloud which is then subject to the motions of the atmosphere. The process of the descent of these contaminated particulates from the debris cloud to the earth's surface is known as ***fallout***. In addition, ***fallout*** is also referred to, in a collective sense, as the particulate matter deposited on the ground.

Fallout may be divided into two categories, ***early fallout*** and ***delayed fallout***. The early fallout, which can also be termed ***local fallout***, has been arbitrarily defined in ***The Effects of Nuclear Weapons*** (Reference 2.1) as those particles which reach the earth's surface within 24 hours after a nuclear explosion. Delayed fallout, which can also be termed ***worldwide fallout***, has been defined as those particles carried into the upper parts of the atmosphere and spread by winds to all parts of the earth. Local fallout consists mainly of larger particles and is primarily deposited due to the effects of gravitational settling. Worldwide fallout, which consists mainly of the smaller particles, is brought to the earth primarily by rain and snow.

During the 1950s and early 1960s, many relatively large nuclear detonations were conducted at the NTS at or near the earth's surface. Contaminated debris was often carried into the upper troposphere and even into the stratosphere. As a result, a large amount of both local and worldwide fallout was produced. These atmospheric detonations ceased in the early 1960s. Most detonations thereafter were designed to be contained underground.

A short series of cratering detonations in the early to late 1960s was an exception to the long series of containment-designed events that followed the Limited Test Ban Treaty of 1963. While these cratering events, as a group, produce much less worldwide fallout than the atmospheric events, each event did produce large amounts of contaminated debris in the lower layers of the troposphere. Thus, local fallout was a significant factor in the cratering detonations. The FOST was developed as a part of an effort to minimize the effects of this local fallout on the populations surrounding the NTS.

After the Limited Test Ban Treaty, only a very small percentage of the containment-designed detonations leaked contaminated debris into the atmosphere. The number of these unexpected leaks decreased markedly during the 1960s. Very few have occurred since 1970. During the early to mid 1960s, when the testing community was in the process of gaining experience in containing nuclear detonations underground, there were a few leaks of a dynamic nature, such as PIKE. Such dynamic leaks (ventings) occurred shortly after detonation and released a significant amount of contaminated particles into the atmosphere. By contrast, there was much less fallout released in association with the ventings than with cratering events. The depths of these prompt-massive-venting debris clouds were usually limited to less than 10,000 ft above ground level (AGL). Consequently, most of the fallout associated with them was local. Relatively little worldwide fallout was produced. The FOST, which had proven quite useful in predicting local fallout for cratering events, was adapted to predict local fallout for containment-designed-prompt-massive ventings.

PARTICLE TRAJECTORIES

Immediately after the larger particles of radioactive debris (those with a radius of greater than about 30 microns) are thrown into the atmosphere, they begin to settle back toward the earth's surface due to the gravitational force of the earth. There are several important factors that determine the time it takes for these particles to reach the ground. These factors include the mass and geometry of the particles and the density of the surrounding air.

As a particle descends through the atmosphere, it is transported horizontally by the winds. Therefore, the horizontal displacement of the particle from its initial elevated position to its impaction point is primarily a function of the wind speeds and directions encountered during its fall. Thus, a good approximation of a particle's impaction point can be determined if the following information is known:

(1) the initial height of a particle,

(2) the particle's shape, size, and mass,

(3) the density of the surrounding air, and

(4) the vertical variation of wind velocity (speeds and directions) encountered by the particle as it falls.

A few simplifying assumptions are helpful in visualizing this fall process. First, let it be assumed that the density of the air remains constant in time and space. The density of the air normally varies with the height above the ground and with time. In a few infrequent situations, the density may vary considerably in the horizontal plane. However, it can be assumed to be nearly constant under certain circumstances. For example, the density of air may be nearly constant (1) if the thickness of the layer through which the particle falls is relatively shallow and (2) if the time it takes for the particle to reach the surface is relatively short.

Next, let it be assumed that the vertical air motions are insignificant and can be ignored. Updrafts and downdrafts affect the fall time of particles, but these effects are usually ignored primarily because they are quite difficult to predict. These effects are small in normal circumstances for particles associated with local fallout. However, significant effects upon local fallout particles may occur during certain infrequent meteorological situations. For example, large vertical wind components may occur near thunderstorms or in connection with strong horizontal winds blowing across mountainous terrain.

Finally, let it be assumed that all the fallout particles are spherical and have a smooth surface. It is realized that there are a large number of different particle shapes generated during a nuclear detonation, but this assumption is made to keep the fallout problem tractable. As stated in Reference 2.1:

> *Actual fallout particles are sometimes quite irregular and angular in shape, although a large percentage tend to be fairly smooth and globular since they result from the solidification of fused spherical droplets of earth and weapon debris.*

With these assumptions in mind, consider a hypothetical debris cloud with its top stabilized at 3000 ft AGL, as exemplified in Figure 2.1. Let us focus upon three identical spherical particles, P1, P2, and P3, at 1000, 2000, and 3000 ft AGL, respectively. The particles are at these altitudes at the time of

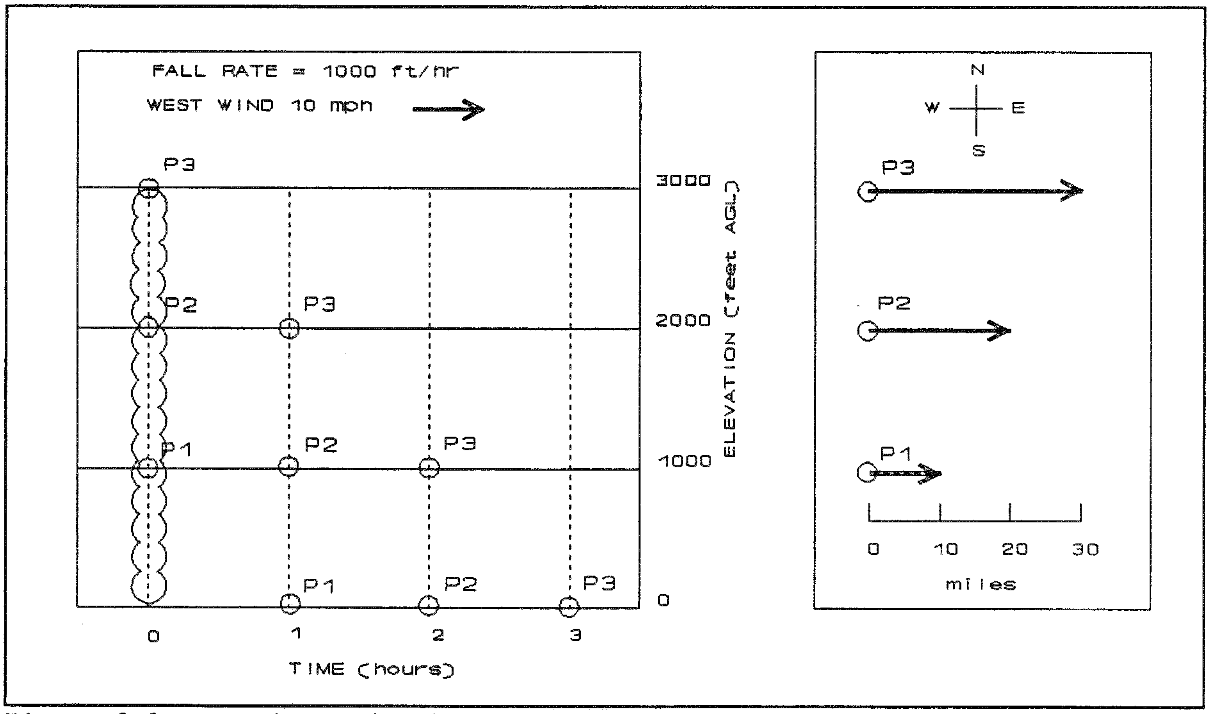

Figure 2.1 Hypothetical Debris Cloud - Case 1

the cloud's stabilization, time = 0. It is assumed that each particle has a fall rate of 1000 ft/hr, and that there is a west wind[1] with a speed of 10 mi/hr below 3000 ft AGL.

As shown in Figure 2.1, the P1 particle reaches the ground at time = 1 hr. The P2 particle, which has fallen to 1000 ft AGL by one hr, reaches the ground at 2 hr. The P3 particle, which has fallen to 2000 ft by 1 hr and 1000 ft by 2 hr, reaches the ground at 3 hr.

The wind velocity, $\vec{v}$, is a vector quantity since it has both speed and direction. It can be graphically represented by an arrow pointing in the direction toward which the wind is blowing. For example, a west wind is represented by the vector, →, and a south wind is represented by the vector, ↑. The length of the arrow is proportional to the wind speed (the longer the arrow, the greater the speed).

The horizontal displacement of a particle from one point to another, $\vec{x}$, is also a vector quantity since there is both distance and direction involved. The displacement is a product of the wind velocity, $\vec{v}$, multiplied by the time it is suspended in the wind, t. The horizontal displacements of the three particles (P1, P2, and P3) are graphically indicated in the right box of Figure 2.1. For example, in the case of the P3 particle, the direction of displacement is toward the east, and the magnitude of the displacement is 30 mi (10 mi/hr times 3 hr).

Of course, the above example is a simplified case in which there is no vertical wind shear (a change in wind speed and/or direction with height). In a more realistic case with vertical wind shear, the following equation can be used to determine the horizontal particle displacement,

$$\vec{x} = \sum_{i=1}^{N} \vec{v}_i \, t_i \qquad (2.1),$$

where,

$\vec{x}$ = the resultant horizontal particle displacement,

$\vec{v}_i$ = the wind velocity in the atmospheric layer, i,

t_i = the time of fall through the layer, i, and,

N = the total number of atmospheric layers.

---

[1] The standard meteorological wind notation conventions will be used in this report. A wind direction denotes the direction from which the wind is blowing. For example, if it is stated that there is a west wind, this denotes that the wind is blowing from the west toward the east.

A more complex, and therefore more realistic, situation is exemplified in Figure 2.2 in which the wind velocity varies with height. In Case 2, the same assumptions are made as in Case 1 except that the winds from the surface to 1000 ft AGL (layer 1) are from the southeast at 5 mi/hr, the winds between 1000 and

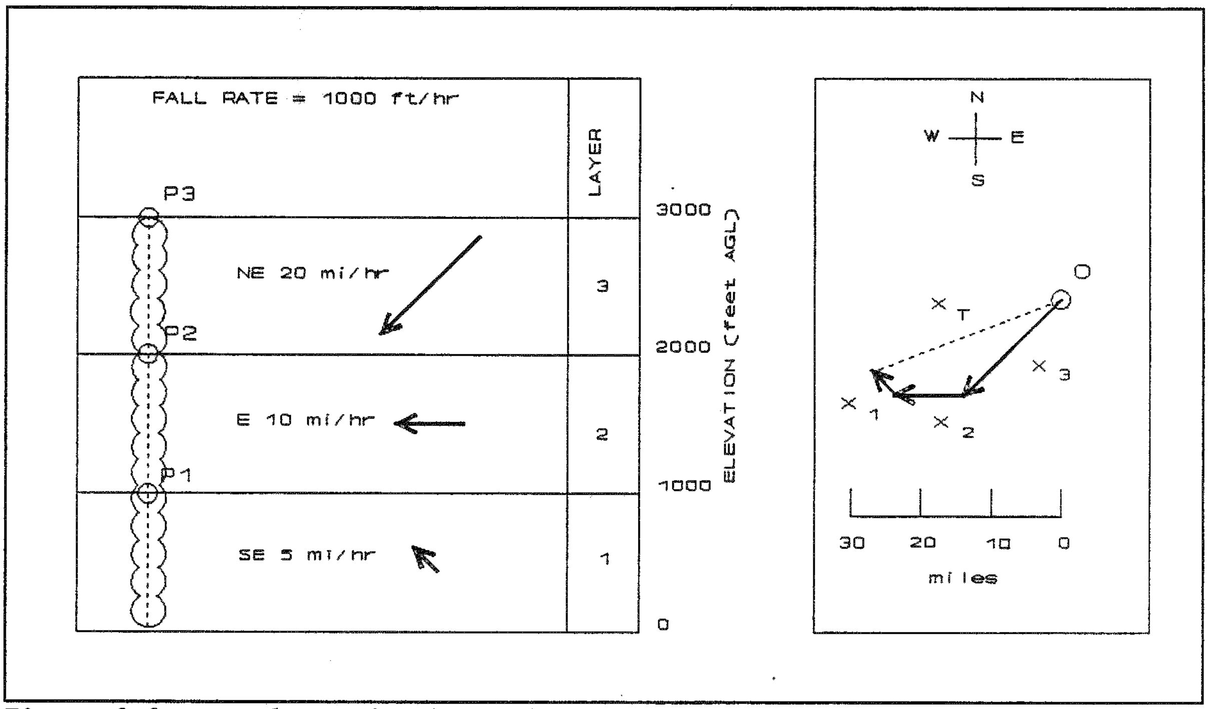

Figure 2.2 Hypothetical Debris Cloud - Case 2

2000 ft (layer 2) are from the east at 10 mi/hr, and the winds between 2000 and 3000 ft (layer 3) are from the northeast at 20 mi/hr.

In this case, the P1 particle would fall through the southeasterly winds of layer 1 and would be deposited on the surface 5 mi to the northwest of its initial position.

The P2 particle would be transported toward the west by the easterly winds in layer 2 for the first hour and toward the northwest by the southeasterly winds in layer 1 for the second hour. The total displacement of the P2 particle, from its initial position to its point of impaction with the surface can be derived using equation 2.1. It would be deposited about 14 mi to the west-northwest of its initial position two hours later.

The P3 particle would first be transported toward the southwest for the first hour by the northwesterly winds in layer 3, would be transported toward the west during the second hour by the easterly winds in layer 2, and would be transported toward the northwest during the third hour by the southeasterly winds in layer 1. Again, the total displacement of the P3 particle can be derived using equation 2.1.

The solution to this equation is graphically shown in the right box of Figure 2.2. The first displacement of the P3 particle is indicated by the vector, $\vec{x}_3$, which was calculated using the product of the wind vector associated with layer 3, $\vec{v}_3$, and the time the particle remained in that layer, t_3. The displacement vectors, $\vec{x}_2$ and $\vec{x}_1$, were calculated in a similar manner. (Of course, in this case $t_1 = t_2 = t_3 = 1$ hr.) The tail of $\vec{x}_3$ was plotted at an arbitrary initial position, O. Next, the tail of $\vec{x}_2$ was plotted at the head of $\vec{x}_3$, and the tail of $\vec{x}_1$ was plotted at the head of $\vec{x}_2$. The point of surface impaction of the P3 particle would be at the head of $\vec{x}_1$. The resultant, $\vec{x}_T$ (the dashed line), which extends from the origin, O, to the head of $\vec{x}_1$, also describes the point of impaction and is the unknown parameter, $\vec{x}$, solved for in equation 2.1.

FALLOUT HODOGRAPHS

The graphical addition of the three P3 displacement vectors ($\vec{x}_3$, $\vec{x}_2$, and $\vec{x}_1$) does not have to be limited to the method shown in the right box of Figure 2.2.[2] These vectors can be plotted head-to-tail from the same origin in *any* order, and the head of the last vector will end at the same point as the head of $\vec{x}_1$ in Figure 2.2. This is exemplified in Figure 2.3. Notice to the south of the origin that the three displacement vectors have been plotted in the same manner as they were in Figure 2.2 (i.e., $\vec{x}_3$ first, $\vec{x}_2$ second, and $\vec{x}_1$ last). Next, notice to the north of the origin that the same three vectors have been plotted from the origin but with $\vec{x}_1$ plotted first, $\vec{x}_2$ plotted second, and $\vec{x}_3$ plotted last. It can be seen that the terminal position for each string of vectors ends at the same place (the head of $\vec{x}_1$ in the lower vector string coincides with the head of $\vec{x}_3$ in the upper vector string).

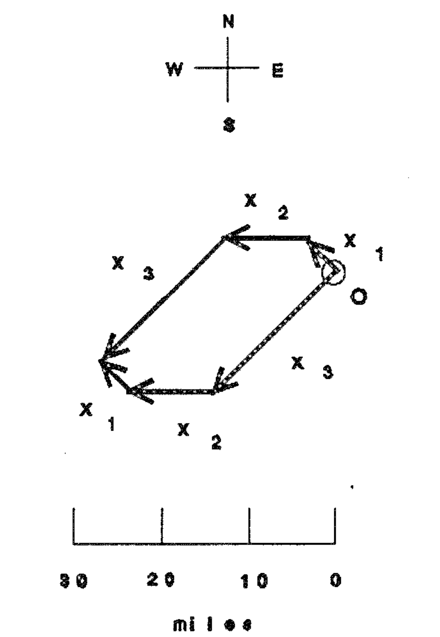

Figure 2.3 Particle Displacement

While the first method of plotting the vectors ($\vec{x}_3$ first) yields a diagram of the path of the P3 particle in the horizontal plane, the second method ($\vec{x}_1$ first) does not. However, by plotting the displacement vectors using the vector associated with the lowest atmospheric layer first and the vector associated with the highest layer last (the second method), the terminal positions of each of the particles is shown. That is, the P1 surface impaction point lies at the head of $\vec{x}_1$, the P2 impaction point lies at the head of $\vec{x}_2$, and the P3 impaction point lies at the head of $\vec{x}_3$. The string of displacement vectors constructed by the second method is referred to as a ***fallout hodograph***.

---

[2]Vector addition is associative. The sum of any number of vectors is independent of the order in which they are added.

Both of the two cases considered so far were simplified considerably by dividing the atmosphere into equal 1000-ft layers. In reality, the atmosphere is seldom characterized by layers of equal thickness having uniform wind velocities throughout those layers. However, upper-air-wind observations are routinely reported in terms of average velocities for layers of equal thicknesses. For example, in an upper-air-wind observation, the wind velocity reported at 5000 ft mean sea level (MSL) is actually an average velocity between 4500 and 5500 ft MSL. Thus, given the upper-air-wind data that is routinely available, it is convenient to visualize the atmosphere as divided into equal thicknesses having uniform wind velocities.

If it is assumed, as it was in case 2, that the depth through which a particle falls is divided into N layers of uniform thickness, then equation 2.1 can be simplified to:

$$\vec{x} = (T/N) \sum_{i=1}^{N} \vec{v}_i \quad (2.2),$$

where,

T = the total time of fall from the starting altitude to the ground, and

T/N = the average time of fall per layer.

Since the time of fall through each atmospheric layer, t_i, is equal to T/N, then:

$$\vec{x} = t_i \sum_{i=1}^{N} \vec{v}_i \quad (2.3).$$

The total time of fall may be expressed as:

$$T = h/s \quad (2.4),$$

where,

h = the starting altitude of the particle, and

s = the particle-fall rate.

Substituting equation 2.4 into equation 2.3 and using (t_i = h / N s) yields:

$$\vec{x} = h/s \ \left(\sum_{i=1}^{N} \vec{v}_i \ / \ N\right) \quad (2.5).$$

The above equation can be simplified if we define:

$$\vec{v}_t = \sum_{i=1}^{N} \vec{v}_i \qquad (2.6),$$

where $\vec{v}_t$ is the resultant wind velocity. This resultant vector is portrayed in Figure 2.4 by plotting the case 2 wind vectors, $\vec{v}_1$, $\vec{v}_2$, and $\vec{v}_3$, starting with the tail of $\vec{v}_1$ plotted at the origin. The resulting string of vectors is quite similar to the hodographs shown to the north of the origin in Figure 2.3, but the vectors shown in Figure 2.4 are ***wind-velocity*** vectors while the vectors in Figure 2.3 are ***displacement*** vectors. In Figure 2.4, the resultant wind vector, $\vec{v}_t$, is indicated as the vector extending from the tail of $\vec{v}_1$ to the head of $\vec{v}_3$. Substituting equation 2.6 into equation 2.5 gives:

$$\vec{x} = \frac{\vec{v}_t\, h}{N\, s} \qquad (2.7)$$

As a final step, let us consider the average velocity along the resultant transport bearing, $\vec{v}_a$, where:

$$\vec{v}_a = \vec{v}_t / N \qquad (2.8).$$

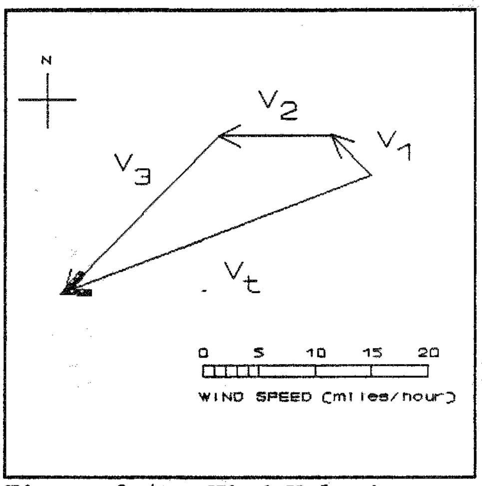

Figure 2.4 Wind-Velocity Vectors

In Figure 2.4, v_a would equal the length of $\vec{v}_t$ divided by N (29.5 ÷ 3). Substituting equation 2.8 into equation 2.7 leads to:

$$\vec{x} = \frac{\vec{v}_a\, h}{s} \qquad (2.9)$$

Equation 2.9 expresses the horizontal displacement of a particle in terms of its initial altitude, its fall rate, and an effective mean transport velocity. Thus, if wind velocities are known for equal-thickness layers beneath a particle, and if the initial height and fall rate of the particle are known, then the impaction point of that particle can be determined using equation 2.9. The vector, $\vec{v}_a$, can easily be derived by plotting a fallout hodograph, such as the one shown in Figure 2.4. Such a hodograph can be constructed from wind vectors, instead of displacement vectors, since the time of fall through each layer is considered constant.

In summary, a fallout hodograph can be constructed in two ways. In the first method the fallout hodograph is the graphical addition of vectors, where:

(1) each vector represents the horizontal displacement of a particle falling through an atmospheric layer having a uniform wind velocity,

(2) the vector representing displacement due to the winds in the lowest atmospheric layer is plotted first,

(3) the vector representing the displacement due to the winds in the second lowest atmospheric layer is plotted next, and

(4) the remaining vectors, if any, are plotted in ascending order with the vector representing the displacement due to the winds in the highest layer plotted last.

A fallout hodograph, constructed as described above, represents the path of deposition on the surface of a group of identical particles dispersed throughout the debris cloud.

In the second method of constructing a fallout hodograph, the atmospheric layers have the same thickness. In such a situation, a fallout hodograph is the graphical addition of vectors, where:

(1) each vector represents the wind velocity of the corresponding atmospheric layer,

(2) the vector representing the wind velocity in the lowest layer is plotted first,

(3) the vector representing the wind velocity in the second lowest layer is plotted next, and

(4) the remaining vectors, if any, are plotted in ascending order with the vector representing the wind velocity in the highest layer plotted last.

Such a hodograph can be used quickly to determine the average velocity, $\vec{v}_a$, of a particle along the resultant transport bearing. This vector can, in turn, be used to determine the horizontal displacement of that particle. This vector also plays an important part in the scaling equations that will be discussed in the next chapter.

FALLOUT SECTORS

Let us again consider the Case-2 scenario, but this time with the addition of three identical fallout particles, P1′, P2′, and P3′. These particles are smaller than the P1, P2, and P3 particles and have a fall rate one half that of the larger particles (500 ft/hr). The P1′, P2′, and P3′ particles are initially located at 1000, 2000, and 3000 ft AGL, respectively. Figure 2.5 shows two fallout hodographs. The smaller hodograph, which is identical to the upper

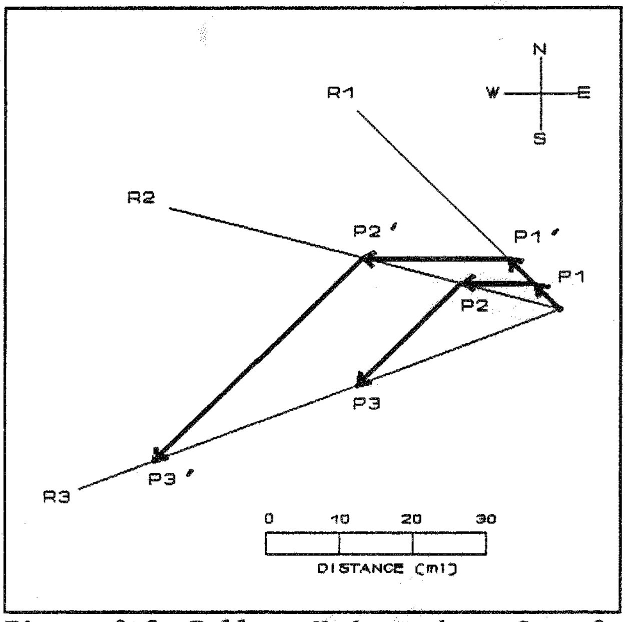

Figure 2.5 Fallout Hodographs - Case 2

vector string in Figure 2.3, is associated with the set of larger particles (P1, P2, and P3). The larger hodograph is associated with the set of smaller particles (P1', P2', and P3'). The surface impaction point of each of the six particles is indicated next to the appropriate vector head.

Notice (1) that each of the particles that initially started from 1000 ft (P1 and P1') lies on radial line R1, (2) that each of the particles that initially started from 2000 ft (P2 and P2') lies on radial line R2, and (3) that each of the particles that initially started from 3000 ft (P3 and P3') lies on radial line R3.

If a third set of identical particles that had a fall velocity even less than the other particles was considered, it would be found that the particle starting at 1000 ft would fall somewhere along R1, the particle starting at 2000 ft would fall somewhere along R2, and the particle starting at 3000 ft would fall somewhere along R3. It follows that all particles initially starting from one particular height, no matter what size, would fall along the same radial line.

It can further be seen that all particles, no matter what size, that initially start between the surface and 1000 ft would fall along the R1 radial. All particles initially starting between 1000 and 2000 ft would fall between R1 and R2, and all particles initially starting between 2000 and 3000 ft would fall between R2 and R3.

As evident from Figure 2.5, the downwind surface area upon which fallout would be deposited would lie between the two outermost radial lines, R1 and R3. This area is termed the ***fallout sector***. Of course, this would be the fallout sector, only if the winds did not vary with time.

Several simplifying assumptions have been made so far in this report in order to explain particle trajectories, fallout hodographs, and fallout sectors. In summary, these assumptions are as follows:

(1) all fallout particles are considered to be spherical,

(2) the air density remains constant with altitude,

(3) the atmosphere is divided into layers of equal thickness each with a particular uniform wind velocity,

(4) the wind velocity varies with altitude but not with time, and

(5) the vertical components of the wind are insignificant.

The above assumptions were also used in the development of the FOST (Reference 1.1). Some additional assumptions that were used in the development of the FOST were that:

(1) all fallout particles are considered to have a uniform density [3],

(2) the air density remains constant not only with altitude but also both in the horizontal plane and in time,

(3) the wind velocity remains constant not only in time but also in the horizontal plane, and

(4) the effects of atmospheric diffusion (i.e., particle transport due to chaotic motions of air) are insignificant.

These additional assumptions, as the ones above them, are not realistic for many actual meteorological situations. However, these assumptions are necessary to explore concepts and to derive the FOST. Later in this report, some of these assumptions will be modified or cancelled. Those assumptions that remain after the derivation of the FOST will be examined to determine the limiting conditions that these remaining assumptions exert upon the operation of the FOST. An obvious example is that if it continues to be assumed that the air density remains constant with altitude, the FOST can only be applied in a relatively shallow layer of the atmosphere near the surface.

As pointed out earlier, fallout particles descend at a rate depending upon their mass and diameter and upon the density of the surrounding air. Since it has been assumed that all the particles have a uniform density and that the air density remains constant in time and space, it would follow that fallout particles would descend at a rate depending upon their diameter. A larger diameter particle would fall faster than a smaller one since the larger particle would have a greater mass to surface area ratio and would, therefore, have a greater terminal velocity. This was exemplified in Case 2 in which the larger-diameter particles (P1, P2, and P3) fell to the earth twice as fast as the smaller ones (P1', P2', and P3').

A fallout pattern can theoretically be derived by considering each particle's displacement as described by $\vec{x} = (\vec{v}_a\ h) / s$ (equation 2.9). Since the wind velocity is considered constant in the horizontal plane and in time ($\vec{v}_a$ is constant), the horizontal displacement, $\vec{x}$, of a particle is therefore only a function of the particle's starting altitude, h, and its fall rate, s. But, since the air density is considered constant in space and time, the fall rate is directly proportional to the particle's diameter (the bigger the particle's diameter, the greater its fall rate). Thus, a fallout pattern can be described

---

[3] A mean particle density of 2.9 g/cm^3 has been assumed for ballistic considerations.

in terms of particle diameters, d, and starting altitudes, h. This is exemplified in Figure 2.6.

In this example (Case 3), it has been assumed that the debris cloud extends up to 3000 ft AGL. The winds from the surface to 1000 ft (h_1) are from the southeast at 5 mi/hr, the winds from 1000 ft to 2000 ft (h_2) are from the south at 10 mi/hr, and the winds from 2000 ft to 3000 ft (h_3) are from the southwest at 5 mi/hr. A hodograph consisting of wind velocity vectors is plotted beginning at 0 and ending at the head of the last vector at T. The dashed line extending directly from 0 to T represents $\vec{v}_a$, the average velocity along the resultant transport bearing.

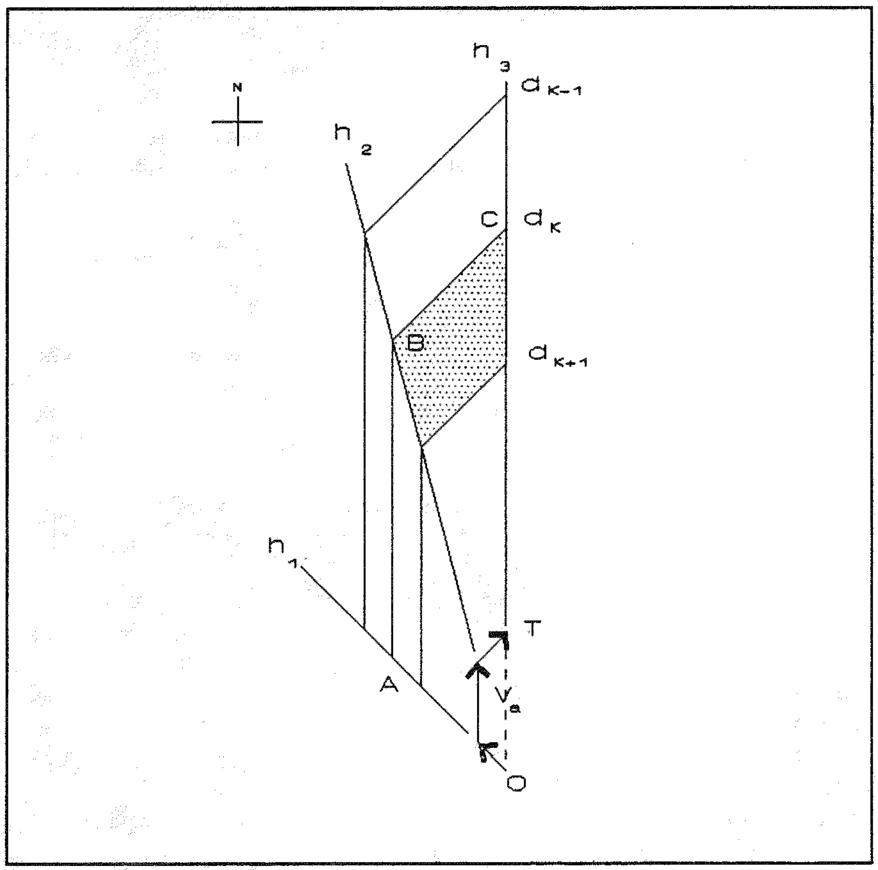

Figure 2.6 Fallout Sector - Case 3

From earlier discussions, it should be evident that all particles initially at 1000 ft or below (regardless of their diameter) will fall along the h_1 radial, all particles initially at 2000 ft will fall along the h_2 radial, and all particles initially at 3000 ft will fall along the h_3 radial. Let it be assumed that all particles initially at h_3 with a particular diameter, d_k, would be deposited at point C on the h_3 radial. Consequently, all particles initially at 3000 ft that were smaller than d_k would be deposited along the h_3 radial to the north of C, and all particles initially at 3000 ft that were larger than d_k would be deposited along that same radial to the south of C.

It follows that all particles initially between the surface and 1000 ft with a diameter, d_k, would be deposited along a line from 0 to A. All particles initially between 1000 and 2000 ft with a diameter, d_k, would be deposited along the line extending from A to B. And, all particles initially between 2000 and 3000 ft with a diameter, d_k, would be deposited along the line extending from B to C. Similar lines have been constructed for all those particles with the smaller diameter, d_{k-1}, and for all those particles with the larger diameter, d_{k+1}. It can be seen that all particles with a diameter from d_{k+1} to d_k that were initially distributed between h_2 and h_3 would be deposited in the hatched quadrilateral.

Thus, based upon the assumptions presented so far in this report, a fallout sector may be visualized as being composed of a group of quadrilateral surface areas. Each of these quadrilaterals is composed of set of particles that:

(1) have diameters of a specific range and

(2) have fallen from a specific range of altitudes.

The next chapter takes the concepts presented in this chapter and shows how the FOST was derived.[4]

[4]It would be quite difficult to describe the derivation and use of the FOST without the use of certain basic radiological terms and their associated units. Some of these terms, such as fallout, have already been defined. Others, such as activity, have been mentioned, but have not been specifically defined. Before progressing farther into the FOST derivation, it is perhaps appropriate to define some of the radiological terms that are crucial to the understanding of the FOST. These terms are presented in Appendix A.

CHAPTER 3

THE FOST FOR CRATERING DETONATIONS

It may first appear to be inappropriate to devote a large portion of this report to the derivation and application of a technique for making exposure estimates for **cratering** detonations. However, the PIKE Model is a special application of the FOST, which was derived not for containment-designed detonations, such as PIKE, but for cratering detonations. Therefore, for thoroughness, it is necessary to present the cratering aspects of the FOST so that the method of applying the FOST to containment-designed events may be understood.

This chapter duplicates much of the material that was presented by Cluff and Palmer in their unpublished 1964 report (Reference 1.1) on the fallout-scaling technique. However, this present report does not describe the validation tests of the scaling technique that were presented in the 1964 report. It has been assumed in this report that the scaling technique described in the 1964 report is an appropriate method of obtaining exposure estimates for cratering events.

While this report duplicates much of that presented in the 1964 report, there are differences. For example, so that the reader may easily follow the development of the FOST from the basic principles that were presented in Chapter 2 to the final scaling equations presented at the end of this chapter, this report presents some of the intermediate derivation steps that are not necessarily obvious in the 1964 report.

By the end of this chapter, the FOST, as applied to cratering events, is fully described. In the next chapter, it will be shown how the FOST has been modified to apply to containment-designed events.

THE BASIC FOST EQUATION

It was demonstrated in Case 3 of Chapter 2 how fallout particles are distributed on the earth's surface as a function of their diameter and initial height in the debris cloud. What was presented in a specific case in Figure 2.6 (page 20) can be generalized as shown in Figure 3.1. In this figure, as was the case in Figure 2.6, the diameter (d) and height (h) lines divide the fallout pattern into quadrilaterals. Within each of these areas is deposited the activity associated with the specified range of particle diameters and initial heights. For example, the hatched quadrilateral area at the left of the figure represents the deposited activity associated with those particles having a diameter between d_k and d_{k-1} and having an initial height between h_k and h_{k+1}. An enlargement of this quadrilateral is presented on the right side of the diagram. Notice that if the quadrilateral is a small area [the angle (ϕ) is quite small], then the diameter lines approximate arcs having their origin at O [ground zero (GZ)]. Thus, the area of the hatched quadrilateral in the left of the figure can be approximated by the hatched area in the right of the figure which is

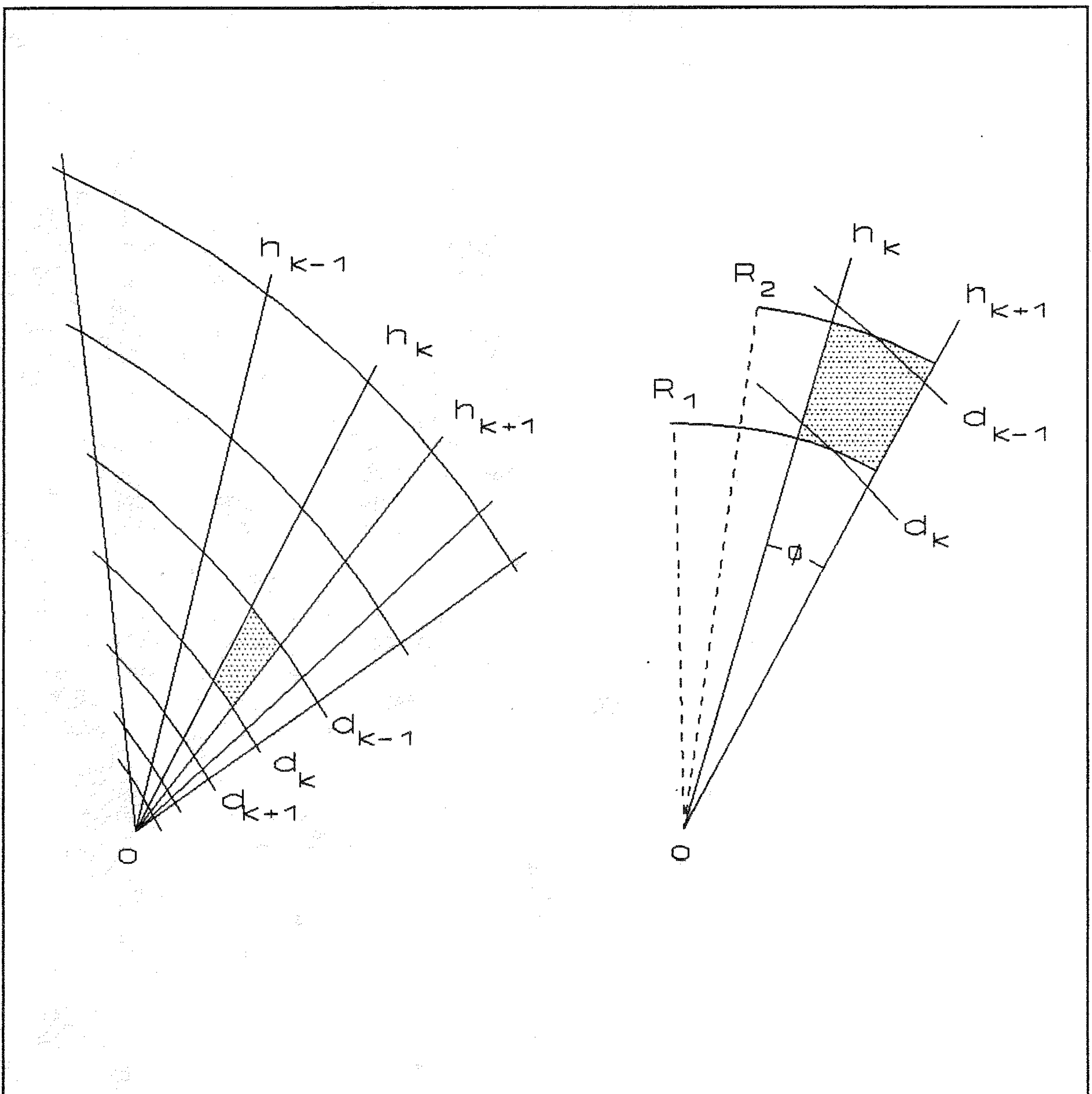

Figure 3.1 Particle-Deposition Pattern

defined by the height lines, h_k and h_{k+1} and by the arcs with radii of R_1 and R_2.

Let it be assumed that the activity within each small area is uniformly distributed and represents k percent of the total activity in the entire deposition pattern. Then:

$$C_s = k\ C_t \qquad (3.1),$$

where,

C_s = the activity within a specified small area,

k = the activity in the specified small area divided by the total activity in the deposition pattern

C_t = the total activity in the deposition pattern.

As stated by Cluff and Palmer:

> *An analysis of fallout patterns for cratering shots has indicated that the total activity deposited in the pattern* [C_t] *is a fraction of the fission activity and induced activity created by the shot.* (Reference 1.1)

Thus,

$$C_t = f\ C_f \qquad (3.2),$$

where,

f = a percentage of the fission plus induced activity available for deposition, and

C_f = the fission plus induced activity created by the detonation.

Substituting equation 3.2 into equation 3.1 yields,

$$C_s = k\ f\ C_f \qquad (3.3).$$

The area of the hatched quadrilateral shown in Figure 3.1 can now be determined. If it is assumed (1) that the area is relatively small and (2) that, therefore, the hatched area shown to the right is approximately equal to the hatched area to the left, then the area can be determined using the formula for calculating the area of a sector of an annulus. Thus,

$$A = (\phi/2)\ (R_2 + R_1)\ (R_2 - R_1)$$

or,

$$A = (\phi/2)\ (R_2^2 - R_1^2) \qquad (3.4)$$

where,

A = the area of the specified small quadrilateral,

ϕ = the angle between the radials h_k and h_{k+1},

R_2 = the larger radius defining the sector, and

R_1 = the smaller radius defining the sector.

Equation 2.9 showed that $\vec{x} = \vec{v}_a h/s$. If we were only interested in the magnitude of $\vec{x}$ (i.e., the distance of displacement without reference to the direction of displacement), then:

$$x = v_a h/s \qquad (3.5),$$

where,

x = the displacement distance (a scaler value), and

v_a = the average speed (not velocity) along the resultant transport bearing.

In Figure 3.1, R_1 can be approximated by x_1, the resultant displacement distance of the particle with a diameter of d_k and with an initial height of h_k. Similarly, R_2 can be approximated by x_2, the resultant displacement distance of the particle with a diameter of d_{k-1} and with an initial height of h_k. (In Figure 3.1, x_1 is the distance along the line extending from 0 to the intersection of the h_k and d_k lines; and x_2 is the distance along the line extending from 0 to the intersection of the h_k and d_{k-1} lines.) Therefore, equation 3.4 can be written as

$$A = (\phi/2)\ (x_2^2 - x_1^2) \qquad (3.6).$$

Substituting equation 3.5 into equation 3.6 gives

$$A = (\phi/2)\ (h^2 v_a^2)\ (s_2^{-2} - s_1^{-2}) \qquad (3.7),$$

where,

s_2 = the fall rate of the d_{k-1} particle,

s_1 = the fall rate of the d_k particle, and

h = the reference height.

This reference height, as strictly defined by the above derivation, is h_k. However, in the computation of the area of the quadrilateral, h would more appropriately be an average between h_k and h_{k+1}.[1]

From equation 3.3, we can calculate the activity (C_s) within the specified small area, and from equation 3.7, we can calculate the area (A) of that small area. Thus,

$$D = C_s/A \tag{3.8}$$

where,

D = the activity per unit area in the specified small area.

The term, D, will be referred to as the activity density in this report. Substituting equations 3.3 and 3.7 into equation 3.8 gives

$$D = \frac{k\ f\ C_f}{(\phi/2)\ (h^2 v_a^{\ 2})\ (s_2^{-2} - s_1^{-2})} \tag{3.9}$$

This is the basic equation upon which the FOST was built.

DEVELOPMENT OF THE SCALING TECHNIQUE

As it was pointed out in Chapter 1, the largest obstacle to accurate fallout predictions is the difficulty of predicting the initial aerial particle-size and activity distributions. As indicated, one of the primary reasons this is difficult is the lack of particle-size and activity data collected in the past.

Successful empirical models are usually based upon comprehensive data that are indicative of the phenomenon to be predicted. Since there is not a comprehensive data base of particle-size and activity distributions upon which to build a fallout-deposition model, one has to utilize whatever data are both abundant and indicative of fallout patterns. The only data that fit these requirements are gamma exposure-rate data.[2]

---

[1] In the above derivation, x_2 could have been defined as the resultant displacement distance of the particle with a diameter of d_{k-1} and with an initial height of h_{k+1} (instead of h_k). If this had been the case, equation 3.7 would not have had an "h" but would have had an h_1 (associated with the d_k particle) and an h_2 (associated with the d_{k-1} particle). However, as can be seen above, both "R's" can be defined using only one "h" radial. This simplifies equation 3.7.

[2] These are surface-based observations of exposure to gamma rays per unit time as measured three feet above the ground.

After each NTS nuclear detonation that produced fallout, radiological-safety monitors surveyed downwind areas with their portable gamma-survey instruments, and, in many cases, installed stationary recording gamma-survey instruments in the downwind fallout sector. Gamma decay rates[3] were determined at those locations where there were enough data collected to provide a relatively continuous trace of exposure-rate values with time. Usually, in association with a particular nuclear detonation, most of the decay rates, regardless of location, were found to be similar. Once this characteristic decay rate was established, any single exposure-rate observation that was indicative of undisturbed deposited debris (not influenced by such processes as cloud passage or redeposition) could then be normalized to a standard time using that decay rate. With all such exposure-rate values normalized to a standard time, it was then possible to construct a fallout pattern analysis (footprint) valid for that particular time. Since gamma-exposure-rate data can be normalized to a standard time, it has a strong advantage over other types of radiological data that cannot be (e.g., particle size and activity distribution data).

ACTIVITY DENSITY VS. EXPOSURE RATE

The analog fallout patterns were constructed using comprehensive gamma-exposure-rate data (usually expressed in mR/hr or R/hr). However, the basic FOST equation, equation 3.9, solves for D, the activity density expressed in activity per unit area (Ci/m^2). Let us consider the relationship between activity densities and exposure rates.

Consider a small surface area upon which uniformly distributed particles having a specified activity have settled. This area would therefore have a certain activity density (Ci/m^2). At a specified time, t_s, the quantity of disintegrations associated with the radioactive material deposited within the area would produce a certain quantity of gamma radiation. One could then think of this amount of radiation per unit area as the gamma-radiation "density." These gamma rays would be emitted from the specified surface area into the volume of air immediately above the surface. A gamma-survey meter within this air would register the amount of ionization per unit volume of air caused by the gamma rays.

Now, consider an identical group of radioactive particles being deposited in a somewhat larger area. These particles, which are also uniformly distributed, have the same amount of activity associated with them as in the above case. Let it be assumed that the air over this larger area is under the same atmospheric conditions as the air indicated above the smaller area. In this larger area at time, t_s, there would be the same quantity of disintegrations as in the smaller area and the same quantity of gamma radiation. However, in this case, these gamma rays would be emitted from a larger surface area. Thus, the gamma-radiation "density" would be lower.

---

[3]The gamma decay rate is the decrease in gamma exposure with the passage of time.

The ratio of the volume of air over the larger sector to the volume of air over the smaller sector would be equal to the ratio of the area of the larger sector to the area of the smaller sector. Thus, if the area of the larger sector was twice that of the smaller sector, then the volume of air above the larger sector would be twice that of the volume of air above the smaller sector. Consequently, since there were equal amounts of gamma radiations in each sector, there would be half as many gamma rays in a unit volume of air over the larger sector. Recall (from Appendix A) that exposure describes the quantity of gamma rays producing electrons that will maintain a certain electrical charge in a unit mass of dry air. Since there would be half as many gamma rays per unit volume of air over the larger sector and since the mass in a unit volume of air over either sector would be the same, then there would be half as much charge per unit mass of air over the larger sector. Thus, the exposure, as measured by a gamma-survey meter, would be half as much over the larger sector as over the smaller sector.

The above exercise indicates that if a group of radioactive particles were equally distributed over a certain initial area, and an identical group of radioactive particles were equally distributed over another area having a different size, then the ratio of the activity density of the initial area to the activity density of the other area would equal the ratio of the exposure rate measured in the initial area to the exposure rate measured in the other area.

THE SCALING EQUATIONS

With the above discussions in mind, it can be shown that equation 3.9 can be used in a ratio form for scaling purposes. As mentioned above, scaling can be accomplished if it is assumed that the initial aerial particle-size and activity distributions associated with the analog event will be the same as those for the new event (the event which exposure estimates are being derived).

> *This implies that the relative spatial particle size distributions are similar regardless of the height or size of the clouds and that the activity available for deposition is partitioned in the same percentage proportions over the spectrum of particle sizes.* (Reference 1.1)

It is contended that if there are two events in which the initial aerial particle size and activity distributions are similar, then there are comparable quadrilateral areas in the two deposition patterns which contain the same percentage of the activity in their respective patterns. This suggestion can be exemplified by using Figure 3.1. The hatched quadrilateral area shown in this figure represents the area occupied by those deposited particles associated with the analog event that have a diameter between d_k and d_{k-1} and had an initial height of between h_k and h_{k+1}.[4] Furthermore, this area contains k percent of the

[4]These heights are in relation to the total height of the cloud. For example, h_k might represent 30% of the total height of the cloud and h_{k-1} might represent 20% of the total height of the cloud. If the cloud were 5000 ft high, then the heights would be 1500 and 1000 ft AGL, respectively.

total deposited activity.

A fundamental assumption of the FOST is that for a new event there exists a similar quadrilateral area (A_p) containing the same percentage of total activity (k) found in the quadrilateral area (A) of the analog event. This quadrilateral area for the new event contains particles having similar diameters (d_k and d_{k-1}) and similar altitudes of origin in relation to the total height of the cloud.[5] It is further assumed that the quadrilateral area (A) associated with the analog event is proportionally equal to the quadrilateral area (A_p) associated with the new event. Thus using equation 3.8, this proportionality can be expressed as

$$A/A_p = (C_s/D) / (C_{sp}/D_p) \quad \text{or}$$

$$D/D_p = (C_s A_p) / (C_{sp} A) \qquad (3.10)$$

where,

A = the area of the analog-event quadrilateral area,

A_p = the area of the new-event quadrilateral area[6],

C_s = the activity within the analog-event quadrilateral,

C_{sp} = the activity within the new-event quadrilateral,

D = the activity density of the analog-event quadrilateral, and

D_p = the activity density of the new-event quadrilateral.

---

[5] In this case, if the total cloud height was 10,000 ft and h_k and h_{k-1} still represented 30% and 20% of the total cloud height, the height lines bounding the new quadrilateral would be 3000 and 2000 ft AGL instead of 1500 and 1000 ft as with the analog example.

[6] For the remainder of this report, parameters associated with the new event will be given the subscript, $_p$, and the comparable parameters associated with the analog event will not be given a subscript notation. This notation scheme evolved from the original FOST derivation where the new-event parameters were noted with a primed value (e.g., A'). The "p" subscript in this report is equal to the "prime" notation in Reference 1.1.

Substituting equation 3.7 into equation 3.10 gives

$$D/D_p = \frac{(C_s / ((\phi/2)\ (h^2\ v^2)\ (s_2^{-2} - s_1^{-2})))}{(C_{sp} / ((\phi_p/2)\ (h_p^2\ v_p^2)\ (s_2^{-2} - s_1^{-2})))} \qquad (3.11)$$

where,

ϕ = the angle between the radials h_k and h_{k+1} for the analog event,

ϕ_p = the angle between the radials h_k and h_{k+1} for the new event,

h = the average starting altitude of the analog event particles,

h_p = the average starting altitude of the new event particles,

v = the average speed along the resultant transport bearing for the analog event,

v_p = the average speed along the resultant transport bearing for the new event,

s_1 = the fall rate of the d_{k-1} particles, and

s_2 = the fall rate of the d_k particles.

Furthermore, substituting equation 3.3 into equation 3.11 gives:

$$D/D_p = \frac{(k\ f\ C_f / ((\phi/2)\ (h^2\ v^2)))}{(k\ f_p\ C_{fp} / ((\phi_p/2)\ (h_p^2\ v_p^2)))} \qquad (3.12)$$

where,

k = the total activity in the pattern divided by the activity in the specified area,

f = the percentage of the fission plus induced activity available for deposition for the analog event,

f_p = the percentage of the fission plus induced activity available for deposition for the new event,

C_f = the fission plus induced activity created by the analog detonation, and

C_{fp} = the fission plus induced activity created by the new detonation.

Equation 3.12 can then be simplified to

$$D/D_p \quad = \quad (\phi_p/\phi)\ (h_p/h)^2\ (v_p/v)^2\ (f\ C_f\ /\ f_p\ C_{fp}) \qquad (3.13).$$

This equation would allow one to compute the activity density, D_p, of the quadrilateral associated with the new event if the activity density, D, of the analog event was known.

The distance at which these two quadrilateral areas are located from GZ can be determined by using equation 3.5, ($x = v_a h/s$). If

x = the distance from GZ to the center of the analog quadrilateral, and

x_p = the distance from GZ to the center of the new quadrilateral, then

$$x/x_p = hv\ /\ h_p v_p \qquad (3.14).$$

Equation 3.14 applies when h and h_p refer to initial altitudes of the particles deposited in the center of the quadrilaterals.

EQUATION MODIFICATIONS

Equations 3.13 and 3.14 are the basic scaling equations which will be modified below for use in making exposure-rate predictions for cratering events. In Chapter 2, it was shown how the wind velocities through the depth of a debris cloud could be plotted as a fallout hodograph and how the outermost radials associated with this resultant hodograph define the fallout sector. This procedure is further exemplified in Figure 3.2, which shows a schematic fallout pattern. Wind vectors representing the winds in layers having the same thickness are plotted from the point representing GZ. The tail of the vector representing the winds in the lowest layer (adjacent to the surface) is plotted at GZ and the vector representing the winds in the highest layer is plotted last.

One of the limits to the fallout sector is the radial extending from GZ to the head of the vector extending the farthest to the right of GZ[7]. The other limit is the radial extending from GZ to the head of the vector extending the farthest to the left of GZ. The fallout sector lies between these two radials. In the example in Figure 3.2, the radial, H_L, is defined by the head of the vector associated with the winds in the lowest layer (the vector beginning at GZ),

---

[7]Right and left are defined in relation to the direction toward which the vectors are pointing. In this case the right-most position is the head of the first vector. This situation is often the case, but there are exceptions. For example, if the second vector had been pointed directly toward the east (right), then the radial would have been constructed from GZ to the head of the second vector, because the head of the second vector would have been farther to the right than the head of the first vector.

and the radial, H_H, is defined by the head of the vector associated with the winds in the highest layer (the vector farthest from GZ).

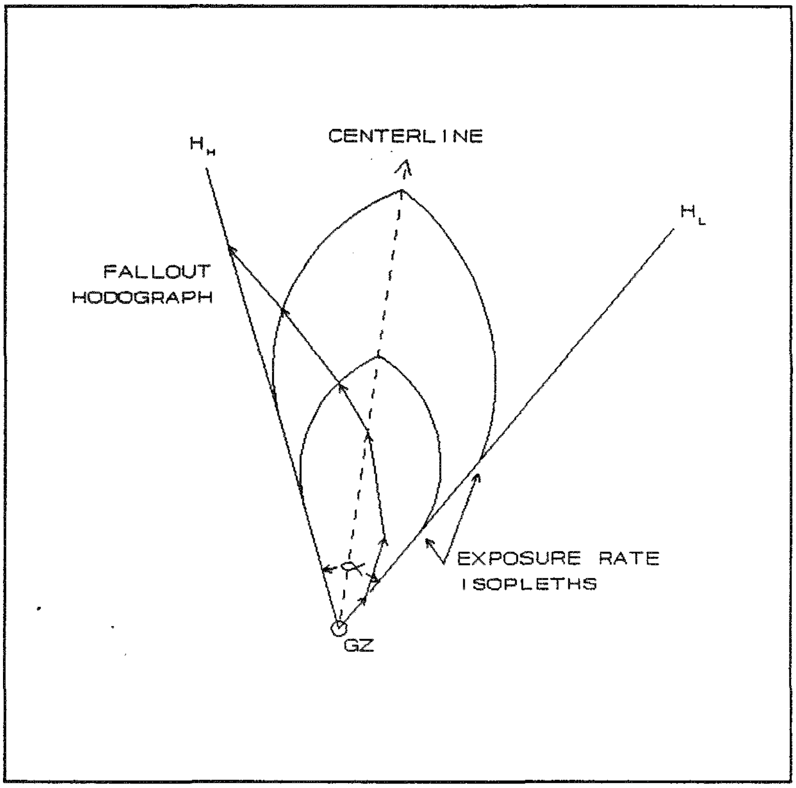

Figure 3.2 Schematic Fallout Pattern

For cratering detonations, Cluff and Palmer assumed that:

(1) the peak exposure rates, as a function of distance from GZ, are found in most cases along the same approximate bearing or "centerline,"[8]

(2) the total deposited activity is contained within the fallout sector, and

(3) that the peak exposure-rate levels and sector limits determine the length and approximate width, respectively, of the exposure-rate isopleths within the pattern.

Instead of trying to develop a method by which all the potential small (quadrilateral) areas in the analog-event fallout sector were related to the corresponding areas in the new-event fallout sector, Cluff and Palmer found it more convenient to limit the calculations to areas along the centerline. In adopting this approach, they were allowing the computation of the maximum exposures as a function of downwind distance while drastically reducing the number of calculations. In this manner, the Test Controller would have access to the most conservative exposure estimates; and the radiation briefer would be able to make the estimates in an expeditious manner.

[8] Cluff and Palmer referred to the centerline as the "hot line."

FISSION YIELD

Earlier, in equation 3.2, C_f, the fission activity plus induced activity[9] created by the detonation, was defined in terms of C_t, the total activity in the deposition pattern. This relationship was established by utilizing the factor, f, which is the fraction of the fission+ activity available for deposition.

It is pointed out in Appendix A that the fission yield of a nuclear detonation is the energy associated with the fission process and that this yield is usually expressed in terms of the equivalent tonnage of TNT required to produce the same amount of energy[10]. For example, a 1 kiloton (kt) fission device would produce energy equivalent to 1 kiloton of TNT (10^{12} calories of energy).

In the FOST, it is assumed that the ratio of the analog event's fission+ activity (C_f) to the analog event's fission+ yield (Y) is equal to the ratio of the new events's fission+ activity (C_{fp}) to the new event's fission+ yield (Y_p). That is

$$C_f/Y = C_{fp}/Y_p.$$

Therefore we can write,

$$Y/Y_p = C_f/C_{fp} \quad (3.15).$$

This equation can be substituted into equation 3.13 to change the input parameters from activities to yields.

The fission+ yield associated with an analog event is calculated from data collected in association with the analog event by the national laboratory that conducted that nuclear detonation. The fission+ yield (Y_p) associated with the new event is estimated by the national laboratory conducting that nuclear detonation. Both of these values are classified.

FALLOUT FRACTION

As discussed earlier, f is the fraction of the fission+ activity available for deposition. The fission+ yield, Y, is directly proportional to the fission+ activity. Thus,

---

[9]The term, "plus induced," will be hereafter replaced by the symbol, "+." Thus, the phrase, "fission activity plus induced activity," will be written as "fission+ activity."

[10]The *total yield* of a nuclear detonation represents all the energy released in association with the detonation. The *fission+* yield represents the energy released in association with the fission process and the energy resulting from the induced activity in the device materials and geological media.

$$Y = K_1 C_f \qquad (3.16),$$

where,

K_1 = a proportionality constant.

Furthermore, the fission+ activity (C_t) deposited in the fallout sector is proportional to a virtual yield, Y_v, associated with C_t.[11] Thus,

$$Y_v = K_2 C_t \qquad (3.17),$$

where

K_2 = another proportionality constant.

Therefore,

$$Y/Y_v = C_f/C_t \qquad \text{when } K_1 = K_2 \qquad (3.18).$$

But, according to equation 3.2, $C_f = C_t/f$. Consequently, after proper substitution in equation 3.18, equation 3.18 becomes,

$$f = Y_v/Y \qquad (3.19).$$

As discussed above, the fission+ yield (Y) for the analog event is a known value which is derived by the national laboratory from data collected after the detonation. Therefore, to calculate f, it is only necessary to calculate Y_v, the virtual yield. This virtual yield is determined by WSNSO through an analysis of the gamma-exposure-rate measurements taken in association with the analog.

The percentage of the fission+ activity available for deposition in association with the new event, f_p, was shown by Cluff and Palmer to be a function of the scaled depth of burial (defined below). It can be calculated using a graph in Reference 1.1 showing f_p versus scaled depth of burial.

CLOUD HEIGHTS

Based upon the assumption that there is a similar particle-size and activity distribution in the new event as in the analog event, it follows that the altitude of the origin of the new-event particles;

(1) having the same size as the analog particles and

---

[11] Y_v is the theoretical yield required to produce the fission+ activity present in the fallout sector.

(2) being deposited in similar quadrilateral areas

are in the same ratio with respect to their total cloud height as the altitude of the origin of the analog-event particles are to their total cloud height. In other words,

$$h/H = h_p/H_p \qquad (3.20),$$

where,

H = the total cloud height of the analog event, and

H_p = the total cloud height of the new event.

Based upon this relationship, the ratio h_p/h in equations 3.13 and 3.14 can be replaced by the ratio H_p/H.

For a cratering detonation, the height of the debris cloud at the time of stabilization is a function of (1) the burial depth and (2) the total yield of the device. These two parameters have been related in a term called the scaled depth of burial, BD_s. The relationship is,

$$BD_s = BD \,/\, Y_t^{1/3} \qquad (3.21),$$

where,

BD_s = the scaled depth of burial ($ft/kt^{1/3}$),

BD = the actual depth of burial (ft), and

Y_t = the total nuclear yield (kt).

The total nuclear yield for the new event is predicted by the national laboratory conducting the nuclear detonation.

Reference 1.1 gives detailed instruction on calculating the cloud height of the new cratering event (H_p) using this scaled depth of burial. The height of the analog cloud (H) is known through observation.

SHEAR ANGLES

Cluff and Palmer also contended that for most cratering-event fallout patterns, it was reasonable that the ratio of the small angle (Figure 3.1), ϕ, to the total directional shear, α, in the fallout hodograph (Figure 3.2) would be approximately the same. Thus,

$$\phi/\alpha = \phi_p/\alpha_p \qquad (3.22),$$

where,

α = the total directional shear in the analog-event fallout hodograph, and

α_p = the total directional shear in the new-event fallout hodograph.

Based upon this relationship, the ratio ϕ_p/ϕ in equations 3.13 and 3.14 can be replaced by the ratio α_p/α. It was pointed out, however, that this approximation appears realistic only when the total variation in wind direction with altitude is less than 90°.

The directional shear associated with the analog event, α, is primarily calculated by an analysis of the winds at the time of detonation of the analog event. The directional shear for the new event, α_p, is based upon wind predictions. This shear can be calculated from a fallout hodograph constructed by using the forecast winds up to the level of the predicted cloud height.

AVERAGE WIND SPEEDS

In equations 3.13 and 3.14, v and v_p are the average speeds along the resultant transport bearings. In their application of the scaler equations to cratering events, Cluff and Palmer chose to determine these average values from the winds from the surface to the *mid-altitude* of the debris cloud.[12] The winds associated with the entire depth of the cloud were used to determine the resultant transport bearing, but only those winds up to the mid-altitude of the cloud were used to determine the average speed. Thus, v and v_p in equations 3.13 and 3.14 can be replaced by V and V_p, where,

V = the average speed from the surface to the mid-altitude of the debris cloud for the analog event, and

V_p = the average speed from the surface to the mid-altitude of the debris cloud for the new event.

For the analog event, V can be derived by an analysis of the winds at the time of detonation. For the new event, V_p is derived from the predicted winds.

H+1 HR EXPOSURE RATES

Earlier, it was pointed out that if a group of radioactive particles were equally distributed over a certain initial surface area, and a similar group of particles were equally distributed over another sector with a different area, then the ratio of the activity density of the initial area to the activity den-

---

[12]In the calculation of exposure rates along the deposition centerline, it was apparently assumed that the centerline debris originated at the cloud's center, which would have been approximately at the cloud's mid-altitude.

sity of the other area would equal the ratio of the exposure rate measured in the initial area to the exposure rate measured in the other area. Thus,

$$D/D_p = ER/ER_p \qquad (3.23),$$

where

ER = the exposure rate in the analog event quadrilateral area, and

ER_p = the exposure rate in the new event equivalent quadrilateral area.

Since these quadrilateral areas are relatively small and the debris in them is assumed to be equally distributed, an exposure rate measured in association with an analog event at a certain point downwind from GZ, X, can be assumed to represent the exposure rate in one of these small areas. As discussed above, the FOST has been structured for making predictions along debris centerlines. Analysis of the analog event results in a plot of centerline exposure rates as a function of distance from GZ. The analog exposure rate at any one distance along this curve can be assumed to represent the exposure rate in one of the small quadrilateral areas.

As discussed earlier, due to radioactive decay, exposure rates measured at different times have to be normalized to a standard time. Though the standard time for most analyses of atmospheric nuclear events has been chosen as H+12 hr, the standard time for cratering and containment-designed events have usually been chosen as H+1 hr.

In equation 3.13, both D and D_p were implied to be for the same time. If a standard time of H+1 hr is assumed, then equation 3.23 can be rewritten as,

$$D/D_p = ER1/ER1_p \qquad (3.24),$$

where,

$ER1$ = the H+1 hr exposure rate at a certain centerline downwind distance for the analog event, and

$ER1_p$ = the H+1 hr exposure rate at the equivalent centerline downwind distance for the new event.

CENTERLINE DISTANCE

As mentioned above, in an H+1 hr-exposure-rate-versus-centerline-distance profile for an analog event, a point on the curve approximates the center of one of the small quadrilaterals. Thus, using this approximation and applying equation 3.20 along with the definitions of V and V_p, equation 3.14 can be written as,

$$X/X_p = (H/H_p)\ (V/V_p) \quad (3.25),$$

where,

X_p = the distance at which an exposure is calculated for the new event, and

X = the distance from GZ along the analog centerline at which lies the deposition area that is being scaled.

Finally, substituting equations 3.15, 3.20, 3.22 and 3.24 into equations 3.13 and 3.14 gives,

$$ER1/ER1_p = (\alpha_p/\alpha)\ (H_p/H)^2\ (V_p/V)^2\ (f\ Y\ /\ f_p\ Y_p) \quad (3.26).$$

Equations 3.25 and 3.26 are the scaling equations used for deriving exposure estimates for cratering events. Because it is not the purpose of this report to give instructions on the method of computing exposures for cratering events, the information about the FOST for cratering detonations will end here. If such estimates were necessary, one should apply the information presented above to the instructions presented in Reference 1.1.

At this point, the operational FOST equations (equations 3.25 and 3.26) have been established. It has also been pointed out how the parameters included within these equations are calculated for cratering detonations. It is now appropriate to describe how to utilize these equations and modify the parameters in order to calculate exposures in association with containment-designed detonations.

CHAPTER 4

THE FOST FOR CONTAINMENT-DESIGNED DETONATIONS

In the last chapter, it was shown how the FOST was developed for cratering-detonation-exposure estimates. The basic FOST equations were presented and *general* information was provided about how cratering-detonation-exposure estimates could be derived. However, since this report pertains to exposure estimates in association with containment-designed detonations, few details about the application of the FOST to cratering detonations will be provided. Instead, the remainder of this report will show how the FOST can be used to derive exposure estimates for containment-designed detonations. Furthermore, in the next two chapters, it will specifically be shown how the FOST can be used with the PIKE analog to calculate such estimates.

The structure of the FOST as applied to containment-designed detonations is generally the same as that derived for cratering detonations. The same basic assumptions are used; namely, that the particle-size and activity distributions of the analog event are similar to the new event. The same basic equations (equations 3.25 and 3.26) are also utilized. However, the manner in which some of the parameters in these equations are calculated is somewhat different.

This chapter is divided into two major sections, radiological aspects and meteorological aspects. They discuss the parameters that need to be extracted from the radiological and meteorological analyses of the analog event and need to be estimated for the new event.

These parameters may be more easily described if equations 3.25 and 3.26 are first rearranged as they are actually used in the FOST for containment-designed detonations. The required parameter is $ER1_p$, or,

$$ER1_p = ER1\ (\alpha/\alpha_p)\ (H/H_p)^2\ (V/V_p)^2\ (f_p\ Y_p\ /\ f\ Y) \qquad (4.1).$$

To determine the value for ER1, the value for the analog downwind distance, X, is needed, so that equation 3.25 becomes,

$$X = X_p\ (H/H_p)\ (V/V_p) \qquad (4.2).$$

RADIOLOGICAL ASPECTS

Once $ER1_p$ is calculated for some downwind distance X_p, then exposure estimates for that location can be made based upon the debris-decay characteristics of the analog event. Therefore, to understand the PIKE Model, it is necessary to comprehend the relationships between exposure rates computed by the FOST and the exposure estimates required by the Test Controller and other safety officials.

EXTERNAL-GAMMA EXPOSURES

Prior to the underground-testing era, one of the major concerns regarding populations exposed to nuclear debris was the dose to the external body due to the gamma radiation associated with fallout. It has always been a relatively straightforward process to calculate such external-gamma doses from exposure-rate measurements. Moreover, many gamma exposure-rate measurements were always made in association with an atmospheric release of nuclear debris.

In assessing health risks, other doses, such as those to internal organs, may be as important, or even more important, than external-gamma doses in certain circumstances. However, calculating these other doses is not as straightforward as gamma-dose calculations, and comprehensive measurements needed to make some of these calculations can not be easily obtained like the gamma exposure-rate measurements. Thus, there has always been emphasis upon obtaining predictions of external-gamma exposures in assessing the safety of nuclear experiments. The FOST satisfies this requirement by using exposure-rate data collected in the past to project gamma exposures and doses in the future should there be an accidental venting of radioactive materials into the atmosphere.

EXPOSURE-RATE OBSERVATIONS

If a recording gamma-exposure-rate instrument was established at a location before the arrival of the debris cloud and was allowed to remain there for a substantial time after the end of the cloud passage, the data recorded could yield an exposure-rate-versus-time profile, such as the example shown in Figure 4.1.

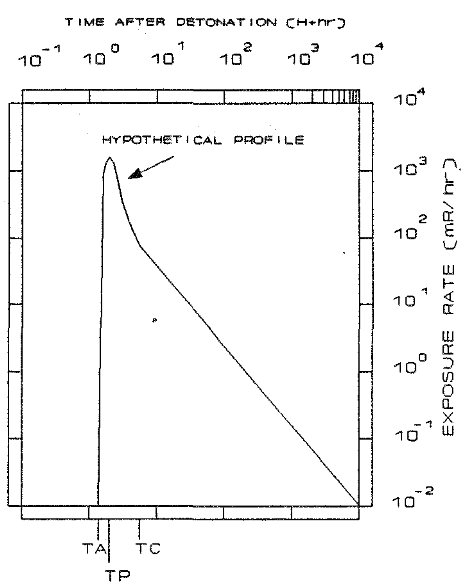

Figure 4.1 Exposure-Rate-Versus-Time Profile

Such a profile indicates the time of cloud arrival, TA. In this case, TA is shown to be about 1.4 hours after the detonation (H+1.4 hr). The profile also shows the time of the peak exposure rate, TP. In this case, TP is about H+2.2 hr. TP would normally indicate the time at which the cloud's axis of maximum activity is directly over the instrument. Furthermore, the end of cloud passage, TC, can be approximated from this profile. As the cloud's maximum activity axis begins moving away from the location, the exposure rate at that location would decrease due to (1) the decrease in the amount of debris suspended overhead and

(2) the decay of the remaining debris, both suspended over and deposited on the ground. After the end of cloud passage, the exposure-rate decrease reflects only the decay of the deposited debris. (That is, the exposure-rate decrease after TC becomes equal to the debris-decay rate.) Consequently, the exposure-rate decrease after TC is slower than that during the period from TP to TC. Thus, an approximation of TC can be gained by finding the time at which the exposure-rate decrease changes from a fast to a slow rate. In Figure 4.1, the exposure-rate decrease becomes slower near H+5 hr.

In Figure 4.1, the exposure-rate decrease after TC (the fallout-decay rate) is shown as a straight line (on a log-log plot). Such a straight line can be described by its slope, N, so that,

$$N = \log(ERX/ERY) \ / \ \log(TX/TY), \qquad (4.3)$$

where,

ERX = exposure rate at time, TX, and

ERY = exposure rate at time, TY.

The decay rate associated with such a straight line is often described as "t^N decay," where t refers to the time after detonation and N to the appropriate slope. In Figure 4.1, the slope after TC is -1.2. Thus, the decay can be described as $t^{-1.2}$ decay. In Reference 2.1, it is stated that the decrease in gamma radiation from most fallout from about H+0.5 hr to H+5000 hr can be approximated within 25 percent by the $t^{-1.2}$ relationship.

Once the decay rate has been established, this rate can be used to evaluate the exposure-rate data collected at individual locations. A line with the associated slope can usually be fitted to those exposure-rate data known to have been collected after cloud passage. The resulting decay curve can be extrapolated both backward and forward in time. If this line is extrapolated backward in time, there will often be a time at which the observed exposure-rate values start to increase dramatically from the extrapolated line. This time is approximately the end of cloud passage (TC).

The point along the decay curve at time TP is defined as the deposition-peak-exposure rate (DPER). This parameter will be discussed later.

INTEGRATED EXPOSURES

With an exposure-rate profile such as the one shown in Figure 4.1, the exposures at that location can be determined for any time period through an integration process. For example, if you need to know the exposure received during cloud passage, an integration under the curve from TA to TC would yield the desired result.

There are several integrated exposures that are of interest to NTS safety officials. Figure 4.2 combined with Table 4.1 show these exposures. In using this figure and table, notice that in addition to TA, TP, and TC, there are also T1, which is H+1 hr, TY, which is H+1 year, and TI, which represents infinity.

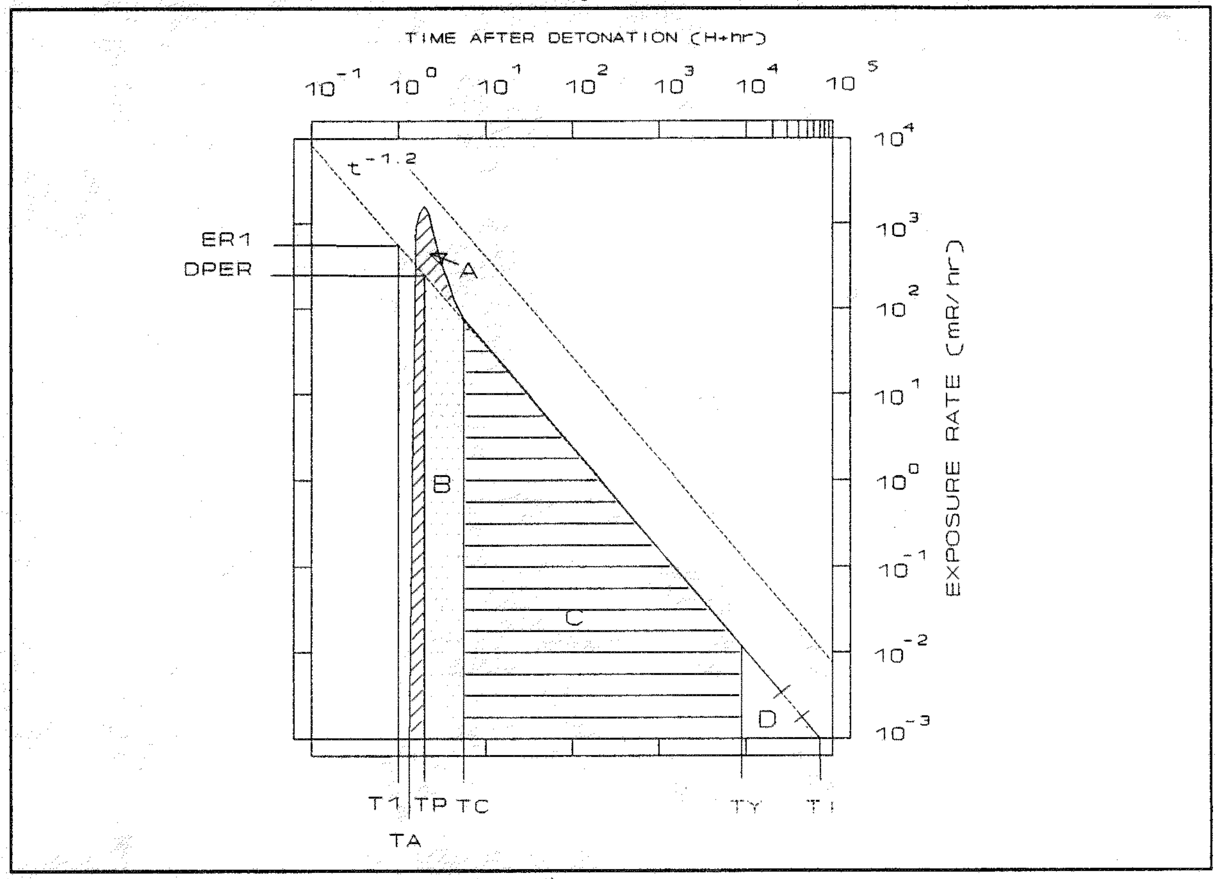

Figure 4.2 Profile Terminology

A $t^{-1.2}$ decay line overlays the profile from TC to TI and extends toward the upper left of the figure. As can been seen in Figure 4.2, the area under the profile (exposures) can be divided into four components, areas A, B, C, and D.

Area A, which has been denoted as the ***Cloud-Airborne-Emitters Exposure (CAE)***, primarily represents the exposure due to the suspended debris during cloud passage. It encompasses the areas (1) under the profile from TA to TP and (2) under the profile but above the $t^{-1.2}$ decay line from TP to TC .

Area B, which has been denoted as the ***Cloud-Deposition Exposure (CDE)***, primarily represents the exposure due to deposited debris (fallout) during cloud passage. It encompasses the area below the $t^{-1.2}$ decay line from TP to TC.

Area C, which has been denoted as the ***Residual-First-Year-Deposition Exposure (RYDE)***, represents the exposure due to deposited debris from the end of cloud passage until one year after detonation. It encompasses the area below the profile (and, therefore, the decay curve) from TC to TY.

Table 4.1 Profile Terminology

TIMES AFTER DETONATION

T1	=	1 hr
TA	=	ARRIVAL OF THE FIRST DEBRIS
TP	=	TIME OF THE PEAK EXPOSURE RATE
TC	=	TIME OF THE END OF CLOUD PASSAGE
TY	=	1 yr (8760 hr)
TI	=	INFINITY

EXPOSURE RATES

ER1	=	EXPOSURE RATE AT H+1 hr
DPER	=	DEPOSITION-PEAK-EXPOSURE RATE

EXPOSURES

TYE	=	TOTAL-FIRST-YEAR EXPOSURE	(A+B+C)
CPE	=	CLOUD-PASSAGE EXPOSURE	(A+B)
TYDE	=	TOTAL-FIRST-YEAR-DEPOSITION EXPOSURE	(B+C)
RYDE	=	RESIDUAL-FIRST-YEAR-DEPOSITION EXPOSURE	(C)
CAE	=	CLOUD-AIRBORNE-EMITTERS EXPOSURE	(A)
CDE	=	CLOUD-DEPOSITION EXPOSURE	(B)
YIDE	=	FIRST-YEAR-TO-INFINITY-DEPOSITION EXPOSURE	(D)
TIDE	=	TOTAL-INFINITE-DEPOSITION EXPOSURE	(B+C+D)
TIE	=	TOTAL-INFINITE EXPOSURE	(A+B+C+D)
RIDE	=	RESIDUAL-INFINITE-DEPOSITION EXPOSURE	(C+D)

Area D, which has been denoted as the ***First-Year-to-Infinity-Deposition Exposure (YIDE)***, represents the exposure due to deposited debris from the end of the first year to infinity. It encompasses the area below the profile (and, therefore, the decay curve) from TY to TI.

At the present time, the most widely used integrated exposure is the ***Total-First-Year Exposure (TYE)***. In the profile, it is represented by the combination of areas A, B, and C. In practical terms, it is the exposure measured at a particular location from the time of cloud arrival (TA) to one year after detonation (TY), assuming that exposure was continuous throughout the period. TYE gains its prominence due to the requirements that a nuclear device can not be detonated until it can be safely assumed that the downwind population will not receive average-whole-body exposures in excess of a certain limit, 170 mR/year in most cases (Reference 4.1). For example, if it were predicted that the TYE at a certain downwind location would be greater than 170 mR and if it was known that remedial actions could not be taken to mitigate the expected exposure (e.g., sheltering the population during and for a period after cloud passage), then the detonation of the device could be delayed.

Another integrated exposure that was used for many years as a safety guide was the ***Total-Infinite-Deposition Exposure (TIDE)***, which was more commonly known as the "infinite exposure." In the profile, it is represented by the combination of areas B, C, and D. This exposure was the primary one for which estimates were made with the PIKE Model for the Test Controller and his safety advisory panel during the 1960s and most of the 1970s.

One integrated exposure in which interest is frequently expressed is the ***Cloud-Passage Exposure (CPE)***. This exposure is represented by areas A and B in the profile. The CPE would be the exposure measured while the debris cloud was passing through a certain downwind location. This exposure becomes important when estimates are made of how much less exposure a person would receive if he was sheltered in a protected place while the cloud was in the vicinity. Note that if that person was properly sheltered during cloud passage, his one-year exposure would be approximated by the RYDE (area C).

There are two remaining exposures defined in Table 4.1. These are the ***Total-Infinite Exposure (TIE)***, and the ***Residual-Infinite-Deposition Exposure (RIDE)***. TIE is represented by a combination of areas A,B,C, and D. RIDE is represented by a combination of areas C and D.

When there is a constant decay rate, such as $t^{-1.2}$, it is relatively easy to integrate using the equation:

$$E = ((ER_s \, t_s^{-N})/(-N-1)) \, (t_s^{N+1} - t_e^{N+1}) \qquad (4.4),$$

where,

E = exposure from t_s to t_e,

ER_s = exposure rate at t_s,

N = slope,

t_s = starting time of the exposure, and

t_e = ending time of the exposure.

If the exposure rate at H+1 hr, ER1, is known, then equation 4.2 can be written as:

$$E = (ER1/(-N-1)) \, (t_s^{N+1} - t_e^{N+1}) \qquad (4.5).$$

This equation can easily be used to compute areas B, C, and D in Figure 4.2.

FALLOUT ANALYSES

Since the scaling analogs used in the FOST are based upon the analysis of gamma exposure-rate data, it is important to have both accurate and sufficient exposure-rate data to develop the analog. Ideally, there should be enough of these exposure-rate readings taken within the fallout field of a particular analog event to construct exposure-rate-versus-time profiles which clearly define:

(1) the debris arrival times (TA),

(2) the peak exposure rates,

(3) the decay rate(s) associated with the deposited debris, and

(4) the times of the end of the debris cloud passage (TC).

Rarely have there been enough exposure-rate data collected in association with NTS nuclear detonations to provide comprehensive exposure-rate-versus-time profiles across the entire fallout field. In the most favorable circumstances, which were associated with the atmospheric detonations of the 1950s, there were often less than a dozen of these profiles per event. In some cases, only one or two of these profiles could be constructed. Since containment-designed detonations which released massive amounts of debris into the atmosphere were "accidents," downwind sampling was generally less organized than that done in association with atmospheric or cratering detonations. As a result, fewer exposure-rate-versus-time profiles could be constructed for the containment-designed-detonation analogs.

Even though ideal exposure-rate data are not available for a fallout pattern analysis, a credible pattern can still be produced as long as (1) at least two exposure-rate-versus-time profiles can be constructed from reliable data collected over a relatively long period of time and (2) there is a substantial amount of accurate exposure-rate data collected after cloud passage and for the entire fallout field. In regards to the second condition, it is not necessary that more than one observation be made at a particular location, as long as that reading is accurate. Assuming that the decay rate derived from the exposure-rate-versus-time profiles is appropriate, then an H+1 hr exposure-rate value can be computed at each location where at least one post-cloud-passage observation was made with an uncontaminated instrument.

If only several comprehensive exposure-rate-versus-time profiles are needed along with one exposure-rate value per location, it might seem that a fallout pattern would not be too difficult to construct. However, with any fallout analysis, there are always many problems that make the analysis quite difficult. These problems result in a large amount of subjectivity being introduced into the pattern derivation.

Most of these problems are concerned with conflicting H+1 hr exposure-rate values. If there is a conflict at a particular location[1], which value is the correct value? Is the conflict the result of an inappropriate decay curve, an observer error, an instrument malfunction, a lingering debris cloud, resuspended debris, contaminated clothing or instrumentation, erroneous location markers, or a combination of several such factors? Thus, it is up to the fallout analyst to recognize a potential problem, eliminate or correct the data associated with that problem, and then view the fallout pattern in light of the changes. If the changes produce a more acceptable solution, then the correction is documented and the next potential problem is addressed. This process continues until all of the apparently conflicting data agree. The analyst then presents the resulting fallout pattern based upon his best assumptions.

In the past, most of the subjective decisions used in deriving fallout patterns were not documented. Only the fallout pattern was presented. Recently, there has been a trend toward documentation.[2] When an undocumented pattern is viewed or when a documented pattern is viewed without reference to its documentation, there is the tendency by some to accept the pattern as a certainty. What is overlooked is that the pattern is only one interpretation of the exposure-rate data.[3]

To utilize the FOST for containment-designed-detonation-exposure estimates, one would need to extract certain factors from the fallout pattern analysis. These factors would include the decay curve, the H+1 hr centerline-exposure-rate-versus-distance curve, the fallout fraction, and the relationship between cloud-passage exposure and the total-first-year-deposition exposure. These factors are discussed below.

THE ANALOG DECAY CURVE

The primary tool for determining the decay curve for the analog event is the exposure-rate-versus-time profile, as presented in Figure 4.2. Each profile for the analog event is analyzed to determine TC, the time of the end of cloud passage. Once this time is known, the data collected after TC is then analyzed to determine the rates at which the exposure rates decrease. If the data are

---

[1]For example, at a particular location one monitor records 14 mR/hr at H+5 hr, another records 12 mR/hr at H+10 hr, and another records 0.5 mR/hr at H+40 hr. If the decay curve were close to $t^{-1.2}$, the H+1 hr values for this location would be 97, 190, and 42 mR/hr, respectively. There are obvious conflicts in this case.

[2]The WSNSO recently reanalyzed 12 atmospheric detonations in association with DOE's Off-Site Radiation Exposure Review Project. The resulting fallout patterns are well documented.

[3]For a comprehensive view of how fallout patterns are constructed, one may refer to the WSNSO SIMON fallout analysis (Reference 4.1). While this report primarily documents the SIMON fallout pattern, it can serve as a tutorial about fallout pattern construction.

accurate and are representative of initial debris deposition (the winds have not significantly redistributed the debris), then it is likely that all the profiles will exhibit similar exposure-rate-versus-time curves when normalized to an exposure-rate value at a standard time (usually H+1 hr).

If all the resulting curves correlate well, then a composite-decay curve can be constructed. The composite curve is a plot of exposure rates versus time with the exposure rate at H+1 hr set to 1.

For the application of the FOST to containment-designed detonation, it is assumed that the debris associated with the new event has the same decay characteristics as the debris associated with the analog event. If a predicted H+1 hr exposure rate ($ER1_p$) is given for a particular location (X_p), then the exposure rate at any other time at this location can be calculated by multiplying $ER1_p$ by the normalized exposure rate indicated by the decay curve.

Earlier in the chapter, it was pointed out that debris-decay rates could often be approximated by a line of constant slope. Up until 1985, it was assumed that the PIKE debris decayed at a rate described by $t^{-1.2}$. With such an assumption, exposure calculations were simple. For example, during the period when safety officials were primarily interested in the Total-Infinite-Deposition Exposure (TIDE), equation 4.4 was simplified to:

$$TIDE = 5\ ER1_p\ TP^{-0.2} \qquad (4.6),$$

where TIDE was expressed in R or mR, ER1 was expressed in R/hr or mR/hr, and TP was expressed in hours after detonation.

There are now theoretical decay curves based upon radiochemical considerations that aid in the interpretation of the exposure-rate-versus-time profiles and allow the extension of the curve to times beyond those at which exposure-rate data were acquired. As a result, it is now possible to more accurately define the decay characteristics of the debris with a more complex (variable slope) decay curve. This procedure will be discussed in more detail in the next chapter.

THE ANALOG EXPOSURE-RATE-VERSUS-DISTANCE CURVE

To solve for $ER1_p$ in Equation 4.1, it is necessary to determine ER1. The ER1 value is determined from the analog-centerline-exposure-rate-versus-distance curve by utilizing the analog distance value (X), as defined in equation 4.2.

As discussed in Chapter 3, in most fallout patterns there is an axis of maximum exposure rates extending from GZ along a certain bearing. (There can be multiple centerlines in situations where there is considerable vertical wind shear, but these cases do not make appropriate scaling analogs.) Once all the normalized exposure-rates are plotted on a chart and exposure-rate isopleths are drawn, it is fairly simple to determine the centerline.

To construct the centerline-exposure-rate-versus-distance curve, those exposure-rate values collected on or very near the centerline are normalized to H+1 hr and plotted versus distance from GZ. In addition, values of the contours can also be plotted on the chart at the distance where they cross the centerline.

THE ANALOG FALLOUT FRACTION

The fallout fraction for a containment-designed-detonation analog can be derived from the fallout analysis by the same method used to derive the fallout fraction for a cratering-detonation analog.

THE ANALOG CLOUD-PASSAGE EXPOSURE VERSUS FIRST-YEAR-DEPOSITION EXPOSURE

As pointed out earlier in this chapter, the total-first-year exposure, TYE, is the primary estimate for which the FOST is employed. As indicated in Figure 4.2, TYE includes areas A, B, and C. If an entire exposure-rate curve as shown in this figure were provided, it would not be too difficult to integrate under the curve from TA to TY to determine TYE. However, the primary FOST equations (4.1 and 4.2) can only be used to calculate the exposure rate at H+1 hr ($ER1_p$). It is therefore necessary to construct a profile based solely upon $ER1_p$.

Since TP and TY are known and since DPER can be calculated using $ER1_p$ in conjunction with the decay curve, it is relatively simple to calculate the area under the curve from TP to TY. This value is the Total-First-Year-Deposition Exposure, TYDE (areas B and C). However, to calculate TYE, the Cloud-Airborne-Emitters Exposure (CAE) (area A) needs to be added to TYDE.

The Cloud-Passage Exposure (CPE) (areas A and B) is another exposure in which safety officials have an interest. Area B can be easily calculated by integrating from TP to TC. However, it is again necessary to know the value of CAE to derive the value of CPE.

The solution to the problem of deriving CPE has been to examine the analog-exposure-rate-versus-time profiles to determine the percentage of TYE that is accounted for by CAE. Once this analysis is complete, the assumption is made that this relationship is applicable to the new event.[4] This approach will be expanded upon in the next chapter.

---

[4]A similar approach was taken in association with the FOST up until the late 1970s. At that time, TIDE (areas B, C, and D) was routinely calculated. It was determined by an analysis of the PIKE exposure-rate-versus-time profiles that CPE was half the value of TIDE. This relationship was considered valid until the reanalysis of the PIKE data in 1985.

SCALING PARAMETERS

To obtain a value for the H+1 hr exposure rate, $ER1_p$, at downwind distance, X_p, one has to input the five radiological parameters, ER1, f, f_p, Y, and Y_p into equation 4.1. As discussed above, ER1 is determined using the analog-exposure-rate-versus-distance curve with the downwind distance, X, calculated with equation 4.2. The methods of determining the other four parameters are discussed below.

FALLOUT FRACTIONS

In Chapter 3, the analog fallout fraction was defined as the percentage of the fission+ activity available for deposition. For cratering detonations, this percentage would primarily be a function of the depth of burial of the device and the total yield of the device. For example, a 10 kt device buried 200 feet should eject more of its fission products into the atmosphere than, (1) a 1 kt device buried 200 feet, or, (2) a 10 kt device buried 400 feet.[5] As discussed in Reference 1.1, the FOST ***new-event*** fallout fraction (f_p) for use with cratering detonations can be calculated as a function of scaled depth of burial, BD_s. While the same method could be utilized to determine the ***analog-event*** fallout fraction (f), a more dependable estimate can be determined by integration of the analog fallout pattern.

The same pattern-integration technique employed to determine the fallout fraction of cratering-analog events can be used to determine the fallout fraction of containment-designed-analog events. However, the simple scaled-depth-of-burial-versus-fallout-fraction relationship used for determining the fallout fraction of cratering-new-event detonations is definitely not applicable to the determination of the fallout fraction of containment-designed-new-event detonations.

Data collected by Germain and Kahn (Reference 4.3) indicate that the burial of devices at scaled depths of 250 or less will likely lead to the venting of debris. A scaled depth greater than about 450 should achieve containment even for yields larger than 5 kt in most geological media. For many years, DOE has mandated that devices have scaled depths of burial much higher than 450.

Today, a containment-designed detonation has a very large scaled depth of burial which insures that the force of the blast will not weaken the structure of the overlying geological media and allow debris to escape. With these large scaled depths of burial, there is no longer a relationship between the scaled depth and the fallout fraction as there was with cratering detonations.

The FOST fallout fraction for containment-designed detonations is a function of the venting mechanism. Because the venting mechanism is very difficult to

---

[5]According the calculations by Cluff and Palmer (Figure 4 of Reference 1.1), the 10 kt cratering device buried 200 feet would have a fallout fraction of about 40%; whereas, the 1 kt device buried 200 feet and the 10 kt device buried 400 feet would have fallout fractions of approximately 3%.

predict, uncertainty enters into the estimation of the fallout fraction for a new event.

To resolve this limitation, it is assumed that the new event will have the same fallout fraction as the analog event, $f = f_p$. This assumption requires that the particle-size and activity distributions of the new event are the same as those of the analog event. Without this fundamental assumption, the FOST would not be applicable.

It is realized that this fallout fraction solution, $f = f_p$, is arbitrary and that many other assumptions would be just as appropriate. For example, to produce more conservative estimates, it can be contended that the new-event fallout fraction should be higher than the analog-event fraction. However, this assumption would suggest that the unknown venting mechanism associated with the new event would probably have more thermal energy released with it and therefore eject additional debris. This assumption would have a significant bearing upon the cloud height.

FISSION+ YIELD

The fission+ yield parameters, Y and Y_p, for use with a containment-designed-detonation FOST application, are determined in the same manner as they are for use with cratering-detonation FOST applications (page 34). Both values are supplied by the national laboratory associated with the analog event and/or new event. Both of these values are classified.

DEBRIS-RELEASE TIME

As has been repeated many times, if the FOST is applied to containment-designed detonations, then the assumption has to be made that the particle-size and activity distributions of the new event are similar to the analog event. It is therefore important to note that the initial activity distribution of a containment-designed detonation is quite dependent upon the time-of-release of the debris. Time-of-release is not a factor in cratering detonations, since cratering debris is released almost instantly. The mix of fission products in a debris cloud which is released a few seconds after detonation would be quite different from that of a debris cloud initially released only a minute after detonation.

Because the mix is dependent on time and since the mix determines the debris-decay characteristics, the decay curve for a particular detonation is dependent on the time of release of the debris. Earlier, it was pointed out that for containment-designed-detonation estimates, it is assumed that the decay curve of the analog event is applicable to the new event. Therefore, it must follow that time of the release of the new event must be similar to that of the analog event.

The decay characteristics are also influenced by the duration of release. Hicks (Reference 4.4) made some theoretical radiochemical calculations of activity densities and exposure rates for NTS events that released radioactive debris

Table 4.2 Containment-Designed Releases

EVENT	DATE	PLACEMENT	CATEGORY	RELEASE
Blanca	581030	tunnel	A	PMV
Antler	610915	tunnel	D	PMV
Feather	611222	tunnel	A	PMV
Pampas	620301	shaft	B	PMV
Platte	620414	tunnel	B	PMV
Eel	620519	shaft	B	PMV
Des Moines	620613	tunnel	A	PMV
Bandicoot	621019	shaft	A	PMV
Yuba	630605	tunnel	F	S
Eagle	631212	shaft	A	PV
Pike	640313	shaft	A	PMV
Alva	640819	shaft	B	S
Drill	641205	shaft	E	S
Parrot	641216	shaft	D	S
Alpaca	650212	shaft	B	S
Tee	650507	shaft	C	S
Diluted Waters	650616	shaft	A	PV
Red Hot	660305	tunnel	F	PS
Pin Stripe	660425	shaft	C	PMV
Double Play	660615	tunnel	G	PS
Derringer	660913	shaft	D	PS
Nash	670119	shaft	F	S
Midi Mist	670626	tunnel	G	S
Umber	670629	shaft	D	PV
Door Mist	670831	tunnel	G	PS
Hupmobile	680118	shaft	C	PMV
Pod	690129	shaft	D	S
Scuttle	691113	shaft	D	S
Snubber	700421	shaft	C	S
Mint Leaf	700505	tunnel	G	S
Baneberry	701218	shaft	C1	PMV
Diagonal Line	711124	shaft	G	S
Riola	800925	shaft	F	S

PV = prompt venting PMV = prompt massive venting
S = seep PS = prompt seep

into the atmosphere. In his publications, exposure rates normalized to H+12 hr are shown from H+1 hr to H+50 yr. Such projections give a theoretical decay curve for each event presented. Included in this study was a group of containment-designed-detonation ventings. A list of these events is shown on the previous page in Table 4.2.

In this containment-designed group, Hicks found enough similarities that he divided the list into eight categories having common decay curves. Table 4.3 lists these categories. Notice in Table 4.2 that these categories are listed for each event. For example, the PIN STRIPE event, which was detonated in a vertical shaft, was assigned to category C, which indicates that it vented between H+30 sec and H+20 min and continued releasing for less than 2 hr.

Table 4.3 Hick's Categories

CATEGORY	DESCRIPTION
A	started before H+30 seconds, continued less than 15 minutes
B	started before H+30 seconds, continued more than 15 minutes
C	started between H+30 seconds and H+20 minutes, continued less than 2 hours
C1	Baneberry is a special case
D	started between H+30 seconds and H+20 minutes, continued more than 2 hours
E	started after H+20 minutes, continued less than 12 hours
F	started after H+20 minutes, continued more than 12 hours
G	effluent either seeped through cables or was filtered through the soil

If the decay curve for an analog event was found to be quite similar to the Hicks' theoretical-decay curve for that event, it should follow that any new event that was scaled to that analog would be expected to have a release time and duration similar to that described by the associated Hicks' category. Thus, if PIN STRIPE were the analog, any new event scaled to it should be expected to vent between H+30 sec and H+20 min and should continue to release for less than 2 hr.

POTENTIAL CONTAINMENT-DESIGNED-DETONATION ANALOGS

As pointed out in Chapter 1, there are few containment-designed-detonation ventings that can be used as analogs for the FOST. In relation to the total number of containment-designed detonations at the NTS, the number that released debris into the atmosphere is quite small.[6] Those that accidently released

[6]From August 5, 1963, (the beginning of the Limited Test Ban Treaty) until May 15, 1989, there were 486 announced nuclear detonations at the NTS. All but four of these were designed to be completely contained. Only 24 of the 482 containment-designed events released debris into the atmosphere in sufficient quantities to be detected offsite.

debris are listed in Table 4.2. Of these 33 events, 18 were seepages and 15 were ventings. As shown in the last column of this table, seepages and ventings may be categorized. These categories are defined below.

A ***venting (prompt venting***[7]) can be defined as a rapid release of radioactive debris that starts within minutes after the detonation but that does not continue for hours. In a venting situation, the major portion of radioactivity consists of very short-lived isotopes which are attached to or imbedded within soil particles. Many of these particles will fall on uninhabited test-range areas where they will decay to safe levels before personnel are allowed to reenter. A much smaller portion of these particles will fall on sparsely-populated areas adjacent to the test-range areas. However, by the time this debris reaches these offsite areas, it will have weakened considerably due to decay and will continue to decay rapidly once deposited.

A ***massive venting (prompt-massive venting***[7]***)*** is a release of relatively large amounts of radioactive material into the atmosphere. By the time it reaches an offsite location, the large amount of debris, though depleted by fallout and weakened by decay, can still cause high exposures in those areas for relatively short periods. With a massive venting, populations near the test-range borders may have to be sheltered or evacuated while the deposited debris decays to acceptable levels.

A ***seepage*** can be defined as a very slow release of relatively small amounts of radioactive debris per unit time into the atmosphere for hours to perhaps days. In general, the fraction of short-lived isotopes released in association with a seepage is quite small. Most of the release is composed of the inert gaseous radionuclides of xenon, krypton, and iodine.

A ***prompt seepage*** is a seepage that begins at a relatively early time after detonation. In such a seepage, there would probably be a significant amount of short-lived isotopes released initially, but the majority of the total release would be the inert gaseous nuclides of xenon, krypton, and iodine.

As pointed out earlier (page 7), the Test Controller is primarily interested in a maximum-credible-prompt-massive-venting scenario upon which to base his public-safety decisions. As shown in Table 4.2, there have been only 12 prompt-massive ventings. Five out of these 12 were associated with tunnel detonations and the rest were associated with vertical-shaft detonations.

---

[7]The terms, "prompt venting" or "prompt-massive venting," are commonly used. However, according to the definition of venting, the word, "prompt," is redundant.

Thus, there are only twelve potential containment-designed-detonation analogs to use with the FOST. Theoretically, the analog should be applicable to new events detonated in similar geological media. Therefore, in theory, there should be at least one analog for tunnel detonations and one analog for vertical-shaft detonations.

TUNNEL ANALOGS

Of the five potential tunnel analogs, only three of them, ANTLER, PLATTE, and DES MOINES, have the necessary radiological data and proper meteorological characteristics to qualify as appropriate FOST analogs.

But, as pointed out in Chapter 1, the Test Controller is interested in a ***credible*** venting scenario.[8] Notice that all five of the prompt-massive ventings occurred in the late 1950s and early 1960s when containment-design techniques for tunnel detonations were being developed. Since it is ***highly*** unlikely that a new tunnel detonation would vent in the manner as these early events, none of the analogs are presently considered credible.

VERTICAL-SHAFT ANALOGS

As shown in Table 4.2, there have been only 7 containment-designed-vertical-shaft-prompt-massive-venting episodes, PAMPAS, EEL, BANDICOOT, PIKE, PIN STRIPE, HUPMOBILE, and BANEBERRY. The characteristics of each of these events are as follows:

PAMPAS AND HUPMOBILE

Mostly volatile gases were released in association with the PAMPAS and HUPMOBILE events. As a result, there was little fallout produced. Since the FOST is based upon deposition (not cloud passage), neither one of these ventings can be considered appropriate FOST analogs.

BANDICOOT

The BANDICOOT event produced a significant amount of fallout. However, there was a very large amount of wind shear associated with it. As discussed earlier, the FOST does not handle situations with a large amount of wind shear. Thus, the BANDICOOT analog is not appropriate to use with the FOST. This is not a shortcoming, since BANDICOOT was not the maximum-case scenario.

---

[8]If the Test Controller were interested in the <u>maximum</u>-prompt-massive-venting scenario (including both tunnels and vertical shafts), the DES MOINES analog would be used.

EEL

The EEL event also produced a significant amount of fallout. However, by the time that the FOST was first utilized, the PIKE event had already occurred. Since greater exposures were observed in association with PIKE then with EEL, the EEL analog was always less conservative and, therefore, has been passed over in favor of PIKE. Although the EEL analog has not been utilized, it is an appropriate FOST analog.

PIKE AND PIN STRIPE

As has been pointed out, the PIKE event has been the analog of choice from the beginning of the FOST. Details about this analog are presented in the next chapter.

The PIN STRIPE event occurred nearly two years after PIKE. The pre-event exposure estimates for PIN STRIPE were derived using the FOST with the PIKE analog. Figure 4.3 shows the observed PIN STRIPE H+1 hr exposure-rate-versus-distance curve (solid line) that was derived from the PIN STRIPE fallout-pattern analysis.

An idea of the performance of the FOST as applied to containment-designed detonations can be gained by comparing this observed PIN STRIPE curve with that of a curve resulting from using the PIKE analog in the FOST with the observed PIN STRIPE radiological and meteorological parameters.[9] This curve ("SCALED PIN STRIPE") is shown in Figure 4.3. Notice, in general, that the FOST slightly underpredicted exposure-rate values. However, it is encouraging to note that the FOST did so well. In fact, this relatively small difference is quite surprising considering that the two events did not vent in the same manner.

Also shown in Figure 4.3 is the H+1 hr exposure-rate-versus-distance curve for the PIKE event. Note that, in general, the PIN STRIPE exposure rates were equal or greater than those of PIKE out to about 15 mi, but that the PIKE exposure rates were larger at distances from 15 mi out to about 100 mi. These small differences could be considered insignificant and in the "noise level." Thus, the PIN STRIPE analog may be just as conservative as the PIKE analog. However, there are several reasons why the PIKE analog may not have been replaced by the PIN STRIPE analog. The first might be that the higher exposure rates at greater distances associated with PIKE would mean that PIKE would provide slightly more conservative estimates for offsite populations. Secondly, for many years, the PIN STRIPE decay rate was thought to be $t^{-1.4}$ and the PIKE decay rate was thought to be $t^{-1.2}$. This difference would mean that the PIN STRIPE debris would decay faster, and,

[9]The PIN STRIPE exposure-rate curve presented to the Test Controller prior to the detonation could be shown in Figure 4.3, but a comparison of this curve with the observed curve would not necessarily show the performance of the FOST but the performance of the meteorological forecast. Using the observed parameters eliminates this problem.

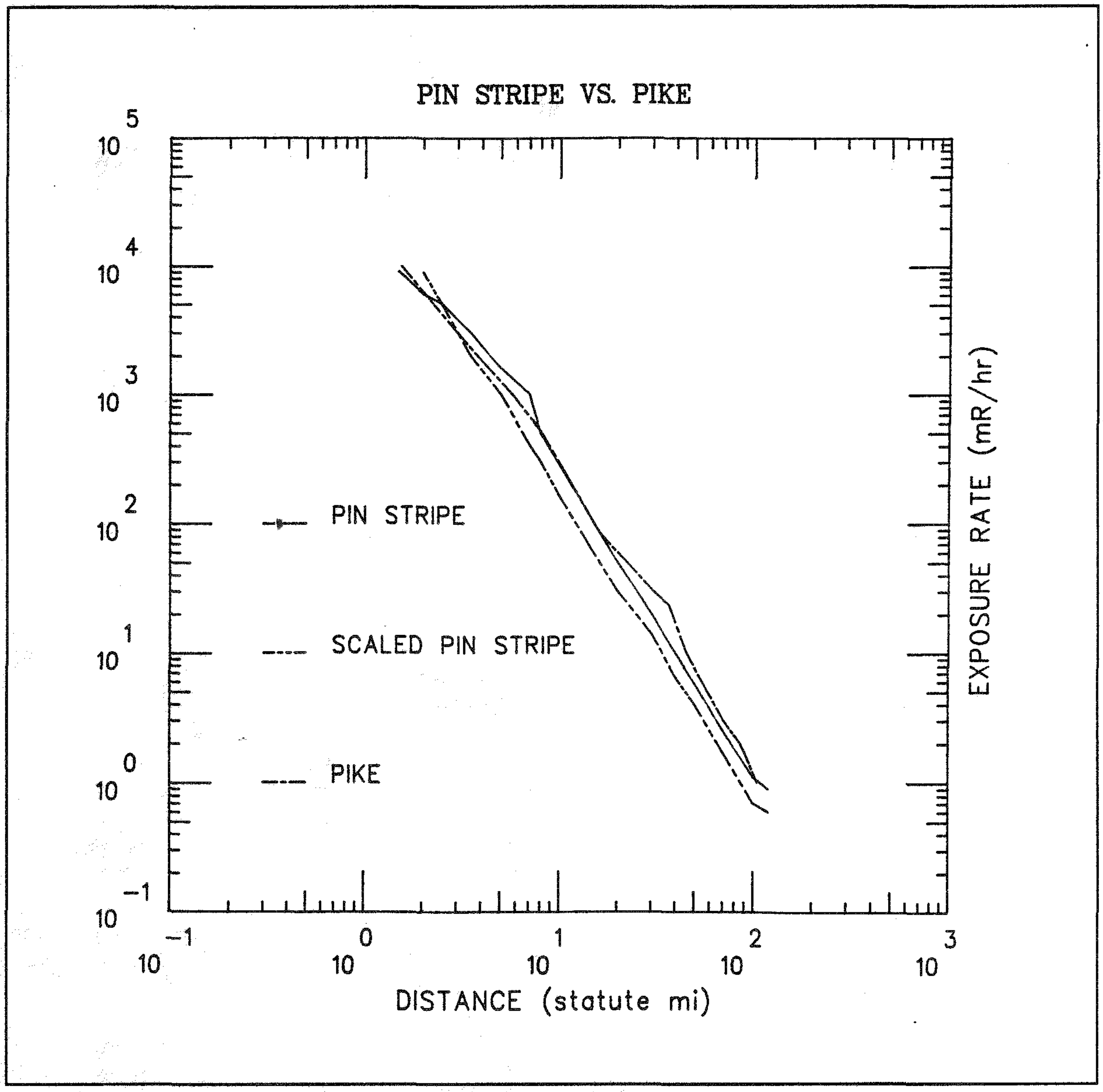

Figure 4.3 PIN STRIPE and PIKE Exposure-Rate-Versus-Distance Curves

therefore, the PIN STRIPE exposures would be less than those of PIKE. Finally, since there was really not that much difference between the two analogs, the PIKE analog may have been retained for its familiarity.

BANEBERRY

There is no doubt that the BANEBERRY event released a massive amount of radioactive debris into the atmosphere. In terms of curies released (normalized to H+12 hr), PIKE had 120,000 while BANEBERRY had 6,700,000, which is about 55 times greater. However, while BANEBERRY released a massive amount of debris, its release characteristics do not match what was defined as a ***venting*** earlier in this chapter (starts within minutes after the detonation but ***does not*** continue for hours). The release commenced at H+3.5 min and continued strongly until H+16.5 min, the time of the surface collapse. The effluent-venting rate decreased steadily thereafter but visible vapor continued to emanate from the fissure for 24 hr after the detonation. These characteristics along with some other factors described below prevent the BANEBERRY event from becoming a FOST analog.

Neither a BANEBERRY fallout pattern or an exposure-rate-versus-distance curve could be constructed due to a lack of offsite ground-survey measurements in large areas of the fallout sector. The lack of positive measurements is usually attributed to the heavy snowfall that commenced shortly after the debris had been deposited. It has been proposed that this deep snow cover evidently attenuated the energy reaching the survey meters.

Disappointment has sometimes been expressed in not having a BANEBERRY analog since it is believed that if there was one and it was used in making exposure estimates, it would produce more conservative estimates than those derived from the PIKE analog. This argument is usually centered around the fact that BANEBERRY released so many more curies into the atmosphere than PIKE. It is sometimes suggested that the PIKE analog should continue to be used but with a fallout fraction (f) based upon some type of relationship between the curies released with BANEBERRY to the curies released with PIKE. For example, instead of (f_p/f) being set to 1 as is the normal case, it is suggested that it be set to 55, or whatever the most appropriate number would be that would reflect a PIKE-type venting with a BANEBERRY-type total release.

It must be noted, however, that the BANEBERRY debris were released at a much later time than the PIKE debris (3.5 min versus a few seconds) and the duration of release was much longer (24 hr versus 1 min). As a result, the BANEBERRY debris were probably composed of a much larger fraction of noble gases. Consequently, a significant portion of the curies released were in association with gases that did not become part of the local fallout.

Thus, it may be postulated that one of the reasons that higher survey-meter readings were not detected in the offsite areas was due to the fact that relatively little fallout was deposited since the debris was more gaseous in nature. Thus, it is possible that the ***local*** fallout from BANEBERRY may not have been greater than that associated with the PIKE event.

In addition, as shown in Figure 4.4, the theoretical BANEBERRY decay curve shows a much higher rate of decay after about H+50 hr than the theoretical PIKE decay curve. Thus, this difference would imply that if the BANEBERRY H+1 hr exposures were equal to or even slightly higher than PIKE H+1 hr exposures, the Total-First-Year Exposure at a particular location might still be higher in association with PIKE.

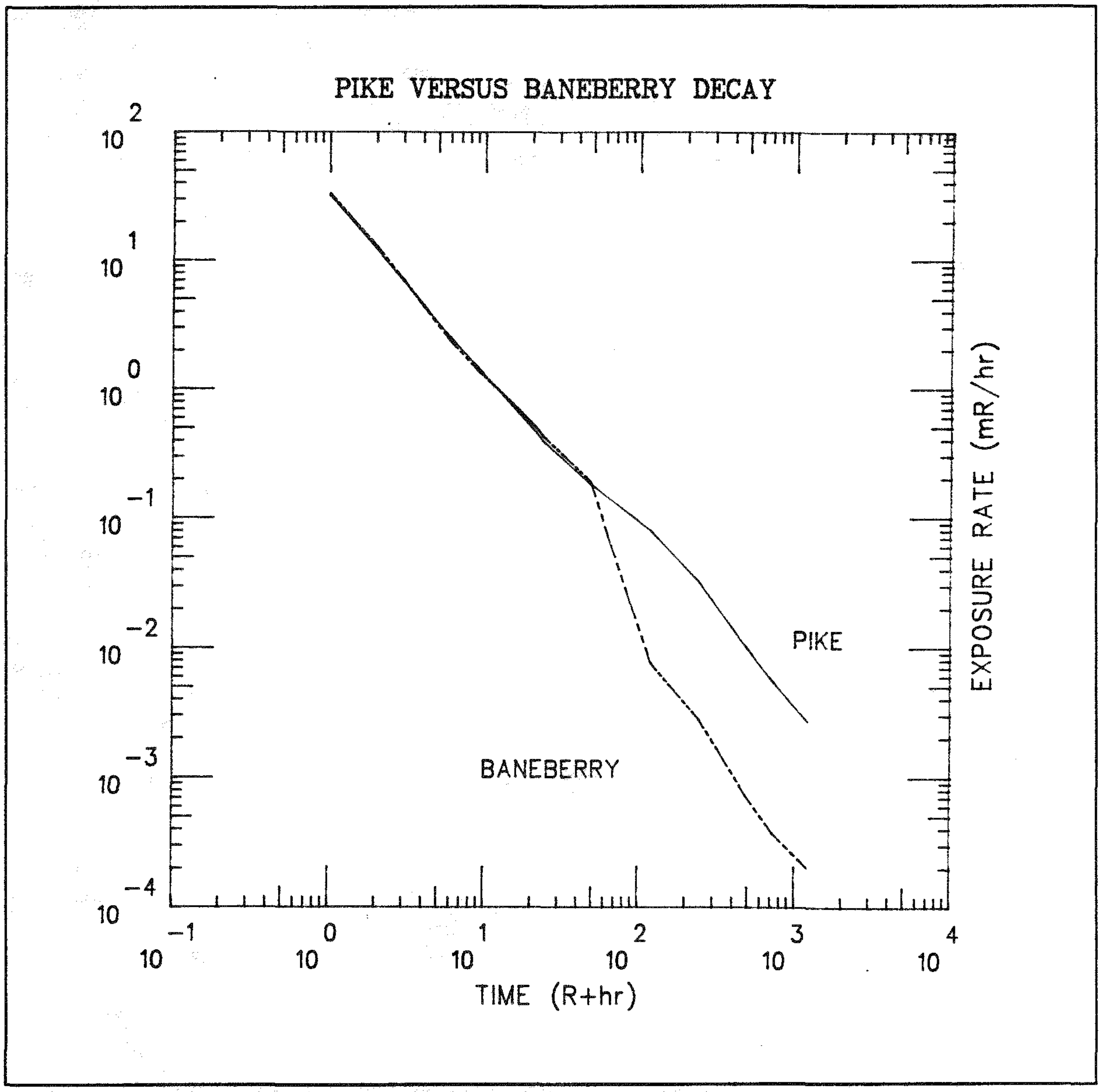

Figure 4.4 Theoretical PIKE and BANEBERRY Exposure-Rate-Versus-Time Profiles

In conclusion, since the FOST was first utilized in the spring of 1964, the PIKE event has been the primary analog. Its use with the FOST definitely provides more conservative estimates than four of the six other possible analogs. In addition, it provides estimates slightly more conservative than the PIN STRIPE analog. Finally, it is possible that the PIKE analog might provide more conservative estimates than could a model based upon BANEBERRY data.

METEOROLOGICAL ASPECTS

As a part of the safety program associated with nuclear testing, the WSNSO maintains a network of surface- and upper-air-meteorological observational sites. At the present time, surface data (wind, temperature, humidity, pressure, and precipitation) are routinely collected every 15 minutes from over 40 remote weather sensors positioned primarily on the NTS but also scattered around areas adjacent to the NTS. Hourly surface-weather observations and 6-hourly upper-wind observations are routinely made at the Desert Rock weather station at the south end of the NTS. The Desert Rock station is part of a network of observatories positioned across the nation, which relay their data not only to the NTS but to the National Meteorological Center where the data are quickly analyzed and utilized in sophisticated prognostic models, which are available to WSNSO.

Meteorological observations are increased in association with nuclear detonations. Upper-wind observations are typically made by mobile units at 7 to 8 locations on and around the NTS. These observations are made at hourly or half-hourly intervals starting 6 hours prior to the scheduled detonation and lasting until at least a couple of hours after detonation. The weather station on Yucca Flat in the central part of the NTS is activated prior to detonation, providing hourly or half-hourly upper-wind observations and upper-air (wind, temperature, and humidity) observations as needed.

If there is an accidental venting, the locations of the mobile units are adjusted to provide the best possible coverage, and observations continue as long as there is a need. The radiation briefer utilizes this vast amount of meteorological data along with the radiological data to estimate the path of the debris and the exposures that downwind populations might receive.

All these data are archived and can be used to construct a FOST analog. While the quantity of meteorological data may have been somewhat less in the 1960s than at the present time, the basic observational structure as described above was in place then. Thus, for each of the massive ventings, there exists large amounts of surface- and upper-air meteorological data. The meteorological parameters used in the FOST are derived from these data.

SCALING PARAMETERS

To utilize equation 4.1 to get a value for the H+1 exposure rate, $ER1_p$, at downwind distance, X_p, one has to input the six meteorological parameters, H, H_p, V, V_p, α, and α_p. The methods of determining these parameters are discussed below.

CLOUD HEIGHTS

In equations 4.1 and 4.2, H and H_p represent the total cloud heights of the analog and new events, respectively. These are the heights above the ground at which the debris cloud tends to stabilize (the height at which the vertical growth associated with the device's thermal energy stops). However, cloud height will increase slowly for many hours after it stabilizes. That portion of the cloud that continues to grow vertically is primarily composed of gases and small particulates that will become part of world-wide fallout and not part of the local fallout. Since the FOST predicts local fallout, the cloud heights needed for the equations are the stabilized heights. The analog cloud height, H, is derived from aerial measurements. Currently, cloud-tracking aircraft, before each detonation, are airborne and are positioned slightly upwind from GZ. Video cameras in at least one of these aircraft are pointed directly at GZ from the time the aircraft is in position until a time well after detonation when it is evident that there could no longer be a massive venting. Thus, if there is a venting, there is good documentation on the visual characteristics of the debris cloud. From such visual records along with observations by the crew of the cloud-tracking aircraft, it is possible to determine the stabilized cloud height used in the analog.

The forecast height of the new-detonation cloud, H_p, is an important parameter in determining both where debris will be deposited and how much will be deposited. If the height of a cloud is underpredicted, there is a chance that debris may fall on a populated area that was not included in the projected fallout pattern. For example, the thermal energy associated with a particular debris cloud may be insufficient to penetrate a temperature inversion[10] based 2500 ft above the surface. If the winds below 2500 ft were light southwesterly (blowing from the southwest toward the northeast), then a debris cloud below 2500 ft would be forecast to be transported northeastward over sparsely populated areas. However, if the venting involved much more thermal energy and if the debris cloud did penetrate the inversion, it could rise several thousand feet higher than predicted (as was the case with the BANEBERRY venting). If the winds above 2500 ft were strong northwesterly instead of light southwesterly, then the top portion of the debris cloud would be rapidly transported toward the Las Vegas area. Though the Las Vegas area would probably be spared from fallout in such a situation (the cloud passes overhead without depositing radioactive debris), populated areas to the north or northeast of Las Vegas (Alamo or Glendale) could receive fallout.

An underpredicted cloud height also affects exposures. For example, consider the above situation but instead of the winds above 2500 ft being strong northwesterly, they were strong southwesterly. First, consider the predicted exposures. They would have been relatively small in offsite areas since (1) much of the debris, which was expected to remain relatively close to the ground, was expected to fall on onsite areas, and (2) the debris that was to reach the offsite areas was expected to decay considerably before being deposited. Next, consider the actual exposures if the debris cloud unexpectedly penetrated the inversion and was transported in the strong southwesterly winds. The exposures in offsite areas would be higher than forecast. This condition would result since (1) a large portion of the cloud, which would be carried much higher and which would have much farther to fall, would fall offsite instead of onsite, and (2) the debris, which would reach the offsite areas much sooner in the stronger flow, would not have as much time to decay before being deposited.

---

[10]Temperature inversions will be discussed in Chapter 5.

The two examples discussed above demonstrate the importance of making a correct cloud height prediction, not only in conjunction with the FOST but also with any fallout prediction technique or model. Unfortunately, it is as difficult to predict the cloud height for a proposed containment-designed detonation as it is to predict the particle-size and activity distribution.

If the quantity and release rate of the thermal energy associated with the venting were known, then it would be theoretically possible to predict the cloud height accurately based upon atmospheric-thermodynamic principles. But, the quantity and release rate are a function of the venting mechanism. And, as pointed out earlier, the venting mechanism can not be predicted accurately.

The solution to this problem has been to assume that the quantity and release rate of the new event's thermal energy is the same as that associated with the analog event. This assumption allows the stability of the atmosphere to be the determining factor in deriving the cloud height. Thus, if the predicted atmosphere for the new event is more stable than that of the analog event, then the new cloud would not rise as high, or if the predicted atmosphere for the new event is more unstable than that of the analog event, then the new cloud would rise higher than the analog cloud.

Even though the cloud height problem has been simplified by the above assumption, the quantity of thermal energy released with any analog event remains unknown. However, rough estimates of this energy associated with several ventings was derived by WSNSO by using equations designed to determine cloud rise (Reference 4.5). Since the cloud rise of an analog event was known from observations, these equations were solved for those parameters related to the amount of thermal energy released. Once the amount of energy was derived for a particular analog, the cloud height of a new event could be estimated using the same equations and assuming that the thermal energy released with the new event was the same as that released with the analog event.

A WSNSO objective cloud-rise technique (CLOUD), which is based upon the above procedure, has been available for many years. This program, which accepts the predicted pressures, temperatures, and wind speeds for appropriate levels within the expected debris cloud, predicts cloud rise for unstable and stable conditions and predicts whether the debris cloud will break through temperature inversions. Unfortunately, the performance of this technique can not be completely evaluated since there have been so few massive ventings. The WSNSO radiation briefers utilize the output from this technique only for guidance. The final cloud height estimate is primarily based upon subjective decisions made by the briefer. The next chapter presents details on how the new-event cloud height is determined in association with the PIKE analog.

AVERAGE WIND SPEEDS

In Chapter 3, V and V_p were defined as the average speeds along the resultant transport bearing from the surface to the mid-altitude of the debris cloud for the analog event and new event, respectively. Figure 3.2 (page 33) can be used to show why Cluff and Palmer (Reference 1.1) chose to use the average speeds along the resultant transport bearing from the surface to the mid-altitude of the cloud instead of from the surface to the top of the cloud.

If the wind hodograph shown in this figure represented the winds through the depth of a 6000-ft debris cloud (there are six 1000-ft layers and six associated wind vectors), then a line drawn from GZ to the head of the third vector from GZ would describe the deposition path of all those particles (regardless of size) positioned at 3000 ft at the time of cloud stabilization. The average transport speed of any of the particles initially at 3000 ft during their period of descent to the ground could be determined by dividing the length of the vector extending from GZ to the head of the third vector by three.

Cluff and Palmer assumed that the debris centerline results from the deposition of particles which originate from the center of the cloud. Such an assumption appears reasonable for cratering-event ventings. Thus, in Figure 3.2, the centerline would correspond to the deposition path of the 3000-ft particles.

In the actual utilization of the FOST, a modification was made to the method presented by Cluff and Palmer. For many years, radiation briefers have computed V and V_p using the winds from the surface to the *top* of the debris cloud. For example, in Figure 3.2, the average speed would be calculated by dividing the vector extending from GZ to the head of the sixth vector by six. The resultant value gives the mean transport speed of any particle that was at the top (6000 ft) of the cloud at the time of stabilization. Those particles would be deposited along the path (H_H) extending from GZ through the head of the sixth vector.

In deriving the position of the centerline, radiation briefers generally use the bearing indicated by the vector extending from GZ to the mid-altitude of the cloud, as proposed by Cluff and Palmer. It therefore seems inconsistent that they should use the average speed based upon the vector extending from GZ to the top of the cloud. Using the top of the cloud for calculations would imply that exposure calculations were being made for the edge of the fallout pattern, but that is definitely not the case. When there is little wind shear, the average speed would be approximately the same whether the mid-altitude or top of the cloud was utilized. Only in those cases where there is a large amount of shear above the mid-altitude of the cloud would there be a significant difference. Perhaps this situation evolved from the practice of estimating cloud-arrival times (TA). If there was little wind shear through the depth of the cloud, then the average speed calculated to the mid-altitude of the cloud would give a good indication of when the cloud would arrive at a particular downwind location. For example, if the winds were 5 mi/hr through the depth of the cloud, then the cloud-arrival time at a location 20 miles from GZ would be 4 hr.

However, if there were much faster speeds above the mid-altitude of the cloud, then an average to the mid-altitude would not be representative of the cloud arrival time. For example, if the winds were 5 mi/hr below the mid-altitude and 35 mi/hr above the mid-altitude, then it would take much less than 4 hours for the cloud to get to the downwind location. An average of the wind speed throughout the entire depth of the cloud (20 mi/hr) would be a more representative estimate of the cloud-arrival time.

Presently, radiation briefers use the average wind speed calculated to the top of the cloud, and mark "arrival times" along the predicted debris centerline based upon this speed. The use of an average wind speed in this manner may be appropriate, but it is questionable whether the same speed should be used in the FOST calculations. Of course, if the major portion of the debris was associated with the upper portion of the cloud, then it would be proper to use the entire depth of the cloud for determining the average wind speed.

Regardless of the reasons why the method of calculating the average wind speed was changed, the fact remains that V and V_p are presently based upon the winds from the surface to the top of the cloud. The average wind speed for an analog event, V, is calculated by plotting wind hodographs using the observed winds collected in association with that event. Average wind speeds from the surface to the top of the cloud are then derived from these hodographs as discussed above. The resulting wind speeds are then analyzed to determine one appropriate value that would be representative of the analog. The next chapter will detail how average wind speeds are calculated for a new event.

SHEAR ANGLES

As discussed in Chapter 3, α and α_p, are the total directional shears in the fallout hodographs of the analog event and new event, respectively. In general, the calculations are made in the same manner they would be for a cratering detonation.

For the analog, the most representative fallout hodograph is plotted and a fallout sector, as defined in Chapter 2 is determined. This can be exemplified by Figure 3.2 (page 33). Note that the fallout sector is defined by radials H_H and H_L, which extend from GZ. The shear angle is the angle between these two radials, α. A similar procedure is preformed to derive the shear angle for the new event. Of course, the hodograph in this case is based upon predicted winds instead of observed winds.

It was pointed out earlier that Cluff and Palmer stipulated that FOST solutions were only realistic when the total variation in wind direction with altitude is less than 90°. It is important to realize that you can have a total variation greater than 90° with α less than 90°. Please examine Figure 3.2 once again. In this example, the winds vary from 230° at the surface to 140° at the top of the cloud, which is a total variation of 90°. However, while the total variation is 90°, α is only about 55°.

Unfortunately, a total variation in wind direction with altitude of over 90° frequently occurs at detonation time at the NTS. Such large wind shears often result from a shallow northerly drainage flow at the surface and southerly flow aloft.

Though the total variation can be greater than 90°, the FOST is still employed since the debris associated with that shallow layer can usually be considered insignificant in relation to the total amount of debris in the cloud. While the fallout-sector prediction might show some debris carried toward the south in this drainage flow, the exposure estimates along the centerline would be based upon a hodograph which essentially ignores the winds in the drainage layer.

There are occasionally times when the total variation of the winds with altitude is greater than 90° and the large shear angle is not due to drainage flow. This condition is associated with relatively light winds; however, it can occur even with moderate wind speeds. Technically, centerline-exposure estimates using the FOST should not be considered valid in these situations. However, there are still those who want to examine such estimates. Thus, if the total variation of the winds with altitude is greater than 90° but the wind shear angle, α, is less than 90°, then the radiation briefer can use this shear angle in the FOST, but he should express a lack of confidence in the resultant estimates.

A wind shear angle greater than 90° should never be used in the FOST. If there is more than 90° of shear, then there are usually multiple centerlines. In such a situation, the radiation briefer would show what he considered to be the primary centerline on his fallout chart. It would most likely be associated with the lower part of the cloud. It would be up to his discretion if he wanted to show the additional centerline(s) on his chart.

For example, consider the situation where the bottom half of a debris cloud is transported toward the north-northeast and the top half is transported toward the south-southeast. In this case, as shown in Figure 4.5, the shear angle (AZB) associated with the bottom half of the debris cloud is 30°, the shear angle (CFD) associated with the top half is also 30°, and the shear angle (AZE) associated with the entire cloud is 120°. At the time of cloud stabilization there would likely be two clouds, as shown in the hatched areas in the diagram to the right.

The debris centerline associated with the north cloud would extend along the radial ZG. All the debris associated with the north cloud would remain in the fallout sector between the radials ZA and ZB. Thus, there would be 30° of shear associated with this sector.

All of the debris associated with the south cloud would be deposited in the fallout sector between the radials ZB and ZE. (Remember, even though the cloud sector lies between ZC and ZD, the debris would eventually fall to the ground toward the northeast due to the southerly winds in the lower layers.) Thus, there would be 90° of shear associated with this sector. Initially, there might be a secondary debris centerline associated with the south cloud extending along the radial ZH. Eventually, however, as the two clouds became separated by more and more distance, this secondary centerline would disappear and the debris associated with the south cloud would be spread over a very wide area.

The main concern would be the highest downwind exposures. These would not be associated with the south cloud since it was spread over a large area, but would be found along the north-cloud centerline, ZG. To get an estimate of the exposures along this centerline, it might be assumed that half of the local fallout would be deposited as a result of the debris in the north cloud. If that were the case, then the fallout fraction, f_p, could be halved, the shear angle, α_p, could be set to 30°, the cloud height, H_p, could be selected as the mid-

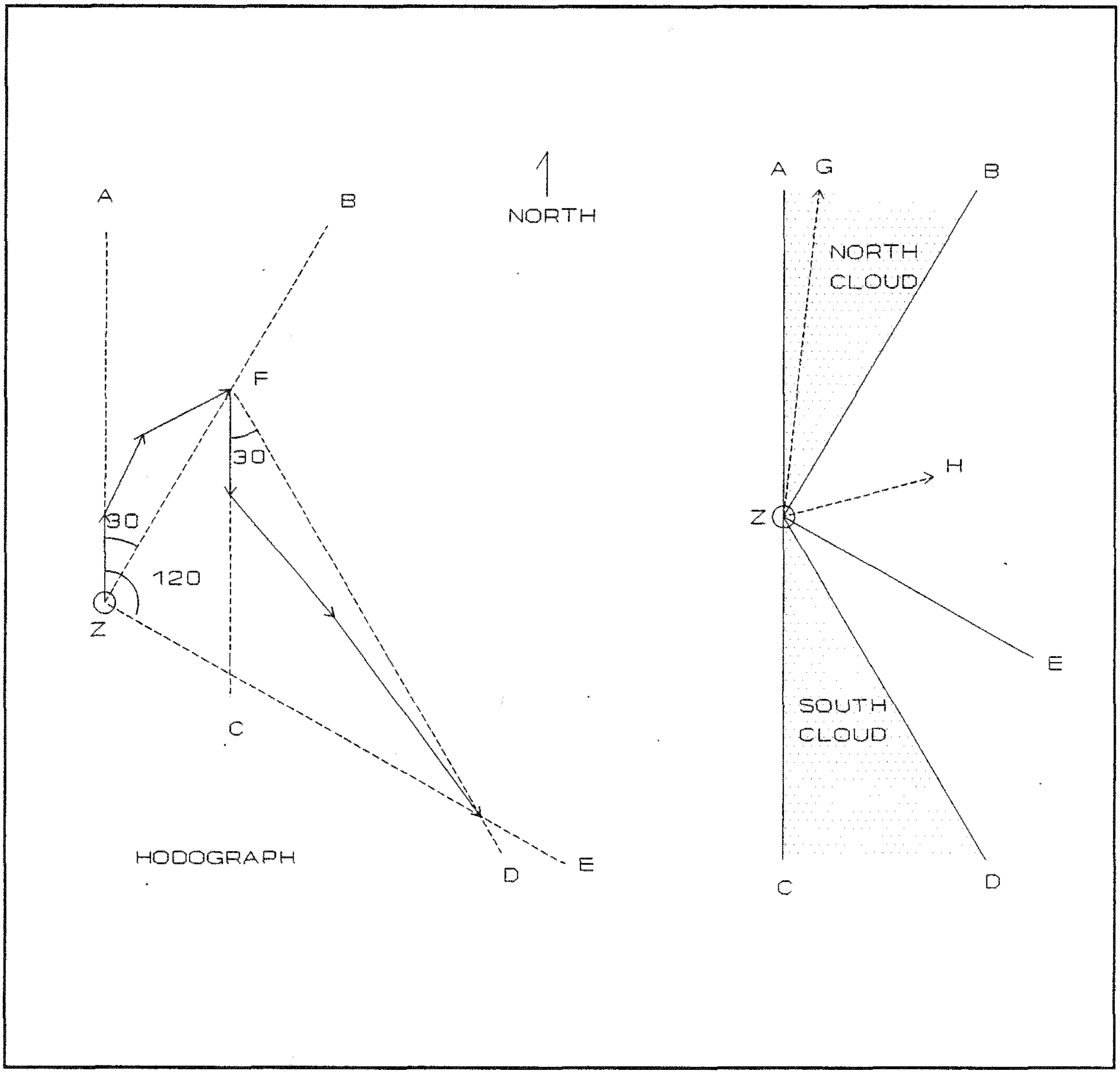

Figure 4.5 Split-Cloud Hodograph

altitude of the total cloud, and the average wind speed, V_p, could be based upon the winds from the surface to the mid-altitude of the cloud.

Such complex situations have to be considered on a case-by-case basis. Those utilizing exposure estimates based upon wind predictions producing large shear angles should be aware of the uncertainties involved.

VARIABLE PARAMETERS

In the derivation of the FOST, it was implied that the winds did not vary in time or space. That is, there is only one fallout hodograph associated with the analog event. However, winds not only vary in time and with height at a particular location, but also change as the cloud moves from location to location due both to atmospheric features (e.g., high and low pressure systems) and to terrain effects (e.g., channeling between mountain ranges). Thus, if there are large, abrupt changes in the wind flow as the cloud moves downwind, then that particular situation has limited application as a suitable FOST analog.

In a strict sense, it is not appropriate to have large changes in the wind flow associated with the new event. In the FOST, it would be completely unrealistic to base a set of new-event meteorological parameters upon averages of highly variable wind speeds or shear angles. For example, if V_p and α_p were 5 mi/hr and 50°, respectively, at H+1 hr and had changed to 25 mi/hr and 20° by H+8 hr, it would not be appropriate to input means of 15 mi/hr and 35° into the FOST.

Perhaps, it may be argued that if the winds were expected to change in such a significant manner, it would be most appropriate to input a wind speed and shear angle of 5 mi/hr and 50°, the initial set of parameters. At least, the estimates at close-in distances would be fairly reliable. Those estimates for distant locations, which would be unreliable since the wind conditions would change before the cloud arrived at those locations, could then be judged in a qualitative sense to determine if it was likely that the exposures there would be higher or lower than indicated. In this case, they would be much higher.

A more quantitative estimate of exposures at these distant locations could be gained by calculating the exposures there using V_p and α_p values based upon the winds at the time the cloud arrived at that location. Thus, in the above example, if the cloud had arrived at a downwind distance at H+8 hr when the wind speed was 25 mi/hr and the shear angle was 20°, then those values could be used to calculate the exposures at that location. Of course, such values would be too high since the debris did not arrive at that location as quickly as indicated by the 25 mi/hr speed.[11] (There would have been more decay of the debris before it arrived.) Also, such values would be too high since the shear angle of 20°, while representative of the winds at the time of arrival, would not be representative of the spread of the cloud, which was initially affected by shear angles of 50°.

---

[11]At first glance at Equation 4.1, the opposite effect might seem to be true (the exposure rate would be lower with an increased new-event wind speed), because $ER1_p$ is inversely proportional to the square of the new-event average wind speed, V_p. However, one must also look at the effects of Equation 4.2. According to this equation, an increased V_p produces a smaller value of X. A smaller value of X produces a greater value of ER1. The increase in ER1 in Equation 4.1 produces an increase in $ER1_p$ that is greater than the decrease in $ER1_p$ that was caused by the increase in V_p in that same equation.

Getting such quantitative "approximations" for distant locations when the meteorological parameters change significantly with time and/or distance has been the practice of WSNSO for many years. This avoids either having to deal with unrealistic mean values or having to abandon the FOST for exposure estimates at distant locations.

In this technique, a value is determined for H_p, V_p, and α_p for each hour from H+1 to H+10 hr. In the notation that will be used in the remainder of this report, a number in parenthesis immediately following one of the meteorological parameters signifies the hour for which that parameter applies. For example, $H_p(2)$ would signify the cloud height from H+1 to H+2 hr, and $V_p(10)$ would signify the mean wind speed from H+9 to H+10 hr. It is assumed that the meteorological parameters remain the same after H+10 hr.

There are several restraints in varying the parameters. While it is possible to vary H_p with time, this variable is usually kept constant. It has already been pointed out that since the FOST estimates are based upon those particles that become a part of the local fallout, it is not appropriate to increase the height of the cloud with time since that portion of the cloud is associated with particles that do not contribute to local fallout. Furthermore, based upon the assumptions used in the derivation of the FOST, it is not appropriate to decrease the height of the cloud with time.

The only time that H_p is varied is when a venting occurs in association with a detonation buried at a location at a relatively high altitude.[12] In such situations, the depth of the cloud would increase as the cloud moved away from the higher terrain and over the adjacent valleys. For example, if surface GZ was at 7500 ft MSL and there was a venting in which a cloud stabilized at 4000 ft AGL, then H_p would initially be equal to 4000 ft. But, if the cloud had moved over a valley with a floor at 4500 ft MSL by H+2 hr, then $H_p(2)$ would be set to 7000 ft.

In the variable parameter technique, α_p can be increased with time but not decreased. There are times in reality when the shear angle may actually decrease with time. For example, consider a relatively low-level debris cloud flowing down a valley bordered by two tall mountain ranges that are converging at the end of the valley toward which the debris is flowing. While some of the debris would strike the sides of the mountains, other debris would be forced inward toward the center of the cloud. This situation could be described by a decreasing shear angle. Though such situations occur, they are usually infrequent, are much more complex than described here, and can not be handled appropriately by the FOST technique. Thus, α_p is not decreased with time.

EXPOSURE CALCULATIONS

At the beginning of this chapter, the two basic equations for computing estimates of exposures in association with containment-designed detonations were

---

[12] On the NTS, such ventings would be in association with tunnel detonations in Area 12 and with detonations under the mesas in Areas 19 and 20.

presented (equations 4.1 and 4.2). After this presentation, it was shown how each of the parameters within these two equations can be derived. At this point, we should now have the ability to compute an H+1 hr exposure rate, $ER1_p$ for a particular downwind distance, X_p. It is now necessary to turn this exposure-rate value into an exposure.

PEAK-EXPOSURE-RATE TIME

If $ER1_p$ for a particular downwind location, X_p, is derived using equations 4.1 and 4.2, it is then necessary to know the value of TP, the time of the peak exposure rate at that location, in order for exposures to be derived for that location. Instead of determining a value for X_p and then finding the appropriate value of TP for that location, it is more convenient to first consider a particular value of TP and then determine the location.

For example, what centerline location at H+1 hr would be experiencing its peak exposure rate? If the distance from GZ to that location (X_p) could be found, then the value of TP would be known (H+1 hr) and the value of $ER1_p$ could be derived at that location using equations 4.1 and 4.2. Thus, the various exposures (e.g. TYE) could be calculated at X_p.

To find this distance, let it be assumed that the peak-exposure rate along the centerline occurs as a function of the average wind speed, V_p, and the time after detonation. Let it first be assumed that if V_p remains constant with time and space, then the distance to the centerline location where TP is occurring can be defined by:

$$X_p(TP) = V_p \, TP \qquad (4.7),$$

where,

$X_p(TP)$ = the downwind centerline distance at which the peak exposure rate is occurring at time, TP,

TP = an arbitrary peak-exposure-rate time, and

V_p = a constant average wind speed.

For example, if the mean wind speed was 10 mi/hr and if we wanted to calculate exposures at the centerline distance where the peak exposure rate occurred at H+2 hr, then using equation 4.7, we would find that the distance where the peak-exposure rate occurred at H+2 hr was 20 mi downwind from GZ. Thus, since both the analog-event and new-event scaling parameters are known, $ER1_p$ could be calculated for this distance. Once $ER1_p$ had been calculated, the exposures could be calculated by integrating under the decay curve utilizing TP as the reference time.

Consequently, if a list of arbitrary TPs was selected, then it would be possible, using the above equation, to determine a corresponding list of X_p's and to compute exposures for each of these distances. An exposure-versus-distance curve could then be constructed, which would allow determination of exposures at any downwind distance along the curve.

Of course, the assumption that the mean transport speed remains constant with time is invalid if we utilize variable parameters, so the computation of X_p(TP) becomes more complicated than indicated in equation 4.7. The method of handling variable parameters in this situation is presented in Chapter 6.

BEST-FIT EXPOSURES

Under normal circumstances, exposures along the centerline would be expected to decrease with distance from GZ. In fact, new-event exposure estimates based upon an analog in which the exposures gradually decrease with distance would definitely be expected to decrease gradually with distance too. However, if variable parameters are employed in the FOST, the resultant exposures rarely result in a smooth curve decreasing with distance. In some cases, these exposure estimates actually increase with distance, though very slightly.

In the discussion above on variable parameters, it was pointed out that once the parameters are varied, then those downwind estimates based upon the varied parameters become more approximate in nature. Thus, at these locations where the exposures may be considered approximations, it is just as appropriate to use these approximate values to construct a best-fit curve as it would be to draw lines from point to point. In fact, a best-fit curve might be a better solution since it smooths out some of the unnatural discontinuities brought about by abruptly changing the meteorological parameters each hour.

Up until the time when the exposure-versus-distance curves were produced entirely by machines, the radiation briefer plotted the exposures and then, using a French curve, drew a smooth curve to those values. The smoothing technique utilized in the present-day computer programs will be discussed in Chapter 6.

CHAPTER 5

THE PIKE ANALOG

The PIKE event, which was part of Operation NIBLICK, was a containment designed underground nuclear weapon experiment conducted on Friday, March 13, 1964, by the Los Alamos Scientific Laboratory in Area 3 (U3cy) of the Nevada Test Site (NTS). Ten to fifteen seconds after detonation time (0802 PST) a massive venting began which lasted until 69 seconds after detonation at which time the overburden collapsed forming a surface crater about 200 feet in diameter and 50 feet deep. Subsequent analysis showed that the radioactive debris, appearing as a dense black cloud, was vented through a surface crack about 130 feet northeast of surface ground zero (SGZ). Near the mid-point of the crack, which was 8 to 10 feet long, was an irregular hole 4 to 6 inches wide at its widest point. The aperture did not appear to be scoured by the escape of high-pressure gas. Radiation readings in and around the drill casing were relatively low which clearly indicated that the stemming held and that the principal venting occurred through the crack and hole.

The vented radioactive debris, consisting of gaseous and particulate material, rose rapidly to about three thousand feet above the surface. The temperature lapse rate was nearly dry adiabatic and the winds were from the northwest throughout the depth of the cloud layer during the period of cloud movement to the Las Vegas, NV, area and beyond. Vertical wind speed shear that existed at shot time caused the upper portion of the cloud to be transported downwind more rapidly than the lower portion, The cloud was described as resembling a huge frankfurter with its convex side up.

Prologue of Reference 5.1

In the last chapter, it was shown how the FOST can generally be applied to containment-designed detonations using applicable analogs. This chapter will give the necessary details about the PIKE analog so that one can implement the "PIKE Model." As discussed in the last chapter, a fallout analog is derived from the analysis of the radiological and meteorological data associated with the analog event. Thus, it is first necessary to examine the PIKE analyses.

RADIOLOGICAL ANALYSES

The original radiological analysis of the PIKE data was completed shortly after PIKE's detonation in 1964. The quality of the gamma exposure-rate data collected in association with the PIKE event was poor. While the analysts encountered problems in the interpretation of these data, they did manage to derive the necessary parameters needed to devise a FOST analog. There were massive ventings that occurred after the PIKE event that had better radiological data than that collected in association with PIKE. Thus, since the PIKE radiological data were marginal, it would have been better if these later analogs could have been used instead of the PIKE analog. However, as pointed out in the last chapter, the PIKE analog became the worst-case analog after it was completed and has remained so to the present time.

Calls for a reanalysis of the PIKE radiological data began soon after the first analysis was released. Several reanalyses were undertaken from the late 1960s until the late 1970s, but the most comprehensive analysis was begun in 1984. This reanalysis is documented in the report, ***1985 Analyses and Evaluations of the Radiological and Meteorological Data for the PIKE Event*** (Reference 5.1). Figure 5.1 shows the PIKE fallout pattern based upon the 1985 analysis.

THE DECAY CURVE

In the original PIKE analysis, it was assumed that the PIKE decay rate was $t^{-1.2}$. Though questioned in later analyses, this assumption was not changed until the 1985 analysis. It continued to be used in the PIKE Model until 1986.

In the PIKE analyses of the 1970s, it was apparent that while $t^{-1.2}$ decay was reflected during certain periods in some of the PIKE exposure-rate-versus-time profiles, there were many profiles which showed exposure rates that did not decrease as indicated by $t^{-1.2}$. While it was evident that $t^{-1.2}$ decay was not appropriate for the PIKE debris, there was so much uncertainty about the validity of the data that it was not possible to unequivocally determine a better PIKE decay rate.

However, as pointed out in Chapter 4, in the early 1980s, LLNL developed a set of theoretical decay rates for many NTS nuclear detonations (Reference 4.4). Applying the theoretical LLNL decay-rate model for the PIKE event to the actual PIKE data greatly aided the PIKE analysts into determining which of the PIKE data were valid. However, once the valid data had been isolated, it became apparent that the theoretical LLNL PIKE decay curve, while appropriate at later times, did not fit the observed data at very early times. As discussed in Appendix C of Reference 5.1, it was shown that the PIKE debris apparently decayed at a rate similar to the theoretical decay that LLNL calculated for the SANTA

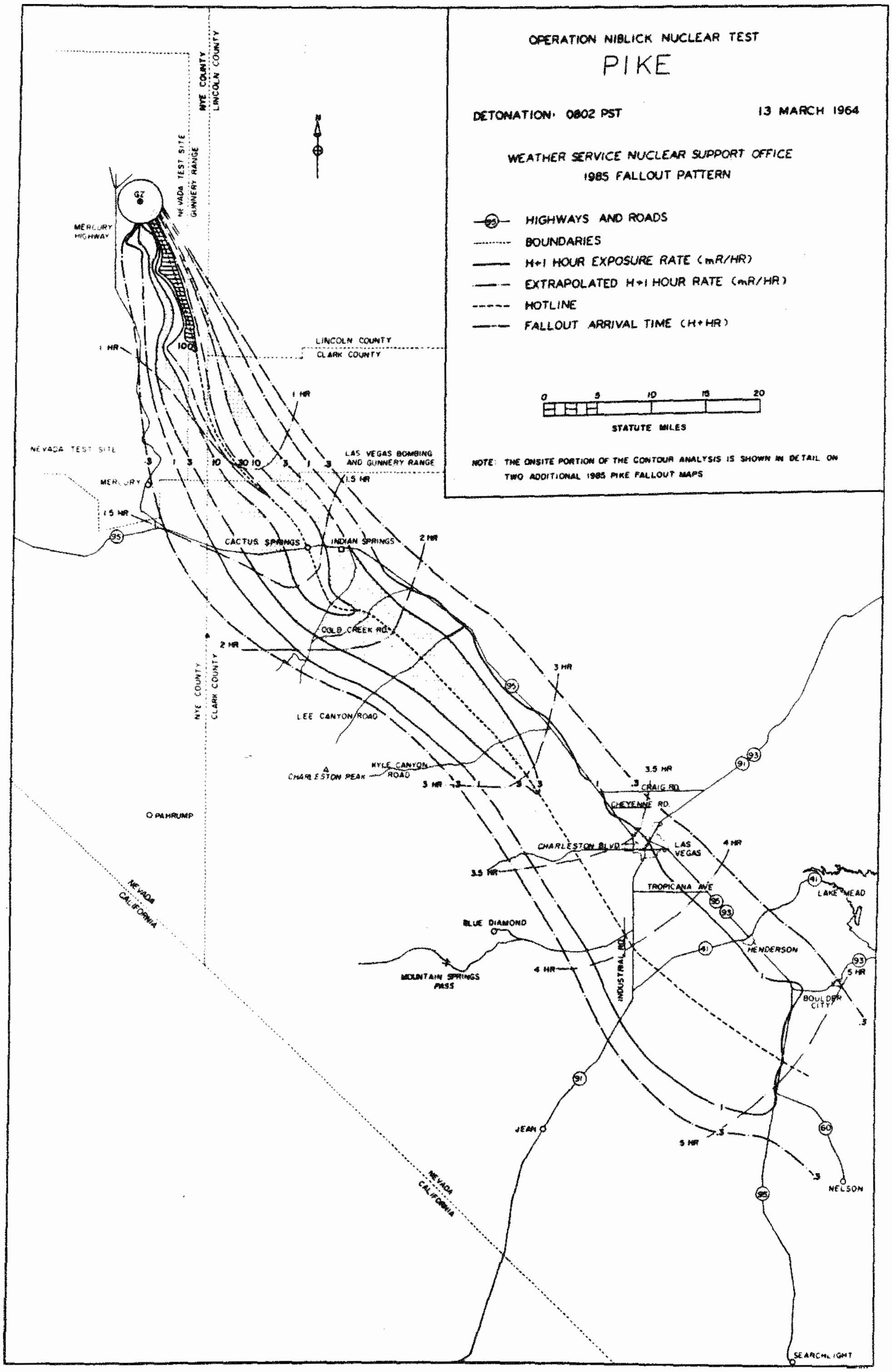

Figure 5.1 The 1985 PIKE Fallout Pattern

FE[1] debris. Thus, the SANTA FE decay scheme was used to normalize PIKE observed exposure-rate data for the derivation of the 1985 PIKE fallout pattern.

In the 1985 PIKE analysis, it was not necessary to normalize any exposure-rate values collected prior to H+1 hr, because no exposure-rate data were collected by monitors prior to H+1 hr. This was fortunate since the LLNL SANTA FE decay scheme was not explicit about what the decay rate was prior to H+1 hr. However, once the 1985 PIKE analysis was completed, it was necessary to update the computer code for the PIKE Model. In order to update this code, it was necessary to know the PIKE decay prior to H+1 hr. Thus, an analysis of PIKE data was undertaken in 1986 by WSNSO to establish the PIKE early-time decay rates. The data primarily used in this analysis were exposure rates from the remote area monitoring system (RAMS) that encircled GZ at close distances.

Table 5.1 PIKE Exposure Rate Versus Time

TIME AFTER DETONATION (hr)	NORMALIZED EXPO. RATE (mR/hr)	SLOPE	TIME AFTER DETONATION (hr)	NORMALIZED EXPO. RATE (mR/hr)	SLOPE
1.670E-01	3.450E 00		1.200E 01	2.923E-02	-1.12
2.000E-01	3.093E 00	- .60	1.400E 01	2.462E-02	-1.11
2.500E-01	2.705E 00	- .60	1.600E 01	2.114E-02	-1.14
5.000E-01	1.785E 00	-. 60	1.800E 01	1.839E-02	-1.18
5.800E-01	1.633E 00	- .60	2.000E 01	1.618E-02	-1.22
1.000E 00	1.000E 00	- .90	2.400E 01	1.290E-02	-1.24
1.500E 00	5.970E-01	-1.27	4.000E 01	6.954E-03	-1.21
2.000E 00	3.944E-01	-1.44	1.000E 02	2.526E-03	-1.11
3.000E 00	2.130E-01	-1.52	2.000E 02	1.236E-03	-1.03
4.000E 00	1.354E-01	-1.56	3.000E 02	7.813E-04	-1.13
5.000E 00	9.458E-02	-1.61	8.500E 02	2.089E-04	-1.27
6.000E 00	7.099E-02	-1.57	1.500E 03	9.299E-05	-1.43
7.000E 00	5.651E-02	-1.48	3.600E 03	2.850E-05	-1.35
8.000E 00	4.710E-02	-1.36	4.800E 03	1.743E-05	-1.71
9.000E 00	4.061E-02	-1.26	7.200E 03	7.024E-06	-2.24
1.000E 01	3.586E-02	-1.18	8.760E 03	4.190E-06	-2.64

Based upon the SANTA FE decay scheme and upon the 1986 WSNSO analysis of pre-H+1 hr RAMS data, a composite PIKE decay curve was established. This curve, which extends from H+0.08 hr to H+10^6 hr (about H+114 yr), is shown in Figure 5.2 on the next page. The $t^{-1.2}$ decay curve is also shown in this figure for comparative purposes. Both curves were normalized so that the H+1 hr exposure rate was 1 mR/hr. Above in Table 5.1 are the PIKE values utilized in this curve from H+10 min to H+1 yr. Also shown in this table are the slopes of lines connecting each point. Notice that the decay slopes are approximately −1.2 from

[1]SANTA FE was a relatively low-yield nuclear event that was detonated at the NTS on October 30, 1958. It was detonated aloft while suspended from a balloon.

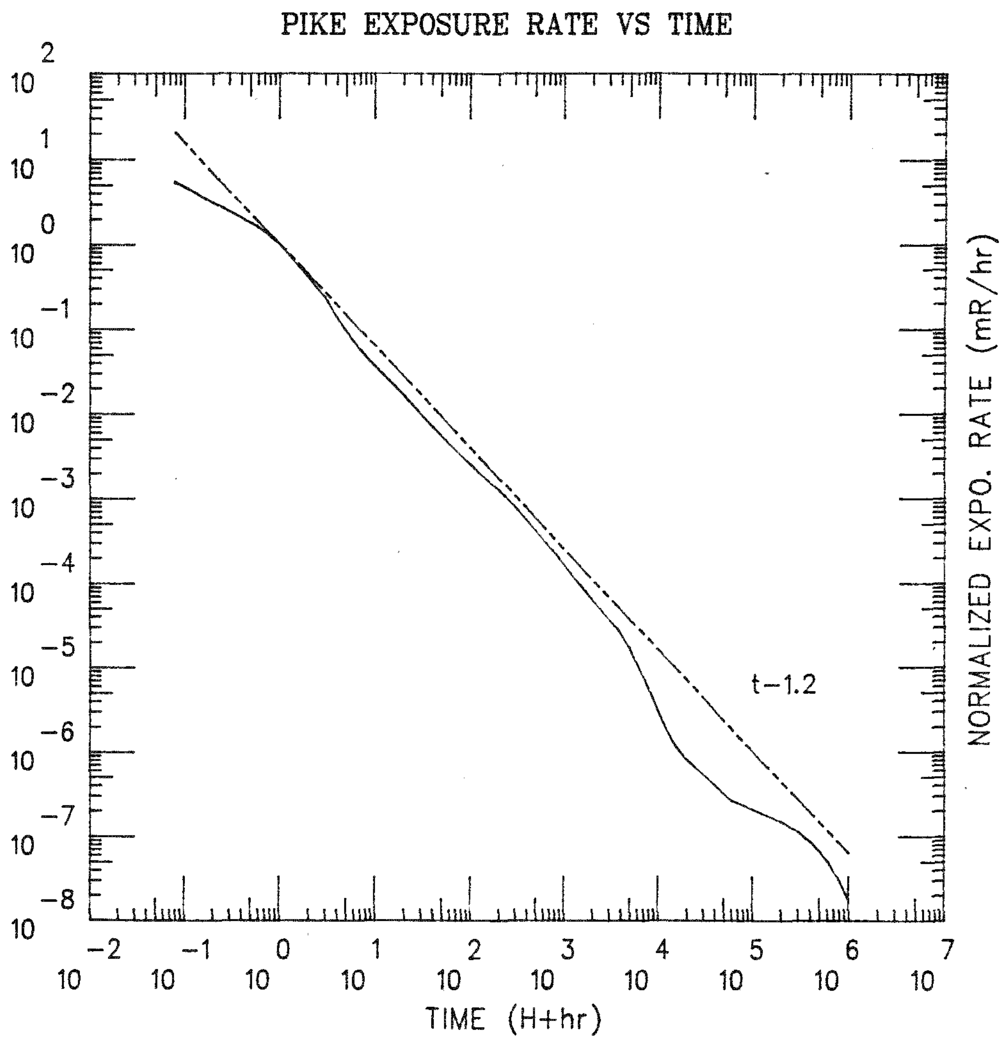

Figure 5.2 PIKE Exposure-Rate-Versus-Time Profile

about H+10 to H+850 hr. In the next chapter, it will be shown how this WSNSO PIKE composite decay scheme is used in the computerized scaling technique.

THE EXPOSURE-RATE-VERSUS-DISTANCE CURVE

A revised PIKE exposure-rate-versus-distance curve was constructed based upon the 1985 PIKE analysis. The first step was to utilize the fallout pattern (Figure 5.1). The centerline distances from GZ where each of the isopleths (1, 3, 10, 30, etc.) crossed the centerline were determined and plotted. For example, it was found that the 100 mR/hr contour crossed the centerline 15.1 miles from GZ as measured along the centerline. The second step was to examine those survey-meter measurements made along or very near the centerline. If these values were considered valid, they were normalized to H+1 hr and plotted versus their centerline distance from GZ.

The resulting 1985 PIKE exposure-rate-versus-distance profile is shown in Figure 5.3. The profile based upon an earlier PIKE analysis is also plotted in this figure for comparative purposes. This "old PIKE" curve was used in the PIKE

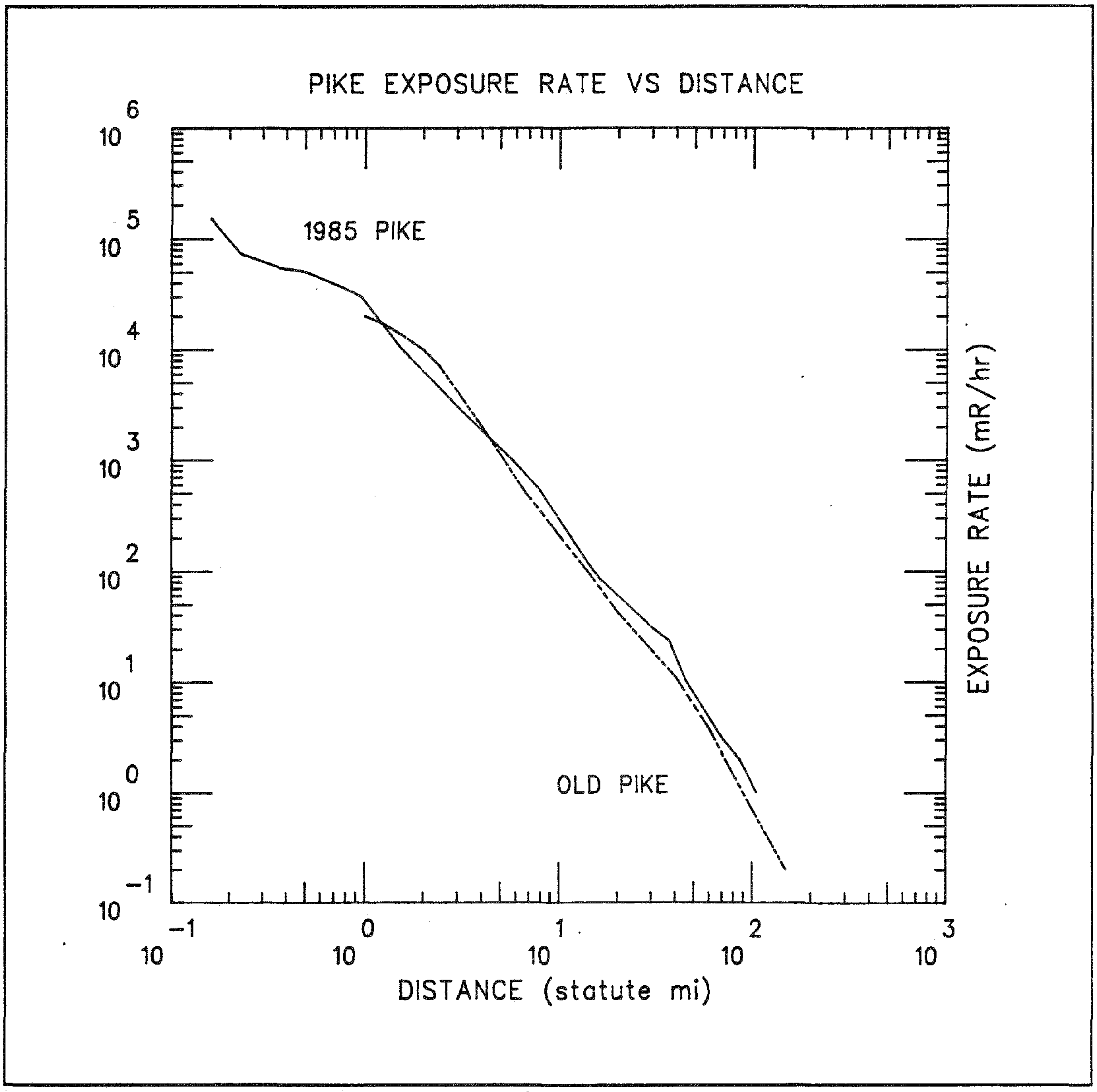

Figure 5.3 PIKE Exposure-Rate-Versus-Distance Curve

model until 1986. The next chapter will show how this 1985 curve was modified for use with the computer model.

THE FALLOUT FRACTION

As discussed in Chapter 4, it is not necessary to determine the fallout fraction for the PIKE analog in order to utilize the FOST, since the assumption is made that the new-event fallout fraction will be the same as that for PIKE. In Equation 4.1, (f_p/f) equals 1.

THE CLOUD-PASSAGE EXPOSURE VERSUS FIRST-YEAR-DEPOSITION EXPOSURE

By now it should be obvious how equations 4.1 and 4.2 can be used to determine the H+1 hr exposure rate, $ER1_p$, at a particular downwind distance, given (1) the derived PIKE meteorological and radiological parameters, (2) the forecast new-event meteorological and radiological parameters, and (3) the PIKE exposure-rate-versus-distance curve. It has also been shown how the peak exposure-rate time, TP, can be determined for this location. In addition, the PIKE decay curve has been specified. With this information, one can then compute TYDE, the total-first-year-deposition exposure.

As exemplified in Figure 4.2 (page 44), TYDE can be computed by integrating under the decay curve from TP to TY (areas B+C). (Of course, the decay curve would be the PIKE decay instead of $t^{-1.2}$, which is shown in that figure.) However, TYDE is not the exposure in which safety officials are primarily interested. As pointed out earlier, they are interested in TYE (areas A+B+C) and CPE (areas A+B). These two exposures are derived by using relationships determined from PIKE exposure-rate-versus-time profiles.

Assume that the profile shown in Figure 4.2 was one derived from PIKE data at a particular downwind distance near the centerline. From this profile, the fraction of TYE (A+B+C) that is associated with TYDE (B+C) can be derived. Thus, even if TYDE and this fraction were the only parameters known, it would still be possible to determine TYE and CPE (A+B), since these two parameters define areas A, B, and C, individually. This type of relationship is used to compute TYE and CPE in the PIKE Model.

An analysis of the comprehensive PIKE exposure-rate-versus-time profiles near the centerline was conducted after the 1985 PIKE analysis. It was found that the percentage of CPE in relation to TYDE decreased as a function of TP. This is in contrast to the assumption used in the pre-1986 PIKE Model that CPE was half of TIDE (areas B+C+D), regardless of TP.

In the current PIKE Model, it is assumed that TYE and CPE have the following relationships to TYDE:

$$TYE = 1.1611\ TP^{-0.02354}\ TYDE \qquad (5.1)$$

$$CPE = 0.28624\ TP^{-0.49365}\ TYDE \qquad (5.2).$$

THE FISSION+ YIELD

The PIKE fission+ yield, Y, has been calculated by LANL, the laboratory that conducted the PIKE event. The fission+ yield for the new-event, Y_p, is an estimate by the national laboratory conducting that event and can be obtained from either the laboratory or from the DOE. Both Y and Y_p are classified numbers.

METEOROLOGICAL ANALYSES

The meteorological situation in association with the PIKE event[2] was fairly stable during the period in which the local fallout was deposited. This was fortunate since abrupt changes or even small steady changes over many hours would have reduced the credibility of the analog. Remember that only one value can be assigned to the analog meteorological parameters.

As was discussed in Chapter 4, though the analog meteorological parameters can not be changed, the new-event parameters can be varied with time. However, there are certain restrictions, which will be discussed below.

CLOUD HEIGHT

According to aircraft measurements, the PIKE cloud quickly rose to 3000 ft AGL or approximately 7000 ft MSL. It continued to rise for the next few minutes and stabilized at 9000 ft MSL, which gives a cloud height of 5000 ft AGL. The 5000-foot value is utilized for the analog cloud height, H, in the PIKE Model.

In order to avoid confusion, it should be pointed out that some aircraft measurements show that the cloud rose to a height greater than 9000 ft MSL. However, it was primarily the gases and small particulates that were mixed to greater altitudes. As pointed out earlier, such debris would not contribute significantly to local fallout, and therefore should not be included in the derivation of the cloud height for the FOST.

It was pointed out in the previous chapter that since the venting mechanism can not be predicted for the new event, the quantity and release rate of the new event's thermal energy can not be predicted. And, since these parameters can not be predicted, the cloud height of the new event, H_p, can not be predicted. As discussed in Chapter 4, the solution to this problem has been to assume that the quantity and release rate of the new event's thermal energy is the same as that for the analog event (PIKE). Thus, the variation in the cloud height in the new event from the PIKE event would primarily be a function of atmospheric stability.

In general, if the temperature lapse rate (the decrease in temperature with altitude) is less than that observed in association with the PIKE event, then the atmosphere is said to be more stable. In this case, a debris cloud with

---

[2]This situation is briefly summarized in Chapter 5 of Reference 5.1.

the same amount of thermal energy as the PIKE cloud would not rise as high. To the contrary, if the lapse rate is greater than that observed in association with the PIKE event, then the atmosphere is said to be less stable. In this situation, a debris cloud with the same amount of energy as PIKE could rise higher than the PIKE cloud.

In many situations, there are atmospheric layers in which the lapse rate is zero (isothermal rate) or the temperature increases with height. This latter condition is referred to as an inversion. Such isothermal or inversion layers, if thick enough, may act as a cap and prevent a debris cloud from rising higher than the base of them.

Figure 5.4 shows the temperature versus altitude curve at the time of detonation for the Yucca Flat Weather Station, which was a few miles from the PIKE GZ. Temperature is plotted along the abscissa and altitude along the ordinate.

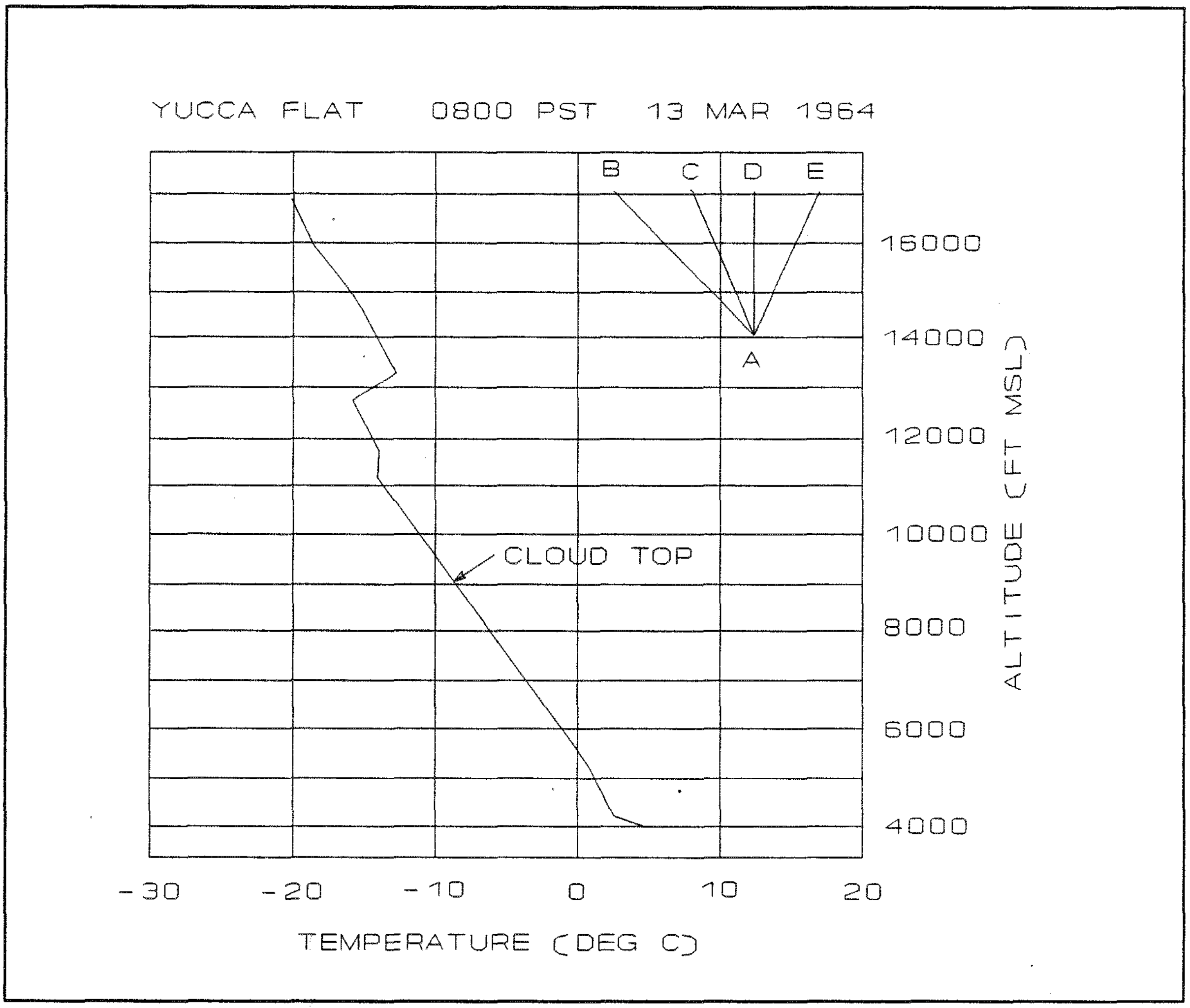

Figure 5.4 PIKE Event-Time Temperature Profile

Note the isothermal layer from about 11,100 to 11,800 ft MSL, and the inversion layer from about 12,800 to 13,200 ft MSL. The layer from the surface to the bottom of the isothermal layer is said to be relatively unstable. That is, a heated parcel of air would easily rise through much of this layer. Temperature profiles are rarely more unstable than this one up to the base of the isothermal layer.

Since the atmosphere was so unstable in association with the PIKE event, it would be difficult to forecast a cloud height greater than the 5000-foot level that was observed with PIKE (assuming that the same amount of thermal energy was released).

Note the four lines emanating from point A in the upper right corner of Figure 5.4. The PIKE lapse rate is similar to the line AB. The forecast cloud height for a new event would be close to 5000 ft if the forecast temperature profile was similar to line AB. However, if the forecast temperature profile was closer to line AC, the forecast cloud height would be lower.

The PIKE-event lapse rate was relatively constant from the surface to 11,000 ft. In many cases, the lapse rate varies considerably in the first few thousands of feet above the surface. In the early morning hours after a clear, calm night, there is often a temperature inversion (line AE) extending from the surface to 500-2000 ft above the surface. Above the inversion, the lapse rate may be more like line AC. If this were the case, the new-event cloud height would probably be forecast to be much lower than the PIKE cloud height (e.g., 2500 ft).

It is obvious that there are a large number of possible temperature-lapse-rate combinations that could occur in association with a new event. It is sometimes difficult for the radiation briefer to determine a cloud height when the forecast temperature profile is vastly different from that of PIKE. As discussed in Chapter 4, the radiation briefer may use the objective CLOUD program to aid in determining how high the new-event cloud would reach. However, after comparing the new-event temperature profile with that of PIKE, the briefer usually exercises his subjective judgment to determine the new-event cloud height. It is unfortunate that such subjectivity has to enter into the estimates, but objectivity can only be gained if the venting mechanism could be forecast or if there was much cloud-height data available from many prompt-massive ventings. Neither of these exist.

AVERAGE WIND SPEEDS

As discussed in Chapter 4, V and V_p, the mean wind speeds for PIKE and the new event, respectively, are based upon the winds from the surface to the top of the cloud.

Hodographs were constructed using the winds in association with the PIKE event. It was determined that the most appropriate value for V in the PIKE Model would be 15 mi/hr.

Hodographs based upon the forecast winds are used to derive the values of V_p for the PIKE Model.

SHEAR ANGLES

Based upon the hodographs constructed from the winds in association with PIKE and upon the PIKE fallout pattern, it was determined that the most appropriate value for α in the PIKE Model would be 20°.

Hodographs based upon the forecast winds are used to derive the values of α_p for the PIKE Model. Remember, that if variable shear angles are utilized, once the shear-angle reaches a certain value, a lower value can not be used for a later time.

CHAPTER 6

COMPUTATIONS

Exposure estimates using the PIKE Model are presently computed utilizing the WSNSO software program, NSCALE (New SCALEr). The NSCALE program is the latest in a series of FOST-computational techniques, that have occasionally changed due to modifications in the PIKE analog and to advancing computing technology. Up until the early 1970s, PIKE-Model calculations were made using a slide rule. By the early 1970s, the PIKE Model was run on programmable calculators. Since the mid 1970s, the PIKE Model has been run on various types of computers. The mechanization of the calculations not only insured that they would be more accurate and would be available more rapidly, but also made it possible for more output products to be created.

The NSCALE program was first implemented in mid-1986 after substantial changes were made in the PIKE analog following the 1985 PIKE analysis.

HARDWARE

Presently, the NSCALE program is primarily run on Data General (DG) computers. Computations are made on DG MV-4000, MV-6000, or MV-10000 machines. NSCALE alphanumeric and graphics output can be displayed on DG D460 (monochrome) or D470 (colored) terminals, but can also be displayed on personal computer (PC) terminals using a D470 terminal emulator. Alphanumeric files are usually printed out on a Digital Decwriter III printer and graphics files are usually plotted on a Hewlett-Packard 7550A pen plotter.

In addition, both alphanumeric and graphics files can be transported to the National Weather Service's AFOS computers, which are also DG machines. Alphanumeric files may be displayed on either the AFOS alphanumeric (monochrome) or graphics (colored) monitors. Graphics files can only be displayed on graphics monitors. Hard copies may be obtained through a Xerox Versatec.

The NSCALE program can also be run on IBM PC's or compatible machines. The type of displays, printouts, and plots depend upon the characteristics of the PC system utilized.

SOFTWARE

The NSCALE computer code was written by the RERB in Fortran 77. The current NSCALE code is listed in Appendix B of this report. There is also a Fortran 77 version of NSCALE which can be run on IBM PC's or PC-compatible machines. (This code is not included in this report.)

The DG version of NSCALE utilizes a plot program referred to as the WSNSO Device-Independent Graphics Package (DIGP). The PC version of NSCALE utilizes a commercial software package, PLOT88.

NSCALE CALCULATIONS

While a detailed description of the NSCALE code is not contained in this report, the basic equations which are utilized in the NSCALE calculations are presented below.

PEAK-EXPOSURE-RATE TIMES

In the last sections of Chapter 4, it was described how the meteorological parameters (H_p, V_p, and α_p) can be varied with time in the FOST. This ability to vary parameters was incorporated into NSCALE.

As described in Chapter 4, the end products of the FOST are exposures (TYE, CPE, etc.). Each exposure is associated with a particular downwind distance, X_p, along the forecast centerline. However, to solve for an exposure, it is first necessary to know the time of the peak-exposure-rate, TP, at that distance.

A method of approaching this problem is to first define a list of arbitrary peak-exposure-rate times. Next, for each of these times, a centerline location would be determined that would have a peak exposure rate corresponding to that time. Thus, if TP is known and if X_p is determined from that TP value, then $ER1_p$ at X_p can be calculated from equations 4.1 and 4.2 since the meteorological and other radiological parameters are known. Finally, the appropriate exposure (TYE, CPE, etc.) at this location can be derived utilizing the analog decay curve, $ER1_p$, and TP. Once exposures have been calculated for each of the arbitrary X_p values, then an exposure-versus-distance curve can be constructed. From this curve, an exposure can be derived for *any* centerline distance along this curve.

Table 6.1 Arbitrary TP Values used in NSCALE

i	TP	i	TP	i	TP
(1)	0.167	(6)	2	(15)	12
(2)	0.200	(7)	3	(16)	14
(3)	0.250	(8)	4	(17)	16
(4)	0.500	(9)	5	(18)	18
(5)	1	(10)	6	(19)	20
		(11)	7	(20)	24
		(12)	8	(21)	40
		(13)	9	(22)	100
		(14)	10		

In NSCALE, a set of 22 standard TP values were arbitrarily chosen. These values, which are in hours after detonation, are listed in Table 6.1.

CENTERLINE DISTANCES FOR THE NEW EVENT

Since there are 22 TP values, there are also 22 distances at which exposures are calculated for the new event. Let the convention be adopted that a number in parentheses following an X_p value signifies the TP value for which the X_p value is calculated. For example, $X_p(1)$ and $X_p(22)$ would signify those centerline distances at which the peak-exposure rate occurred at TP(1) [H+0.167 hr] and TP(22) [H+100 hr], respectively (as defined in Table 6.1).

Furthermore, as discussed in Chapter 4, there are ten sets of variable-meteorological parameters. In the equations below, a number in parentheses following one of these variables (H_p, V_p, or α_p) signifies the hour for which the variable applies.[1] For example, $V_p(2)$ would signify the average wind speed from the first to the second hour. It is assumed that the meteorological parameters are constant after H+10 hr and retain the H+10 hr values. Below are the equations which determine the new event's downwind distances.

For i = 1 to 5:

$$X_p(i) = V_p(1)\ TP(i) \qquad (6.1).$$

For i = 6 to 14:

$$X_p(i) = (V_p(i-4)\ TP(5)) + X_p(i-1) \qquad (6.2).$$

For i = 15 to 22:

$$X_p(i) = ((TP(i) - 10)\ V_p(10)) + X_p(14) \qquad (6.3).$$

CENTERLINE DISTANCES FOR THE PIKE EVENT

As discussed in Chapter 4, to obtain the forecast exposure rates at a particular downwind distance, X_p, we first need to relate that distance to a corresponding distance, X, on the analog centerline. Equation 4.2 shows how X can be computed using the average winds speeds and cloud heights of the analog event and the new event.

---

[1]To avoid confusion when considering the remaining equations of this report, please remember that the integer in parenthesis following H_p, V_p, or α_p refers to the hour for which the variable applies (1 through 10); whereas, the integer in parenthesis following any other variable (e.g., X_p, TP, F) refers to one of the 22 arbitrary times that determine the locations for which exposures estimates are calculated.

Based upon equation 4.2, the next few equations solve for X, and, at the same time, allow for variable parameters. Remember that H for the PIKE event is 5000 ft[2], and V is 15 mi/hr ((H)(V) = (5)(15) = 75). Thus,

for i = 1 to 10:

$$F(i) = 75 / (V_p(i)\ H_p(i)) \qquad (6.4),$$

for i = 11 to 22:

$$F(i) = F(10) \qquad (6.5),$$

where,

F = a factor used in deriving X.

As a result of this definition, X can be defined as follows:

for i = 1 to 5:

$$X(i) = X_p(i)\ F(1) \qquad (6.6)$$

and,

for i = 6 to 22:

$$X(i) = X_p(i)\ F(i\text{-}4) \qquad (6.7).$$

H+1 HR EXPOSURE RATES FOR PIKE

In Chapter 5, the PIKE centerline H+1 hr exposure-rate values as a function of distance were presented in Figure 5.3 (page 78). This curve can be approximated by a curve composed of 5 line segments. The equations for these five lines are as follows:

#1	$X < 1$ mi	ER1	=	2.486×10^4	$X^{-0.9808}$	(6.8)
#2	$1 \text{ mi} \le X < 8$ mi	ER1	=	2.486×10^4	$X^{-1.8691}$	(6.9)
#3	$8 \text{ mi} \le X < 37$ mi	ER1	=	4.0069×10^4	$X^{-2.0986}$	(6.10)
#4	$37 \text{ mi} \le X < 90$ mi	ER1	=	5.3117×10^5	$X^{-2.8144}$	(6.11)
#5	$X \ge 90$ mi	ER1	=	6.3545×10^6	$X^{-3.3659}$	(6.12).

---

[2]When dealing with the cloud heights in the FOST and associated NSCALE equations, it is customary to express the heights in thousands of feet. Thus for a cloud height of 5000 feet, H = 5.

A comparison of the curve resulting from these five segments with the observed PIKE exposure-rate-versus-distance curve is shown in Figure 6.1. The solid line represents the observed PIKE values and the dashed line represents the values utilize in NSCALE.

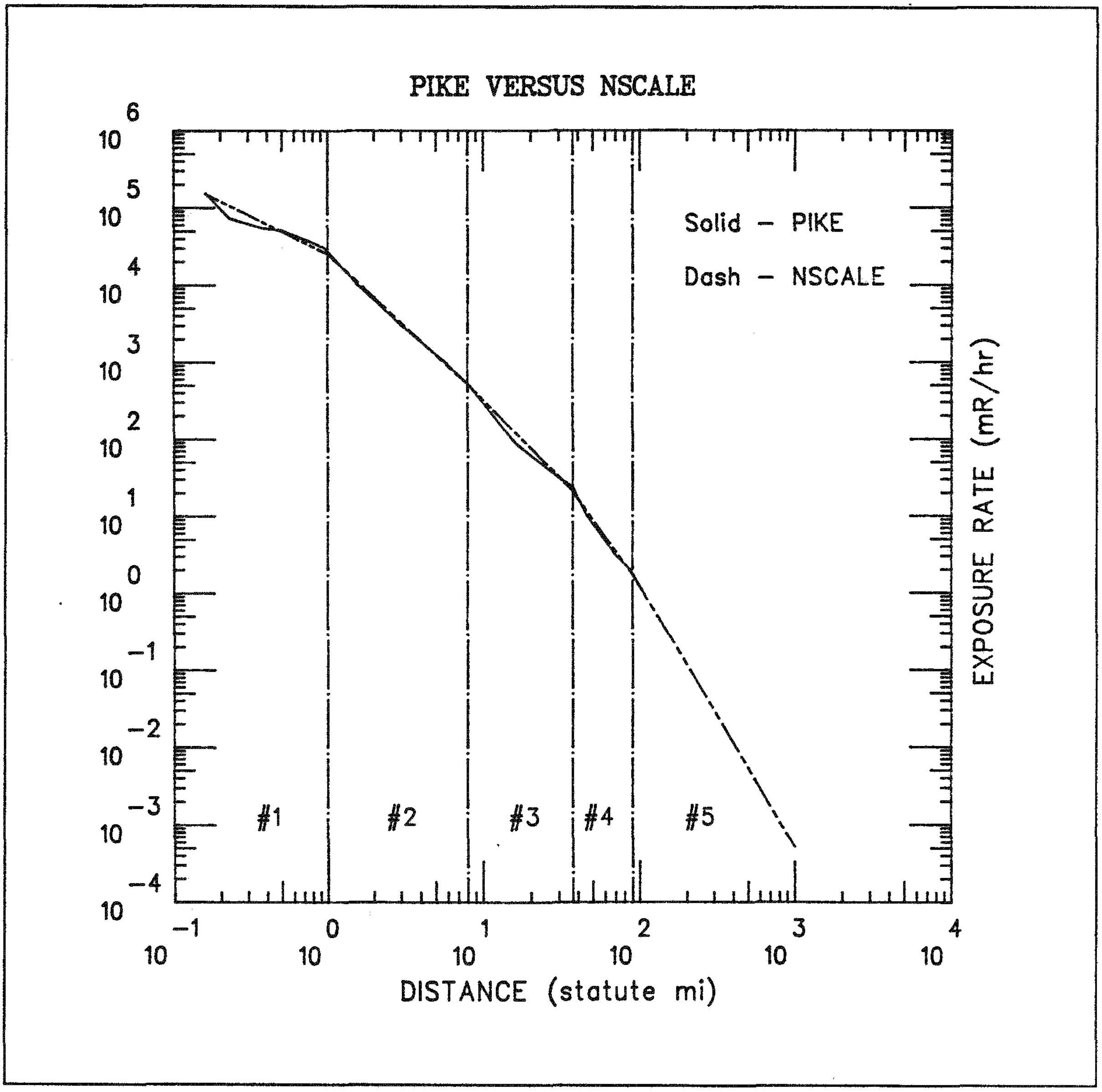

Figure 6.1 NSCALE Exposure-Rate-Versus-Distance Curve

H+1 HR EXPOSURE RATES FOR THE NEW EVENT

At this point in the NSCALE calculations, by using equation 6.1 through 6.3, we have defined 22 centerline distances, X_p, for which we can calculate the various exposures for the new event. We also know the TP values for each of these 22 distances. By using equations 6.4 through 6.7, we have calculated the PIKE centerline distances, X, each of which correspond to one of the X_p values. And, by using equations 6.8 through 6.12, we have calculated the PIKE H+1 hr exposure rates (ER1) for each of the 22 X values. We are now in a position to calculate H+1 hr exposure rates for the new event ($ER1_p$) for each of the 22 X_p distances, using a form of equation 4.1.

The new-event meteorological parameters (H_p, V_p, and α_p) have been derived from the forecast weather conditions and have been input into NSCALE. As pointed out earlier, the ratio, f_p/f, is assumed to be one. The three PIKE meteorological parameters, H, V, and α, are known from PIKE analyses. Since these values do not vary, they can be included as a constant in the NSCALE equation that is equivalent to equation 4.1. Thus, $(\alpha)(H^2)(V^2)$ for the PIKE analog equals $(20)(5^2)(15^2)$ or 1.125×10^5.

While the PIKE fission+ yield is also known and does not vary, it could be included in this constant, but it can not be due to security considerations. Instead, the ratio of the new-event fission+ yield to the PIKE fission+ yield, Y_p/Y, is set equal to R. Once the new-event fission+ yield is received from the national laboratory, it is divided by fission+ yield of PIKE to produce the R value. This R value is then input into NSCALE.[3]

The new-event H+1 hr exposure rates are calculated in NSCALE with the following equations, all of which are based upon equation 4.1.

For i = 1 to 10:

$$f(i) = (1.125 \times 10^5 \ R) \ / \ (V_p(i)^2 \ H_p(i)^2 \ \alpha_p(i)) \qquad (6.13),$$

and

for i = 11 to 22:

$$f(i) = f(10) \qquad (6.14),$$

where,

f = a factor used in deriving $ER1_p$.

[3]Actually, for security reasons, there are other factors included in the derivation of the R value. These factors, which are not reflected in the code shown in Appendix B, are periodically changed.

As a result of the above definitions, then

for i = 1 to 5:

$$ER1_p = f(1)\ ER1(i) \quad (6.15),$$

and

for i = 6 to 22:

$$ER1_p = f(i-4)\ ER1(i) \quad (6.16).$$

Thus, by using equations 6.13 to 6.16, we can derive an $ER1_p$ value for each X_p value. Since we also know the TP values for each X_p value, we could now compute exposures for each location and plot an exposure-versus-distance curve.

However, if we had varied the meteorological parameters, the resulting curve would probably not show a smooth continuous decrease in exposures with distance as would be expected. This predicament was briefly discussed at the end of Chapter 4. The solution is to first establish a best-fit curve (least squares method) based upon the calculated $ER1_p$ values. Then, instead of using the $ER1_p$ values as calculated above to compute exposures, one would use the $ER1_p$ values as indicated by the best-fit H+1 hr exposure-rate-versus-distance curve.

The NSCALE $ER1_p$ best-fit curve is constructed by taking the $ER1_p$ values computed using equations 6.15 and 6.16 and using them as follows:

(1) for $X_p(1)$ through $X_p(5)$, use the corresponding $ER1_p(1)$ through $ER1_p(5)$ value as calculated,

(2) for $X_p(6)$ to $X_p(7)$, use the value calculated from a best-fit curve based upon $ER1_p(4)$ through $ER1_p(9)$,

(3) for $X_p(8)$ to $X_p(9)$, use the value calculated from a best-fit curve based upon $ER1_p(4)$ through $ER1_p(11)$,

(4) for $X_p(10)$ through $X_p(14)$, use the value calculated from a best-fit curve based upon $ER1_p(8)$ through $ER1_p(20)$,

(5) for $X_p(15)$ through $X_p(19)$, use the values calculated from a best-fit curve based upon $ER1_p(12)$ through $ER1_p(21)$, and

(6) for $X_p(20)$ through $X_p(22)$, use the corresponding $ER1_p(20)$ through $ER1_p(22)$ value as calculated.

Once these steps are taken, there would then be 22 H+1 hr exposure-rate versus distance values, which, when plotted, would produce a relatively smooth curve. Since the exposure-rate values produce a smooth curve, the exposures based upon the exposure rates would also produce a smooth curve.

TOTAL-FIRST-YEAR-DEPOSITION EXPOSURE

As discussed earlier, the two exposures in which the safety officials are primarily interested are the Total-First-Year-Exposure (TYE) and the Cloud-Passage Exposure (CPE). In order to derive these exposures, it is first necessary to compute the Total-First-Year-Deposition Exposure (TYDE).[4]

If the decay was constant, such as $t^{-1.2}$, then TYDE at each of the 22 downwind locations could be calculated from the following equation which is based upon equation 4.5 (page 46).

$$TYDE(i) = (ER1_p(i) \ / \ (-N-1)) \ (TP(i)^{N+1} - 8760^{N+1}) \qquad (6.17).$$

As explained in Chapter 5, the decay slope, N, is no longer considered constant for the PIKE analog, so the above equation would not be applicable. However, it can be used in a modified form if the decay curve is divided into straight-line segments.

The PIKE normalized exposure rates as a function of time are shown in Table 5.1 (page 76). Notice in this table, that there are 32 times from H+10 min to H+1 yr (H+0.167 to H+8760 hr), and that 22 of these times correspond to all of the arbitrary TP values used in NSCALE. Plotting these 32 points produces the PIKE decay curve shown in Figure 5.2 (page 77). Thus, this curve is actually composed of 31 straight-line segments each with the constant slope indicated in Table 5.1.

Since for each centerline distance, $X_p(i)$, there is a corresponding TP(i), and because each TP(i) is the starting point for one of the straight-line segments within the PIKE decay curve, then the TYDE for that $X_p(i)$ can be calculated by integrating under each of the straight-line segments from TP(i) to TY (8760 hr) and summing the results.

If we assume that $ER1_p$ equals 1, then equation 4.5 (page 46) can be written:

$$E = (t_s^{N+1} - t_e^{N+1}) \ / \ (-N-1) \qquad (6.18).$$

For TP(1), exposure values could be computed using the above equation for each of the areas underneath the 31 straight-line segments in the PIKE decay curve from H+0.167 to H+8760 hr. Adding these 31 exposures gives a value of 4.363 mR. In a similar manner, for TP(2), exposure values could be computed using the above equation for each of the areas underneath the 30 line segments from H+0.2 to H+8760 hr. This procedure could then be repeated for all the TP values out

[4] It might be easier to follow this discussion if reference was once again made to Figure 4.2 (page 44).

Table 6.2 TYDE Factors

(i)	FTYDE
1	4.363
2	4.254
3	4.110
4	3.570
5	2.904
6	2.278
7	1.990
8	1.820
9	1.707
10	1.626
11	1.562
12	1.511
13	1.467
14	1.429
15	1.364
16	1.311
17	1.265
18	1.226
19	1.191
20	1.133
21	0.983
22	0.740

to TP(22). Table 6.2 shows these values, which are referred to as TYDE factors, FTYDE.

Since $ER1_p(i)$ is known for a particular centerline distance, $X_p(i)$, then it is only necessary to multiply $ER1_p(i)$ times FTYDE(i) in order to calculate the TYDE at that location.

OTHER EXPOSURES, EXPOSURE RATES, AND DOSES

At this point in our NSCALE calculations, we now have 22 centerline locations, $X_p(i)$, at which we know TP(i), $ER1_p(i)$, and TYDE(i). From these parameters, we can derive other exposures, exposure-rates, and doses that are of interest to the radiation briefer and/or the safety officials.

TOTAL-FIRST-YEAR AND CLOUD-PASSAGE EXPOSURES

Equations 5.1 and 5.2 (page 79) defined the relationships between TYDE and TYE and between TYDE and CPE. Below, these equations have been rewritten in the form that has been used to describe the other NSCALE equations.

$$TYE(i) = 0.1611 \quad TP(i)^{-0.02354} \quad TYDE(i) \qquad (6.19)$$

$$CPE(i) = 0.28624 \quad TP(i)^{-0.49365} \quad TYDE(i) \qquad (6.20)$$

DEPOSITION-PEAK-EXPOSURE RATE

One estimate that is sometimes requested of the radiation briefer is the peak-exposure rate at a particular centerline distance. Presently, it is not possible to make a definitive estimate of this parameter. However, it is possible to give a value for the deposition-peak-exposure rate, DPER, which is the H+1 hr exposure rate normalized to TP, using the decay curve. This is exemplified in Figure 4.2 (page 44). DPER always lies directly below the peak-exposure rate. Thus, one can approximate the peak-exposure rate by multiplying DPER by a factor somewhat larger than 1. In using the PIKE analog, a credible, conservative estimate would be given by multiplying DPER by 2. However, at the present time, this relationship has not been studied thoroughly; thus, this factor should be used with caution.

The DPER values in NSCALE are calculated by multiplying $ER1_p$ by a decay factor, DF. This decay factor is merely the PIKE exposure rate relative to unity at H+1 hr. These values, which are shown in Table 5.1 (page 76) as a function of time after detonation, are also shown in Table 6.3 as a function of the 22 TP values.

Table 6.3 Decay Factors

(i)	DF
1	3.450
2	3.093
3	2.705
4	1.785
5	1.000
6	0.3944
7	0.2130
8	0.1354
9	0.09458
10	0.07099
11	0.05651
12	0.04710
13	0.04061
14	0.03586
15	0.02923
16	0.02462
17	0.02114
18	0.01839
19	0.01618
20	0.01290
21	0.006954
22	0.002526

RESIDUAL-FIRST-YEAR-DEPOSITION EXPOSURE

The Residual-First-Year-Deposition Exposure (RYDE), as first described in Chapter 4, is that exposure due to deposited debris from the end of cloud passage until H+1 yr. It is graphically shown as area C in Figure 4.2 (page 44).

The U.S. Environmental Protection Agency (EPA) has the responsibility for protecting downwind off-site populations from adverse exposures from nuclear fallout. The RYDE is sometimes utilized by EPA in their planning for nuclear tests.

As discussed earlier, the DOE follows certain guidelines for population exposure in association with NTS nuclear activities. These guidelines (Reference 4.1) state that based upon the most appropriate hypothetical release model (normally the PIKE Model), nuclear events should be postponed until more favorable weather conditions prevail when:

(1) whole-body gamma exposure estimates exceed 170 mR/yr and thyroid doses exceed 500 mrads for offsite populations in areas where remedial actions to reduce exposures are not feasible, and

(2) whole-body gamma exposure estimates exceed 500 mR/yr and thyroid doses exceed 1.5 rads/yr for off-site populations in areas where remedial actions to reduce exposures are feasible.

EPA has designated certain areas surrounding the NTS as "controlled areas." These sparsely populated areas are areas where, as mentioned above, remedial actions can be taken to reduce exposures should there be an accidental venting. In these areas, EPA is in close contact with all the residents and can quickly shelter or move them. If, in conjunction with a containment-designed detonation, a predicted TYE for one of these controlled areas is slightly over 500 mR, EPA becomes interested in what the exposure would be to that population if it were sheltered or moved entirely out of the area during cloud passage. This mitigated exposure would be TYE minus CPE which, as exemplified in Figure 4.2, would be RYDE. Thus, if TYDE was over 500 mR, but RYDE was below 500 mR, then EPA could assume that they could protect the population from excess exposure. EPA could therefore recommend to DOE that the detonation should proceed.

Furthermore, in some cases, when the predicted RYDE is well over the guideline limits, it is sometimes of interest to EPA to determine at what time during the RYDE period (TC to TY) would the remaining portion of RYDE equal 500 mR. For example, if the predicted RYDE was 1.5 R, and if it was assumed that an individual who lived at the location for which the prediction was made could be evacuated prior to the arrival of the cloud, then at what time could he return to that location and still receive only 500 mR external exposure? Based upon RYDE values, these "stayout times" can be calculated.

In NSCALE, RYDE can be calculated by the following equation:

$$RYDE(i) = TYDE(i) - CPE(i) \qquad (6.21).$$

INFANT THYROID DOSE

DOE is also concerned about the potential radiation doses to thyroids of downwind populations due to the ingestion of milk produced by cows or goats that feed upon vegetation upon which fallout is deposited. It was realized many years ago that infants were especially susceptible to this form of exposure. Thus, EPA must assure the Test Controller that the Infant Thyroid Dose (ITD), based upon the NSCALE estimates, does not exceed the guidelines (1.5 rads).

For over 20 years, EPA, in making estimates of ITD, has utilized relationships between exposure rates and ITD which were developed by Knapp (Reference 6.1). They use Knapp's most conservation estimate, which is that the ITD is equal to 16.4 times the exposure rate at H+24 hr. The resultant dose (rad) is based upon the assumption that the animals were on green feed and that the measurements are gamma-exposure rates measured at 3 ft above the ground in association with deposited debris. The EPA assumes that if the animals were on dry feed, then the dose would be one fifth of the above product.

The WSNSO routinely provides EPA with ITD-dose estimates based upon the following equations:

$$ITD_g(i) = 16.4 \quad DF(20) \quad ER1_p(i)$$

$$= 0.2116 * ER1_p(i) \qquad (6.22),$$

where,

$ITD_g(i)$ = infant thyroid dose with a green-feed assumption at the downwind distance, $X_p(i)$.

$$ITD_d(i) = ITD_g(i) / 5$$

$$= 0.0423 \; ER1_p(i) \qquad (6.23),$$

where,

$ITD_d(i)$ = infant thyroid dose with a dry-feed assumption at the downwind distance, $X_p(i)$.

BENCHMARK EXPOSURES

At this point in the NSCALE calculations, an exposure-versus-distance curve can be constructed for the various doses (e.g., TYE, CPE, etc.) from $X_p(1)$ to $X_p(22)$. Thus, the exposure at any distance can be derived from the appropriate curve. To the contrary, the distance at which a certain exposure occurs can also be derived from the appropriate curve. This latter use is frequently exercised since safety officials want to know at what distance along the centerline does the predicted exposure drop below certain values. For example, at what centerline distance does the TYE drop below 170 mR? Any location having a distance from GZ along the centerline that is greater than the distance of this "benchmark" exposure (170 mR) would have an exposure less than 170 mR. In order that the distances to such benchmark exposures may be readily available and do not have to be picked manually off a curve, they are routinely calculated by NSCALE.

Calculations are made of the distances at which the TYE and CPE values equal 5R, 500 mR, 170 mR, 100 mR, 10 mR, and 1 mR. Also, calculations are made of the distances at which ITD_g and ITD_d values equal 500 mrad and 50 mrad.

NSCALE OPERATION

This section will detail how to run NSCALE on one of the DG computers. The operation of NSCALE on a PC is essentially the same.

INPUT

In order to better illustrate how NSCALE operates, an example run has been constructed and is shown in Appendix C. It is perhaps best to follow the instructions below while actually running NSCALE at a terminal. However, if this is not possible, one can follow along by using the example in Appendix C.

Obviously, the first step in running NSCALE is to log on the computer. NSCALE may be run on any WSNSO DG computer in the radiation briefer's directory or any associate subdirectory. Since over two dozen files can be created by running NSCALE, it is often advisable to run NSCALE in a directory especially set up for NSCALE calculations. If this is not done, the NSCALE files may get dispersed among other files, making it more difficult to quickly locate NSCALE files should it be necessary. To run NSCALE, first type the word NSCALE.

FISSION-YIELD TERM

The first prompt to appear on the screen is *R =*, the radiological source term corresponding to the ratio, (f/f_p). Type in the value of this ratio and strike the ENTER key.[5]

METEOROLOGICAL PARAMETERS

The NSCALE operator will next be asked to input the meteorological parameters: speed, cloud height, and shear. These three values are entered (in the order specified) in response to the hour prompt (H+1 hr = 1, H+2 hr = 2, etc.). They may be separated by a comma or a space. Though ten sets of meteorological parameters can be entered, a lesser amount may be entered by typing in three zeros (0,0,0) next to the hour prompt at which the parameters first remain constant.

Once the parameters have been entered, the operator will have a chance to make corrections if necessary. When the operator is satisfied with the input parameters, the entire list of parameters can be displayed on the screen for verification.

OUTPUT

After the input parameters have been listed and verified, NSCALE makes its calculations and writes the data to disk files.[6] At this point, the NSCALE operator has many options from which to chose in order to get the output into the most appropriate form.

SCREEN DISPLAYS AND PRINTOUTS

The operator will be asked if a printout is wanted. If the answer is "no," then the input parameters and resultant calculations are presented on the terminal screen. If the answer is "yes," then the input parameters and resultant calculations are not presented on the screen but will be printed out at the end of the run.

---

[5]Although the value of the f/f_p ratio is used in running the version of NSCALE listed in Appendix B, it is not used in the actual versions on the DG computers. The radiation briefer should check with the chief of the RERB to determine what number should be input for R.

[6]These data files are:
ns_a_tye_bf.dat, ns_a_tye_pbf.dat, and ns_a_spl_tye_bf.dat (TYE vs distance data)
ns_a_cpe_bf.dat and ns_a_cpe_pbf.dat (CPE vs distance data)
ns_a_tdg_bf.dat and ns_a_spl_tdg_bf.dat (ITD_g vs distance data)
ns_a_tdd_bf.dat (ITD_d vs distance data)
ns_a_dper_bd.dat (DPER vs distance data).

R = 1.000

TIME (H+HRS)	SPEED (MPH)	CLD. HGT. (*1000 FT)	SHEAR (DEG.)
1	12.	5.0	20.
2	15.	5.0	30.
3	15.	5.0	30.
4	15.	5.0	30.
5	15.	5.0	30.
6	15.	5.0	30.
7	15.	5.0	30.
8	20.	5.0	30.
9	20.	5.0	30.
10	20.	5.0	30.

TP (H+HRS)	X (MILES)	TYE (mR)	CPE (mR)	ITD_GF (RADS)	ITD_DF (RADS)
.167	2.00	7.405E+03	4.238E+03	2.965E+02	5.928E+01
.200	2.40	5.113E+03	2.686E+03	2.109E+02	4.216E+01
.250	3.00	3.238E+03	1.532E+03	1.390E+02	2.778E+01
.500	6.00	7.575E+02	2.587E+02	3.804E+01	7.605E+00
1.	12.0	1.437E+02	3.542E+01	9.015E+00	1.802E+00
2.	27.0	1.338E+01	2.382E+00	1.088E+00	2.175E-01
3.	42.0	3.930E+00	5.780E-01	3.693E-01	7.383E-02
4.	57.0	1.546E+00	1.986E-01	1.599E-01	3.197E-02
5.	72.0	8.019E-01	9.277E-02	8.890E-02	1.778E-02
6.	87.0	4.736E-01	5.029E-02	5.536E-02	1.107E-02
7.	102.0	2.788E-01	2.753E-02	3.405E-02	6.807E-03
8.	122.0	1.556E-01	1.443E-02	1.970E-02	3.939E-03
9.	142.0	9.472E-02	8.312E-03	1.239E-02	2.477E-03
10.	162.0	6.153E-02	5.138E-03	8.282E-03	1.656E-03
12.	202.0	3.262E-02	2.500E-03	4.619E-03	9.236E-04
14.	242.0	1.700E-02	1.212E-03	2.514E-03	5.027E-04
16.	282.0	9.772E-03	6.543E-04	1.502E-03	3.004E-04
18.	322.0	6.043E-03	3.828E-04	9.613E-04	1.922E-04
20.	362.0	3.948E-03	2.380E-04	6.482E-04	1.296E-04
24.	442.0	1.910E-03	1.057E-04	3.310E-04	6.619E-05
40.	762.0	2.618E-04	1.140E-05	5.293E-05	1.058E-05
100.	1962.0	7.995E-06	2.262E-07	2.194E-06	4.387E-07

EXPOSURE	DISTANCES (MILES)		DOSE	DISTANCES (MILES)	
(mR)	TYE	CPE	(RADS)	ITD_GF	ITD_DF
5000.	2.43	1.87	.500	37.10	19.62
500.	7.13	4.64	.050	89.94	48.42
170.	11.19	6.95			
100.	13.58	8.36			
10.	29.99	17.55			
1.	66.56	35.40			

Figure 6.2 First Page of NSCALE Alphanumeric Output

Figures 6.2 and 6.3 show an example of the alphanumeric output that is either displayed on the screen or typed on a printer, depending upon the option chosen. The input parameters are listed in the upper left corner of Figure 6.2. The 22 standard TP values are listed in the far left column in the middle of this figure. Calculations of X, TYE, CPE, ITD_GF, and ITD_DF are listed for each of these 22 values. The distance (statute miles) along the centerline of the new event, which has been denoted by X_p up to this point in this report, is denoted by X in this listing. Of course, TYE and CPE represent the Total-First-Year and Cloud-Passage Exposure in association with the new event. And, and ITD_GF and ITD_DF represent the Infant-Thyroid Dose calculations for green and dry feed, respectively, for the new event.

TP (H+HRS)	X (MILES)	ER1 (mR/HR)	DPER (mR/HR)	TYDE (mR)	RYDE (mR)
.167	2.00	1.401E+03	4.835E+03	6.114E+03	3.167E+03
.200	2.40	9.967E+02	3.083E+03	4.240E+03	2.427E+03
.250	3.00	6.568E+02	1.777E+03	2.699E+03	1.706E+03
.500	6.00	1.798E+02	3.209E+02	6.419E+02	4.988E+02
1.	12.0	4.261E+01	4.261E+01	1.237E+02	1.083E+02
2.	27.0	5.143E+00	2.026E+00	1.171E+01	1.100E+01
3.	42.0	1.745E+00	3.718E-01	3.473E+00	3.352E+00
4.	57.0	7.557E-01	1.023E-01	1.375E+00	1.347E+00
5.	72.0	4.202E-01	3.975E-02	7.173E-01	7.092E-01
6.	87.0	2.617E-01	1.857E-02	4.255E-01	4.233E-01
7.	102.0	1.609E-01	9.094E-03	2.514E-01	2.513E-01
8.	122.0	9.312E-02	4.386E-03	1.407E-01	1.411E-01
9.	142.0	5.856E-02	2.378E-03	8.590E-02	8.640E-02
10.	162.0	3.915E-02	1.404E-03	5.594E-02	5.639E-02
12.	202.0	2.183E-02	6.382E-04	2.978E-02	3.012E-02
14.	242.0	1.189E-02	2.926E-04	1.558E-02	1.579E-02
16.	282.0	7.102E-03	1.501E-04	8.984E-03	9.118E-03
18.	322.0	4.544E-03	8.357E-05	5.571E-03	5.660E-03
20.	362.0	3.064E-03	4.957E-05	3.649E-03	3.710E-03
24.	442.0	1.565E-03	2.019E-05	1.773E-03	1.804E-03
40.	762.0	2.502E-04	1.740E-06	2.460E-04	2.504E-04
100.	1962.0	1.037E-05	2.619E-08	7.674E-06	7.769E-06

TP = Time of peak exposure rate at distance X
X = Centerline distance from ground zero
TYE = Total first year gamma exposure [total exposure from both suspended and deposited debris from arrival time out to 1 year]
CPE = Cloud passage gamma exposure [total exposure during cloud passage...includes exposure due to early deposition]
ITD_GF = Infant thyroid dose (green feed)
ITD_DF = Infant thyroid dose (dry feed)
ER1 = Exposure rate at H+1 hours
DPER = Deposition peak exposure rate [exposure rate at time TP]
TYDE = Total first year gamma deposition exposure [exposure from deposition during and after cloud passage out to 1 year]
RYDE = First year residual deposition exposure [exposure from deposition after cloud passage out to 1 year]

Figure 6.3 Second Page of NSCALE Alphanumeric Output

In the lower left corner of Figure 6.2 is a list of centerline distances as a function of the benchmark TYE and CPE exposures. And, in the lower right corner of the figure is a list of centerline distances as a function of the benchmark ITD_GF and ITD_DF exposures. For example, the distance along the centerline at which the TYE is predicted to drop to 170 mR is about 11 miles.

In the top half of Figure 6.3, the 22 standard TP values and their associated X_p values are once again listed in the first two columns from the left. To the right of these values are computations of ER1, DPER, TYDE, and RYDE. The H+1 hr exposure rate in association with the new event, which has been denoted as $ER1_p$ to this point in this report, is denoted by ER1 in column 3. The predicted Deposition-Peak-Exposure Rate (DPER), the Total-First-Year-Deposition Exposure (TYDE), and the Residual-First-Year-Deposition Exposure (RYDE), all of which are for the new event, are listed in columns 4 through 6 in mR.

As a handy reference, the bottom half of Figure 6.3 identifies the output symbols.

If the option to have a printout is taken, the operator then has the option to have the bottom two thirds of Figure 6.2 printed twice. This additional output is requested when there is a need to give a hard copy of the exposures to EPA.

The printouts are not initialized on the printers until at the very end of the program when NSCALE asks if the print file should be sent to AFOS and/or to the Decwriter.

PLOTS

There are four basic graphic plots that can be generated using NSCALE. The first, as exemplified in Figure 6.4, is a semi-log plot of TYE and CPE versus centerline distance. There is also a log-log plot of TYE and CPE versus centerline distance (not shown here). The third plot, as exemplified in Figure 6.5, is a log-log plot of ITD_GF and ITD_DF versus centerline distance. Finally, there is a log-log plot of DPER versus centerline distance (not shown here). NSCALE will ask the operator if plot files should be created. If the answer is "yes," then the plot files for the HP plotter will automatically be created.[7]

---

[7]These files are:

ns_tye_cpe_sl.spl	(TYE and CPE vs distance, semi-log plot)
ns_tye_cpe.spl	(TYE and CPE vs distance, log-log plot)
tdg_tdd.spl	(ITD_g and ITD_d vs distance, log-log plot)
dper.spl	(DPER vs distance, log-log plot).

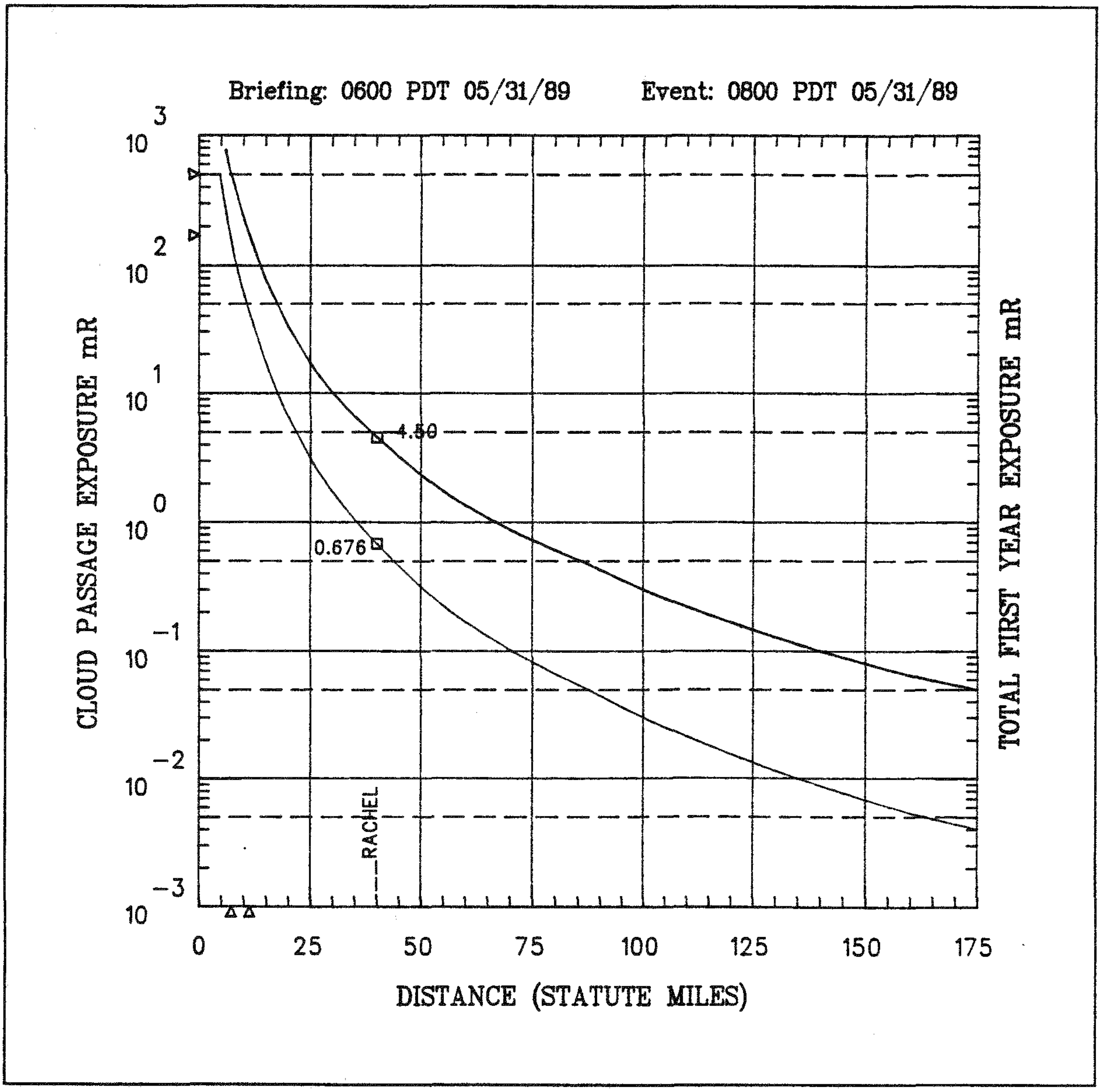

Figure 6.4 Example TYE and CPE Graphics Product

It is the operator's option to create plot files to be sent to the AFOS computer.[8]

---

[8]These files are:

2tb, 2tl, and 2tn	(TYE and CPE vs distance, semi-log plot)
2pb, 2pl, and 2pn	(TYE and CPE vs distance, log-log plot)
2gb, 2gl, and 2gn	(ITD_g and ITD_d vs distance, log-log plot)
2db and 2dl	(DPER vs distance, log-log plot).

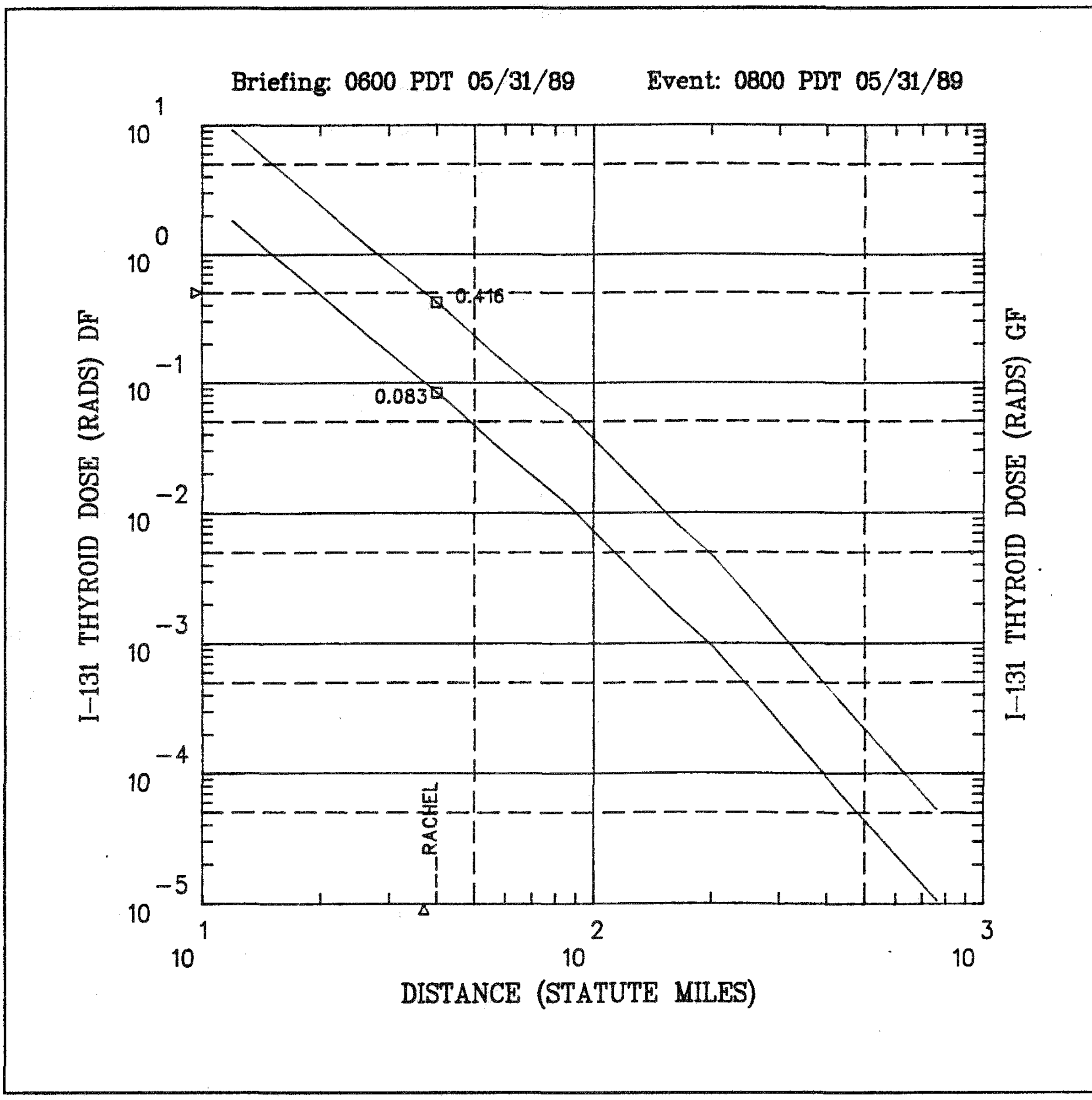

Figure 6.5 Example ITD_g and ITD_d Graphics Products

The TYE and CPE vs distance plot (semi-log) is automatically sent to the HP plotter.[9] The other three plot files can be sent to the HP plotter manually, if desired, by utilizing the graphics spooler commands described in WSNSO's DIGP. Furthermore, all four plots can be displayed on a terminal using the DIGB plot commands. If the operator opts for AFOS plots, all four plots will automatically

[9]This is the exposure chart normally displayed to the Test Controller for the readiness briefings prior to a detonation. This plot file is sent to the HP plotter where a transparency is made for the overhead projector and a hard copy is made for the event files.

be created on AFOS. These plots can be displayed on one of the AFOS graphics monitors and plotted on the Versatec printer.

An option exists to ship the AFOS files either by the line to the DOE building in Las Vegas or by the line to the Control Point 1 (CP-1) at the NTS.

Before any of the plot files are generated, the operator has the option of entering additional information on the plots. First, the names of locations may be entered on the chart in respect to their distance from GZ. Second, the operator may enter the ***briefing*** time and date (the time of the readiness briefing prior to detonation) and the *event* time and date (the proposed time of the event detonation). For example, in Figure 6.4, the town of Rachel is indicated at the bottom of the chart at 40 miles from GZ, and the briefing and event times are shown at the top of the chart. The method of entering this information is exemplified in Appendix C.

At this point in the program, all the calculations and files have been completed. The operator now has the option of entering new data or changing the parameters. If no changes or calculation are wanted, then the program approaches its end. As indicated in Appendix C, a series of messages are displayed following the option not to enter more data. These messages indicate when and where the various files are sent.

CHAPTER 7

PREDICTIONS, OBSERVATIONS, AND CONCLUSIONS

So far in this report, it has been shown how the PIKE analog can be used with the WSNSO Fallout-Scaling Technique to produce external-gamma-exposure estimates in association with containment-designed nuclear testing at the NTS.

This final chapter will (1) present some of the products that are routinely derived from the PIKE Model, (2) offer some observations about the technique, and (3) present conclusions.

FALLOUT PREDICTIONS

While the PIKE Model is, in a strict sense, the method of deriving exposure estimates for a new event from the FOST by utilizing the PIKE-event analog, some people probably associate the PIKE Model with the entire group of fallout predictions that are routinely presented to the Test Controller prior to a containment-designed nuclear detonation.

There are two fallout-prediction products which are based entirely upon the PIKE Model as presented in this report. These are the "Exposure-Versus-Distance Curve" and the "Circle Chart."

The two other fallout-prediction products, the "Onsite-Fallout Pattern" and the "Offsite-Fallout Pattern," are constructed through the utilization of many of the same principles presented in this report. Furthermore, most of the parameters that are input into NSCALE are used in the construction of these two charts. And, some of the exposures calculated in NSCALE are displayed upon these charts. However, the construction of the fallout patterns is a process separate from that of determining exposures by the PIKE Model. It is beyond the scope of this report to discuss the method by which these fallout patterns are derived.

Below are discussions of the four fallout-prediction products (mentioned above) that the radiation briefer routinely presents at readiness briefings prior to the detonation of a nuclear device.

The Exposure-Versus-Distance Curve

The Exposure-Versus-Distance Curve is merely the computer-generated plot of TYE and CPE versus distance, as discussed in Chapter 6 and as exemplified in Figure 6.4 (page 101). While there is also a computer-generated plot of TYE and CPE versus distance displayed on a log-log presentation, only the semi-log presentation (Figure 6.4) is customarily presented at the readiness briefings.

The range of downwind-centerline distances, which are plotted along the abscissa, is dependent upon the average wind speeds, V_p (the greater the speeds, the greater the range). Since CPE is a component of TYE, the TYE values are always higher. Thus, the TYE curve is always the top curve in the plot.

The two small arrowheads along the left side of the ordinate mark the 500 and 170 mR positions. There are two related arrowheads along the bottom of the abscissa, which show the distance at which the 500 and 170 mR TYE values are predicted to occur.

As discussed in Chapter 6, locations of cities, towns, camps, etc. can be shown on these charts. In Figure 6.4, the town of Rachel is indicated to be on (or close to) the predicted centerline about 40 miles (along the centerline) from GZ. The two values next to the two squares on the TYE and CPE curves are the predicted values of TYE and CPE at Rachel.

The Circle Chart

The Circle Chart for a new event shows the centerline distance of the 170 mR TYE estimates from GZ for four meteorological situations. This chart, which is usually presented to safety officials about a week before the detonation, can be used as an aid in isolating offsite areas where there might be a potential problem in association with the 170 mR-TYE-guideline limitation. An example Circle Chart is shown in Figure 7.1. This was the Circle Chart for the TEXARKANA event.

The four meteorological cases used in constructing a Circle Chart cover a wide range of possibilities. Case 1 is a typical light-wind situation where there is a large amount of wind shear. Case 4 is a typical strong-wind situation where the cloud height is inhibited somewhat and the wind shear is relatively small. Cases 2 and 3 involve parameters between the Case-1 and Case-4 extremes. Obviously, due to the slower wind speeds and greater amounts of dispersion associated with a Case-1 scenario, the centerline distance to the 170 mR value is much less than that for the Case-4 scenario.

A circle chart neglects wind directions. In using a circle chart, it is assumed that the wind might be blowing in any direction at the time of detonation. Thus, the 170 mR distance for a particular case is used to draw a circle with its center positioned at GZ. The intersection of this circle with a line extending from GZ in the direction toward which the wind is forecast to blow, shows where the 170 mR position might be.

The hatched area in a circle chart shows the areas where the population is too dense to be controlled. That is, if there were a massive venting, it would be highly unlikely (and impossible in certain cases) that EPA personnel could properly shelter or evacuate the populations in the hatched area. The un-hatched area shows the areas where the populations could be sheltered or evacuated if there was a massive venting.

Consequently, if a town in the uncontrolled area lies inside of a particular circle, then the population there would be subject to TYE exposures of greater than 170 mR if the centerline extended over that town.

For example, in Figure 7.1, the town of Alamo (about 50 mi east-northeast of GZ) is in the uncontrolled area. In a Case-1 scenario, Alamo would be outside of the circle. This would indicate that there would not be a problem if the debris was carried toward Alamo under Case-1 conditions. However, there would be a problem under a Case-2 scenario since Alamo lies within the Case-2 circle.

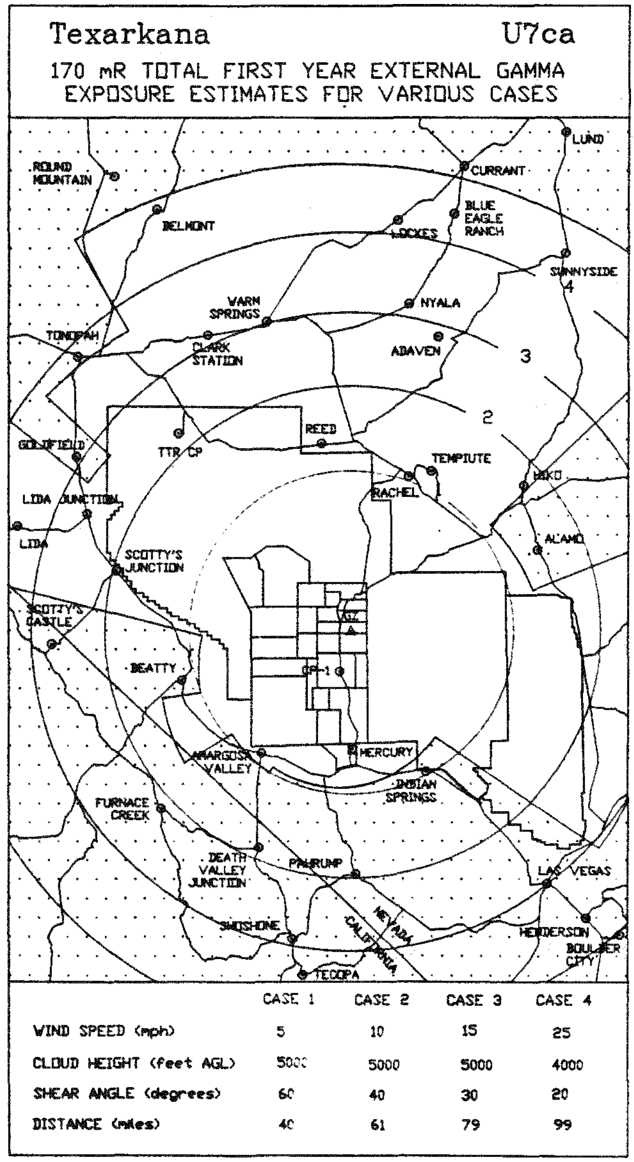

Figure 7.1 Circle Chart Example

The Onsite-Fallout Pattern

An example of an Onsite-Fallout Pattern is shown in Figure 7.2. This is a fallout pattern for the hypothetical HUSHPUPPY event. [The NSCALE calculations shown in Figures 6.2 and 6.3 (pages 98 and 99) and in Appendix C were made in association with this hypothetical case.]

For the HUSHPUPPY event, GZ was located in NTS Area 2. The line extending from GZ north-northeastward is the predicted centerline. The positions of the predicted 500 and 170 mR values are indicated by the two small arrows pointing toward the centerline. These downwind positions (7.1 and 11.2 mi) were taken from the benchmark locations shown at the bottom of Figure 6.2 (page 98).

The predicted centerline position of the leading edge of the fallout at H+1 hr is shown slightly downwind from the exposure arrows. This distance is marked using the derived mean transport speeds, which are shown in the middle of the legend box on the left side of the figure.

The hatched area within the lines on either side of the centerline is the predicted fallout sector.

As stated above, the only parts of this chart that are directly derived from the PIKE Model (NSCALE) are the positions of the 500 and 170 mR values.

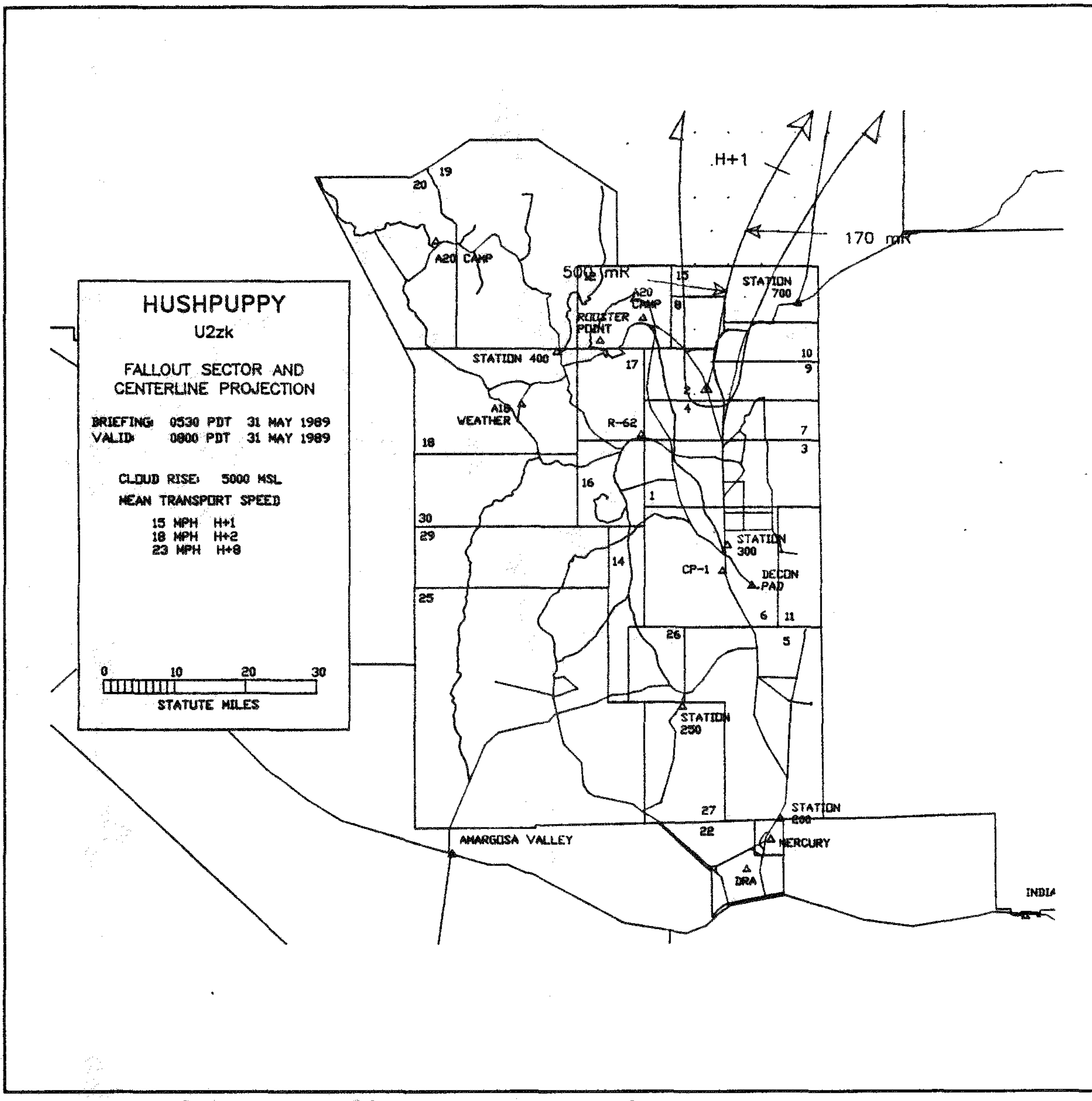

Figure 7.2 Onsite-Fallout-Pattern Example

The Offsite-Fallout Pattern

Figure 7.3 shows the Offsite-Fallout Pattern for the hypothetical HUSHPUPPY event. The same basic predictions are shown in this figure as where in the onsite pattern. However, in this case, the fallout pattern is extended much farther downwind.

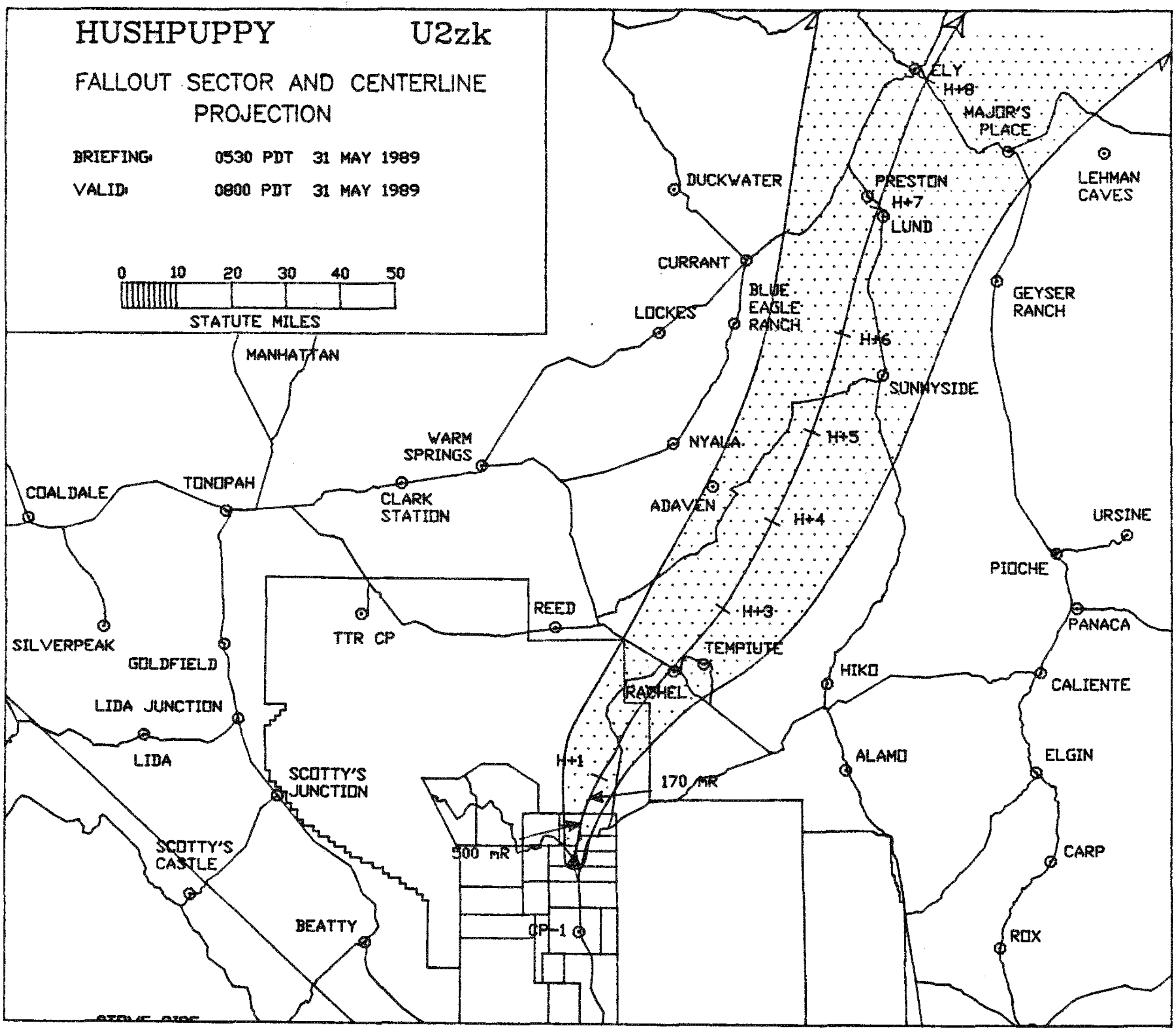

Figure 7.3 Offsite-Fallout-Pattern Example

POST-EVENT PREDICTIONS

As mentioned in Chapter 1, the PIKE Model can be utilized in association with an actual massive venting. Once such a venting does occur, there is initially very limited radiological data that can be used to help derive estimates of downwind exposures. During the first 15 minutes after such a venting, the downwind exposures would most likely have to be based upon the pre-event estimates.

However, when the debris cloud stabilizes, an actual cloud height would be known from aircraft measurements and actual winds through the depth of the cloud would be available. With this information, NSCALE could then be run using the actual meteorological conditions and assuming that the venting was like PIKE. Obviously, these estimates would be gross approximations, especially it is apparent from visual observations and GZ RAMS data that the new event was very different from PIKE.

A more reasonable set of exposure predictions could be available about an hour after the venting, assuming that the national laboratory conducting the detonation could provide a preliminary radiological source-term estimate. This estimate is the number of beta curies released, normalized to H+12 hr. It is known that there were 120,000 H+12 hr beta curies released in association with PIKE. To create the source term, R, for NSCALE, the estimated value of curies released for the new event would be divided by the value of curies released in association with PIKE. Then NSCALE could be run using this R value along with the latest available wind data.

These estimates would remain approximations since the assumption is still made that the new venting is similar to the PIKE venting. Obviously, these estimates would be in error if the fission products released were considerably different from PIKE. Comparing H+12 hr curies from ventings that had different venting times, and therefore different fission products, would be like comparing apples with oranges.

Thus, while the PIKE Model can be used in association with actual ventings to provide preliminary downwind exposure estimates along the predicted centerline, it must be realized that such estimates are merely "first guesses." Only when downwind radiological data are collected for analyses of decay rates and fallout intensities can more accurate fallout predictions be made.

OBSERVATIONS

In the final sector of this chapter, conclusions about the PIKE Model will be presented. However, before going into these conclusions, there are several aspects of the PIKE Model that need to be brought into focus.

The Effects of Parameter Changes

The radiation briefer, at a readiness briefing, is sometimes asked to comment about the effects upon a certain set of exposure estimates if one of the parameters were changed. For example, "What would be the effect upon the TYE estimates at Alamo if the winds speeds were actually twice as strong as predicted?" Or, "How much farther out would the 170 mR TYE position extend if twice as much debris was released as predicted?" Of course, the obvious solution would be to rerun NSCALE with the desired parameter changes. However, the briefer does not always have this option. Appendix D discusses the sensitivity of PIKE-Model exposure estimates to various changes in parameters.

Limiting Assumptions

In Chapter 2 (pages 18-19), a summary of simplifying assumptions used to derive the FOST were presented. Since these assumptions are not realistic at times, it is important to assess their effect upon the FOST's estimates.

Obviously, the assumptions that (1) all fallout particles are considered to be spherical and (2) all fallout particles are considered to have a uniform density are not realistic. However, it would be extremely difficult to develop a fallout model which could handle the entire range of particle shapes and densities. Furthermore, it would be impossible to predict the initial distributions of particle shapes and densities even if such a model could be developed. The FOST, as well as any other fallout model, is apparently stuck with these two assumptions no matter what their effects on the final estimates. However, since the FOST was proven to be successful in predicting exposures in association with cratering detonations (Reference 1.1), it appears that these two simplifying assumptions are appropriate.

The assumption that the air density remains constant not only with altitude but also both in the horizontal plane and in time could be a problem if the technique was applied to a relatively deep debris clouds or was used to derive exposure estimates for distances well downwind of the NTS. While differences in air densities exist even in atmospheric layers only several thousand feet thick, they are usually minor. In most instances, a debris cloud would have to be much higher than the PIKE cloud to be affected by significantly different air densities. Furthermore, while air densities do vary in the horizontal and with time, such variances are usually minor for local-fallout areas unless there is a significant change of air mass (e.g., a cold-front passage).

Another problem associated with air densities could be the difference between the air densities associated with the PIKE event and those densities associated with the new event. The PIKE Model implies that those densities should be similar. Obviously, the mid-March air densities associated with PIKE could be considerably different from the mid-August air densities associated with a new event. Such differences could affect the performance of the PIKE Model but it would be quite difficult to establish quantitative effects.

As discussed earlier, the assumption that the atmosphere is divided into layers of equal thickness each with a particular uniform wind velocity, is not an unrealistic assumption as it is applied to the FOST. The WSNSO routinely collects upper-wind data for 1000-ft layers to 10,000 ft MSL and for 2000-ft layers from 10,000 to 20,000 ft MSL. Wind predictions are usually made for the same layers. The wind-velocity values for each layer are derived by averaging the velocities within each layer. Since the layers are relatively shallow, it is reasonable to assume that the average wind velocity is representative of the wind throughout the layer. Thus, uniform wind velocities for layers of equal thickness can easily be made available for use with the FOST.

The method of varying the meteorological parameters, as discussed in Chapter 4 (page 68), gets around the initial assumption that the wind velocity remains constant not only in time but also in the horizontal plane.

The assumption that the vertical components of the wind (updrafts and downdrafts) are insignificant is a reasonable assumption. However, safety officials should be aware that this assumption does not apply well when there are thunderstorms in the vicinity or when weather conditions favor orographic lifting. Both the horizontal and vertical movements of debris in the vicinity of a thunderstorm or near mountain ridges during very windy conditions can be radically changed from what might be expected. For example, a downdraft could rapidly transport debris to the surface which, under normal circumstances, would have been deposited much farther downwind. As a result, there could be areas of enhanced exposures due to vertical components of the wind associated with thunderstorms.

The assumption was also made that the effects of atmospheric diffusion are insignificant. This assumption is probably appropriate when the atmospheric stability in association with the analog event is similar to that in association with the new event. For the PIKE event, the effects upon the transport of particles by chaotic motions of the air were relatively minor. This is typical for a moderate- to strong-wind situation. However, in light-wind situations, the effects of chaotic motions are more pronounced. In a light-wind situation, the debris would probably be spread out more than indicated by the PIKE Model due to atmospheric dispersion. Thus, PIKE-Model exposure estimates for light-wind situations might be overestimated.

Finally, one assumption that has not been specifically stated but that should be obvious is that it is assumed that the debris is not affected by precipitation scavenging. Rain in downwind areas can have a significant influence upon fallout exposures. It is often assumed that an exposure at a downwind location could be ten times higher if rain occurred during cloud passage.

Awareness of the Limitations of the PIKE Model

Like any predictive technique, there are recognizable shortcomings in the PIKE Model which have to be considered when evaluating resultant estimates. These limitations were presented to the nuclear-testing community before the PIKE Model was ever utilized and have been carefully scrutinized every few years by various committees composed of members throughout the testing community. For each nuclear detonation, the Test Controller has always had safety advisors that were familiar with the limitations of the PIKE Model, who could interpret the PIKE Model output.

This report has enumerated the limits of the PIKE Model and can be used as an aid in keeping these limitations in the open.

The PIKE Model Versus Mathematical Fallout Models

Since the inception of the PIKE Model, there has been almost continuous pressure from various groups for a more sophisticated approach to making exposure estimates. Committees formed to recommend other models have usually expressed dissatisfaction with the PIKE Model at the onset of their inquiries, but have always failed to agree on a better approach.

Ideally, a mathematical fallout model would be more acceptable than the PIKE Model. If an atmospheric-transport model, which could predict small-scale air circulations over mountainous terrain, could be merged with a fallout model, which could simulate the deposition of radioactive particles transported by the winds, then the alleged "guesswork" sometimes attributed to the PIKE Model could be eliminated.

But, as shown in this report, there are two major obstacles that have prevented such an ideal model from replacing the PIKE Model. One has been the lack of a sophisticated prognostic air-transport model, and the other is the inability for anyone to predict realistic initial particle-size and activity distributions.

There are currently a few mathematical models which are advertized to "predict" where fallout will be deposited. While these models incorporate atmospheric-transport models, they are not necessarily predictive in nature. It is true that such models can be manipulated to approximate actual deposition patterns. However, the meteorological conditions input into the model to produce these fallout patterns are ***observed*** and not predicted. Thus, the models may be good diagnostic tools, but are not necessarily good prognostic tools. (They can be used to predict but will fail when the meteorological conditions change.)

Furthermore, while such models might handle particle transport reasonable well in a diagnostic sense for areas well downwind from GZ, they do not normally do well in describing local fallout. This is primarily due to the inability of the model to properly handle the local terrain effects that are crucial to local-fallout estimates.

At the present time, WSNSO meteorologists, armed with (1) the latest predictions derived from some of the most highly sophisticated prognostic atmospheric models available, (2) objective predictive techniques utilizing a comprehensive local meteorological network, and (3) the intimate knowledge of local weather and terrain features, have a much better chance of accurately predicting downwind fallout areas than any of the current mathematical fallout models.

However, prognostic atmospheric models which can handle local terrain effects are now becoming available. WSNSO should obtain such a model in the near future. The availability of such a model should further enhance WSNSO's radiological-prediction capabilities.

Even if a reliable prognostic atmospheric-transport model is utilized, the second major obstacle, predicting the initial particle-size and activity distributions, will still have to be overcome. Of course, the solution of this problem is not entirely the responsibility of WSNSO. If the national laboratories can provide such distributions, then WSNSO will be able to provide the fallout patterns based upon them.

The fact remains that, at the present time, such initial radiological distributions are not available. In order to deal with this void, the current mathematical fallout models partition the initial cloud into a number of layers containing a certain number of particles with an arbitrary range of sizes. A certain percentage of the total activity released into the atmosphere is assigned to each of the layers. The model then allows the particles to be deposited based upon the atmospheric-transport portion of the model.

If one of these diagnostic models is used to "predict" a fallout pattern, the credibility of the resultant estimates would be severely challenged due to the arbitrary and simplistic manner in which the cloud was partitioned. If the particle-size and activity distributions can not be forecast, how would anyone know how to partition the cloud in the model? In order to mitigate this situation, the mathematical fallout model would have to be compromised somewhat by adopting an analog event.

It could be assumed, in a manner similar to the FOST, that the new event would vent like a worst-case analog (e.g., PIKE) and that this new event would have the same particle-size and activity distributions. Then, using the observed analog radiological and meteorological data, one could repeatedly run the mathematical fallout model, each time changing the size of the cloud partitions and/or the activities and particle sizes attributed to the partitions until the resultant analog pattern approximated the actual analog pattern. It would then be assumed that the "successful" partition/parameter combination which approximated the actual fallout pattern would be applicable to the new event. Thus, the "mathematical fallout model" could have a PIKE analog. It would be assumed that the new event would have the same partition/parameter combination as that used in the mathematical fallout model to approximate the PIKE fallout pattern.

The problem with this approach is that while one simplistic partition/parameter combination may approximate the analog pattern, it is not necessarily a unique solution. There would probably be other combinations that would also approximate the analog pattern. But in order to utilize such an analog mathematical fallout model, it would have to be assumed that such a solution was unique.

In the future, when reliable prognostic atmospheric-transport models are available, such a partitioning technique may be employed by WSNSO if a better technique can not be found. But until reliable prognostic models are put into service, it remains doubtful that mathematical fallout models with their simplistic partitioning assumptions can do as well as the PIKE Model.

CONCLUSIONS

For 25 years, the PIKE Model has served as the primary technique for which exposure estimates are made for immediate-downwind populations in association with containment-designed nuclear testing at the NTS. To many safety officials, it has become a convenient, reliable yardstick to measure potential hazards from one nuclear detonation to the next.

Many assumptions were made in the derivation of the PIKE Model. Obviously, if any of these assumptions are seriously violated in applying the PIKE Model, then the resultant estimates should be suspect. Based upon these assumptions, one can deduce that the PIKE Model should function very well if:

(1) the new-event particle-size and activity distributions were quite similar to those of PIKE,

(2) the new-event radiological source term, f_pY_p, was properly predicted,

(3) the thermal energy released during the new event was similar to that released with PIKE,

(4) the new-event meteorological parameters, V_p, H_p, and α_p, were based upon accurate meteorological predictions,

(5) the new-event meteorological parameters did not vary significantly in time or space,

(6) the wind directions through the depth of the debris cloud did not vary more than 90°, and

(7) there were not any significant, abrupt changes in the weather (e.g., thunderstorms, rain, or frontal passages) as the cloud moved downwind.

To the contrary, the PIKE Model would definitely fail if conditions opposite to all those listed above occurred. Realistically, one would not expect all seven of the above conditions to be either fulfilled or violated.

As discussed in this report, it is unlikely that conditions (1), (2), and (3) would verify. This situation, of course, is due to the inability to predict the venting mechanism and is a common problem shared by all fallout-prediction models. However unlikely it may be that these three conditions verify, it is necessary to assume that they will. This follows from the reasoning that it is better to have estimates based upon these unlikely assumptions than to have either no estimates at all or estimates based upon pure speculation.

It is quite likely that the meteorological forecast will verify, and, therefore that the PIKE-Model meteorological parameters should be correct. The Test Controller does not allow a detonation if the forecast conditions are significantly different from those being experienced shortly before a detonation is scheduled. If there is a discrepancy between the forecast and what is observed, a revised forecast is issued and new parameters are input into the PIKE Model before the detonation is allowed. Thus, condition (4) is usually fulfilled.

Though it would be best if the meteorological parameters did not significantly vary in time and space, they often do. While the PIKE Model performs best when they do not vary, reasonable estimates can still be obtained when they do. If there is considerable variance (contrary to condition 5), estimates made for locations close to the NTS should be reliable with some deterioration in the estimates at locations farther downwind. Usually, the estimates made at closer distances are more critical to safety officials; thus, this situation is not normally much of a problem.

Violation of condition (6) is often a problem. In light-wind situations, there is frequently more than 90° of difference in wind directions within the depth of the debris cloud. This report has discussed how the PIKE Model can be applied to such situations to give reasonable estimates. However, safety officials should be aware that exposure estimates in such circumstances are not as reliable. Fortunately, when the winds are light and there is much wind shear, much of the debris would be deposited on the NTS and the debris that did reach offsite areas would be depleted due to radioactive decay and atmospheric dispersion. Thus, the reliability of the estimates is not as critical in these situations.

While it is always assumed that condition (3) will verify in order to get meaningful exposure estimates, safety officials should not overlook the possibility that more energy will be released and that the new-event debris cloud could rise much higher than assumed in the PIKE-Model calculations. Failure to consider this possibility might result in some debris being deposited on populated areas such as Las Vegas.

The PIKE Model, which was adopted as a "temporary solution" to a very complex problem, is still in use after 25 years of service to the nuclear testing community. It is far from an ideal fallout model and will eventually be replaced. However, it will continue to be used until other models manage to establish the thread to reality that the PIKE Model established 25 years ago.

REFERENCES

1.1 Cluff, F.D., and Palmer, T. R., *A Fallout Scaling Model for the Prediction of Gross Gamma Dose Rates from Earth Cratering Detonations*, Weather Bureau Research Station (currently, Weather Service Nuclear Support Office), Las Vegas, Nevada, 1964. Unpublished manuscript.

1.2 Stopinski, O.W., *Fallout Predictions as of 1957*, LA-9993-MS UC-11, Los Alamos National Laboratory, Los Alamos, New Mexico, March 1984.

2.1 Glasstone, S., et al., *The Effects of Nuclear Weapons*, U.S. Energy Research and Development Administration (currently, U.S. Department of Energy), Washington, D.C., 1977.

4.1 Malik, J.S., et al., *Radiological Criteria for Underground Nuclear Tests*, LA-8776-MS, Los Alamos Scientific Laboratory (currently, Los Alamos National Laboratory), Los Alamos, New Mexico, 1981.

4.2 Steadman, C. R., *Analysis of Operation UPSHOT-KNOTHOLE Nuclear Test SIMON Radiological and Meteorological Data*, NVO-315, Weather Service Nuclear Support Office, Las Vegas, Nevada, July 1988.

4.3 Germain, L.S., and Kahn, J.S., "Phenomenology and Containment of Underground Nuclear Explosions", *Technical Discussions of Off-site Safety Programs for Underground Nuclear Detonations*, NVO-40, U.S. Atomic Energy Commission (presently, U.S. Department of Energy), Nevada Operations Office, Las Vegas, Nevada, February 1969.

4.4 Hicks, H.G., *Results of Calculations of External Gamma Radiation Exposure Rates from Fallout and the Related Radionuclide Compositions*, UCRL-53152 (8 parts), Lawrence Livermore National Laboratory, Livermore, California, July 1981.

4.5 Briggs, G.A., *Plume Rise*, TID-25075, Air Resources Atmospheric Turbulence and Diffusion Laboratory, Environmental Science Services Administration (currently, the National Oceanic and Atmospheric Administration), Oak Ridge, Tennessee, November 1969.

5.1 Quinn, V.E., and Steadman, C.R., *1985 Analyses and Evaluations of the Radiological and Meteorological Data for the PIKE Event*, NVO-308, Weather Service Nuclear Support Office, Las Vegas, Nevada, December 1986.

6.1 Knapp, H.A., *Iodine-131 in Fresh Milk and Human Thyroids Following a Single Deposition of Nuclear Test Fallout*, U.S. Atomic Energy Commission (currently, the U.S. Department of Energy), Washington, D.C., June 1963.

APPENDIX A

RADIOLOGICAL TERMS

As pointed out at the end of Chapter 2, there are certain radiological terms that should be specifically defined for a better understanding of the derivation of the FOST.

Radioactivity is the spontaneous emission of radiation, generally alpha or beta particles and often accompanied by gamma rays, from the nuclei of an unstable (radioactive) isotope. As a result of this emission, the radioactive isotope is transformed into the isotope of a different element which may or may not be radioactive. The number of nuclear transformations which occur per unit of time is defined as the ***activity*** of a radioactive sample. A common unit of activity is the ***curie (Ci)***, which is 3.7 x 10^{10} transformations per second. A ***gamma-curie*** is the activity of material in which 3.7 x 10^{10} gamma rays are emitted per second.

A ***photon*** is a unit or "particle" of electromagnetic radiation, carrying a quantum of energy which is characteristic of the particular radiation. Electromagnetic radiation, in the form of one or more gamma photons is generally emitted during a nuclear disintegration.

Ionizing radiation is electromagnetic radiation (e.g., gamma ray) or particulate radiation (e.g., alpha particle) that is capable of producing *ions* (electrically charged particles) in its passage through matter. *Ionization* is the separation of a normally electrically neutral atom or molecule into electrically charged components. Air is ionized when exposed to gamma radiation and electrical charges are liberated. ***Exposure*** is a measure of ionization of air by gamma rays. A special unit of exposure is the ***roentgen (R)*** and is the quantity of electrical charge liberated in a known mass or volume of air. (Technically, the roentgen is that amount of gamma or X-rays required to produce ions carrying 1 electrostatic unit of electrical charge in 1 cubic centimeter of dry air under standard conditions.)

The ***dose*** is the quantity (total or accumulated) of ionizing radiation received. As can be seen in Reference 1.1, at the time the FOST was first derived, the term "dose" was used to indicate what today is referred to as exposure or ***exposure dose***. The exposure dose is expressed in roentgens, which, as pointed out above, is a measure of the total amount of ionization that the quantity of radiation could produce in <u>air</u>. Exposure should be distinguished from the ***absorbed dose***, which is measured in rads. Absorbed dose represents the energy absorbed from radiation in a gram of <u>any material</u>.

Fission is the process in which the nucleus of a heavy element, such as uranium-235, splits into nuclei (usually two) of lighter elements with the release of substantial amounts of energy. All nuclear detonations employ the fission process; but, in some cases (such as in thermonuclear devices), only a fraction of the energy released is directly due to fission. The ***yield*** (energy yield) of a nuclear detonation is the total effective energy released by the explosion. It is usually expressed in terms of the equivalent tonnage of TNT required to produce the same amount of energy. The ***fission yield*** of a nuclear detonation is the energy associated with the fission process. The ***fission plus induced activity yield***[1] of a nuclear detonation is the energy associated with the fission process plus the energy associated with the induced activity.

Induced radioactivity is radioactivity produced in certain non-radioactive materials, such as those found in the casings of nuclear devices or in the soil or air surrounding the devices. This radioactivity is produced as a result of nuclear reactions, especially the capture of neutrons. The reactions are accompanied by the formation of unstable (radioactive) nuclei.

---

[1]The fission plus induced activity yield is referred to as the fission+ yield in this report.

APPENDIX B

NSCALE COMPUTER CODE

As mentioned in Chapter 6, the NSCALE computer code has been written in Fortran 77.[1] The version of this code which runs on the WSNSO Data General machines is presented in this appendix.

[1]NSCALE has been developed by Robert Duke of WSNSO.

```
      PROGRAM NSCALE

c new scaler   1987
      character*1 icyc, nplt, plt_afos, plt_hpdoe, plt_hpnts, afos_line_doe
      character*1 plt_tye_hpdoe, plt_tdg_nts, text_afos, text_qla, ians
      character*30 nfile, nblank
      character*30 print_file
      character*9  afos_file
      character*3  route

      include 'scaler_params'
      logical yes, exist

      include 'data_int'

      print_file = 'NSCALE.PRINT'
      afos_file  = 'DOELSCALE'
      route      = 'NTS'

c enter data
      icnts = 0
   10 call scinp(tp, r, vp, hp, alfa, last_input, icnts)
c compute data
      call scaler_a(icyc)

c plot graphs
     IF(yes (' <007> <012>  Create plot files (y/n)? [n] ',nplt) ) THEN

        write (10, '(" <012> When sending plots to AFOS the semi_log plot ",
    +"will be sent to the HP plotter!")' )
      if(yes (' <012>    Send plots to AFOS (y/n)? [n] ',plt_afos) ) then
         nfile = nblank
         nfile = 'tye_tdg_afos'
     open (1, file=('='//NFILE), IOSTAT=IOS,ERR=20,STATUS='NEW',RECFM='DS')
         close (1, IOSTAT=IOS, ERR=20)

c.. default tocpl line
         write (10, '("    Using line to DOE(y/n)? [n] ",$)' )
         read  (11, '(al)' ) afos_line_doe
         if( afos_line_doe .eq. 'Y' ) afos_line_doe = 'y'
      endif
   20 continue
c.. locations on plots
     if(yes (' <007> <012>  Enter Locations  (y/n)? [n] ',ians) ) then
           call ns_locations(plt_afos, afos_line_doe)
     else
           call plot_graphs(plt_afos, afos_line_doe)
     endif

      write (10, '(/," <007> AFOS PLOTS sent .... Plot sent HP when ",
    +"program exited..last plot saved")' )

     ENDIF

c recycle for new data entry or changes to last input
```

```
        if(yes (' <012>  New data or change parameters (y/n)? [n] ',icyc) )
     +go to 10

        inquire (file = ('='//'nolptfile'), exist=exist)
       IF( .not. exist) then

c output text file can be sent to AFOS and/or decwriter
         if(yes (' <012>   Send PRINT file to AFOS (y/n)? [n] ',text_afos)) then
          open (1,status='old', file = ('='//'no_doelscale'), iostat=ios)
            if(ios .eq. 0) close (1,status='delete',err=140)
            close (12)
  140       call afos_text_file(print_file, afos_file, route)
        endif

        if(yes (' <012>  Send PRINT file to decwriter (y/n)? [n] ',
     +text_qla ) ) then
            open (1,status='old', file = ('='//'no_qla120'), iostat=ios)
            if(ios .eq. 0) close (1,status='delete',err=160)
  160       continue
        endif

       ENDIF

        stop
        end


        Subroutine Afos_text_file(product, afos_file, route)
        integer unit_num_prod/20/, unit_num_afos/21/
        character    afos_line(80)
        character*30 product
        character*9  afos_file
        character*3  route
        character*9  afos_header_1/"<cr><lf><lf><lf>ZCZC "/
        character*2  afos_header_2/"<305><200>"/
        character*2  cr_lf/"<cr><lf>"/
        character*4  cr_cr_lf/"<nul><cr><cr><lf>"/, blank_4/"    "/
        character*2  null_blank/"<nul> "/
        character*1  afos_??/"*"/
        character*10 afos_trailer/"<nul><cr><cr><lf>NNNN <nul>"/

c A text file converted to a AFOS text file with proper heading and trailer
C This portion will take a filename, or pathname and open a channel for
c reading on AOS

        open(unit_num_prod, file = ('='//product), status= "old", iostat= ier,
     +  err= 999, recfm= "ds", pad= "yes")

C Open the file to be shipped to AFOS, and write in the AFOS header

        open(unit_num_afos, file = ('='//afos_file), status= "fresh", carriage
     +  control= "none",recfm="DS")

        write(unit_num_afos, fmt= 203) afos_header_1, afos_file, afos_??
     +  , route, cr_lf, afos_header_2, CR_CR_LF
```

```
 203   format(8A)
 200   format(7A)

C Read a line into array from product file

 1000   read(UNIT_NUM_prod, fmt= 201, RETURNRECL= IBYTE, iostat= ier, err= 998
     + ,END= 800) AFOS_LINE
 201    format(80A1)


C Write a line into the AFOS product

        write(unit_num_afos, fmt= 100)(afos_line(I),I=1,IBYTE), Cr_cr_lf

 100    format(a,a)

        go to 1000

C write the trailer into the AFOS product

 800    write(unit_num_afos, fmt= 202) afos_trailer
 202    format(a)

C Close up shop

        close(unit_num_afos)
        close(unit_num_prod)
        return

C error messages

 999    write(*,300) product, ier
 300    format("<nl><NL><tab>Unable to open file ",a,". Error = ",i5)
        return

 998    write(*,301) product, ier
 301  format("<nl><nl><tab>Problem in reading from file ",a,". Error = ", i5)
        return
        end


        Subroutine Comb_bf(xbf, ybf, xbf_spl, ybf_spl,xbf_comb, ybf_comb)
        dimension xbf(*),ybf(*),xbf_spl(*),ybf_spl(*),xbf_comb(*),ybf_comb(*)

c this routine combines two arrays with ascending centerline distances
c into one array for plotting

        j = 1
        k = 1
        l = 0
        xbf_comb(32) = -9999.
        do 10 i = 1, 31
              l = l + 1
              if(l .gt. 31) go to 20

              if(xbf(j) .eq. xbf_spl(k) ) then
```

```
                  if(xbf(j) .eq. -9999.) go to 20
                  xbf_comb(l) = xbf(j)
                  ybf_comb(l) = ybf(j)
                  j = j + 1
                  k = k + 1
           endif

           if(xbf(j) .lt. xbf_spl(k) ) then
                  if(xbf(j) .eq. -9999.) then
                     xbf_comb(l) = xbf_spl(k)
                     ybf_comb(l) = ybf_spl(k)
                     k = k + 1
                  else
                     xbf_comb(l) = xbf(j)
                     ybf_comb(l) = ybf(j)
                     j = j + 1
                  endif
           else
                  if(xbf_spl(k) .eq. -9999.) then
                     xbf_comb(l) = xbf(j)
                     ybf_comb(l) = ybf(j)
                     j = j + 1
                  else
                    xbf_comb(l) = xbf_spl(k)
                    ybf_comb(l) = ybf_spl(k)
                    k = k + 1
                  endif
           endif

 10   continue
      l = l + 1
 20   if(l .le. 32) xbf_comb(l)  = -9999.
      if(l .gt. 32) xbf_comb(32) = -9999.

      return
      end


      Subroutine Define_data( id )

c definitions of column abbreviation on text printout

      write (id, '(////)' )
      write (id, '(4x,
     +" TP        =  Time of peak exposure rate at distance X")')
      write (id, '(4x,
     +" X         =  Centerline distance from ground zero")')
      write (id, '(4x,
     +" TYE       =  Total first year gamma exposure  [total exposure from")')
      write (id, '(4x,
     +12x," both suspended and deposited debris from arrival time")')
      write (id, '(4x,
     +12x," out to 1 year ]")')
      write (id, '(4x,
     +" CPE       =  Cloud passage gamma exposure  [total exposure during",
     +" cloud")')
```

```
      write (id, '(4x,
     +12x," passage...includes exposure due to early deposition]")')
      write (id, '(4x,
     +" ITD_GF   =  Infant thyroid dose (green feed)")')
      write (id, '(4x,
     +" ITD_DF   =  Infant thyroid dose (dry feed)")')
      write (id, '(4x,
     +" ER1      =  Exposure rate at H+1 hours")')
      write (id, '(4x,
     +" DPER     =  Deposition peak exposure rate  [exposure rate at time ",
     +"TP]")')
      write (id, '(4x,
     +" TYDE     =  Total first year gamma deposition exposure  ",
     +"[exposure from")')
      write (id, '(4x,
     +12x," deposition during and after cloud passage out to 1 year]")')
      write (id, '(4x,
     +" RYDE     =  First year residual deposition exposure  [exposure ",
     +"from")')
      write (id, '(4x,
     +12x," deposition after cloud passage out to 1 year]")')
c
      return
      end


      Subroutine Dskw  (NFILE,NBLANK,NFCOM,X, Y)
      CHARACTER*30 NFILE, NBLANK, NFCOM
      DIMENSION X(*),Y(*)

c  write data to disk from a one dimension array

      OPEN (1,FILE=('='//NFILE), IOSTAT=IOS, ERR=999, STATUS='NEW',RECFM='DS')
    5 WRITE (1, '(A30)' ) NFCOM
      DO 10  I = 1,300                        !WRITE  DATA TO DISK
            IF(X(I).EQ.-9999. .OR. Y(I).EQ.-9999.) THEN
               xend = -9999.
               yend = -9999.
               write (1,  '(1P2E13.5)' ) xend, yend
               GO TO 20
            ELSE
               write (1,  '(1P2E13.5)' ) x(i), y(i)
            ENDIF
   10 CONTINUE

   20 CLOSE (1, IOSTAT=IOS, ERR=88)
      RETURN

  999 continue                                 !OVERWRITE DEL OLD
         OPEN (1, FILE=('='//NFILE), IOSTAT=IOS, ERR=888, STATUS='OLD')
         CLOSE(1,IOSTAT=IOS,ERR=888,STATUS='DELETE')
     OPEN (1, FILE=('='//NFILE), IOSTAT=IOS, ERR=888, STATUS='NEW',RECFM='DS')
         GO TO 5

  888 WRITE (10,'(/," UNABLE TO OVERWRITE  ",A30," IOS = ",I5)' ) NFILE,IOS
      NFILE = NBLANK
```

```
      RETURN

88    WRITE (10, '(/," UNABLE TO CLOSE CHANNEL AFT WRITE   IOS = ",I5)' )  IOS
      RETURN
      END

      Subroutine Find_xy(itype_fit,ixfind,xold,yold,xspecial,yspecial,
   +  mina,maxa,ynfit)
      dimension xold(*), yold(*), ynfit(*)
      character*1 ixfind

c  Find  X if Y is know   or  Find  Y if X is known

c itype_fit  type of fit,  1 = linear, 2 = exponenital, and 3 = power fit
c ixfind     determines whether to solve for x or y.
c            If ixfind .eq. 'y'   solve for x
c            If ixfind .ne. 'y'   slove for y
c xold       x array
c yold       y array
c xspecial   x value
c yspecial   y value
c mina       min value of array
c maxa       max value of array
c ynfit      new array for y best_fit [not used]

      if( ixfind .eq. 'y') go to 15
      do 10 i = mina, maxa                            !x known fine y

            if( xold(i) .eq. xspecial ) then
                  yspecial = yold(i)
                  go to 30
             endif

             if( xold(i) .gt. xspecial ) then
                if( i .eq. 1 ) then
                      minl = 1
                      maxl = 2
                      go to 20

                else
                      minl = i -1
                      maxl = i
                      go to 20
                endif
             endif

 10   continue
      minl = maxa - 1
      maxl = maxa
      go to 20

 15   do 17 i = mina, maxa                             !y known fine x
            if( yold(i) .eq. yspecial ) then
                  xspecial = xold(i)
                  go to 30
             endif
```

```
            if( yold(i) .lt. yspecial ) then
                 if( i .eq. 1 ) then
                     minl = 1
                     maxl = 2
                     go to 20
                  else
                     minl = i -1
                     maxl = i
                     go to 20
                 endif
            endif
17    continue
      minl = maxa - 1
      maxl = maxa

20    continue

      if(itype_fit .eq. 3) then
              call fit_power(xold,yold,minl,maxl,aone,azero,rcc,ynfit,sn)
              if(ixfind .ne. 'y') yspecial = azero * (xspecial ** aone)
              if(ixfind .eq. 'y') xspecial = (yspecial/azero) ** (1. / aone)

         else if(itype_fit .eq. 2) then
              call fit_expon(xold,yold,minl,maxl,aone,azero,rcc,ynfit,sn)
              if(ixfind .ne. 'y') yspecial = azero * (10.0**(xspecial * aone))
              if(ixfind .eq. 'y') xspecial = alog10(yspecial / azero) / aone

      else
              call fit_lin(xold,yold,minl,maxl,aone,azero,rcc,ynfit,sn)
              if(ixfind .ne. 'y') yspecial = azero + (aone * xspecial)
              if(ixfind .eq. 'y') xspecial = (yspecial - azero) / aone
      endif

30    return
      end


      Subroutine Fit_expon(xp,ybfit,minl,maxl,aone,azero,rcc,ynfit,sn)
      dimension xp(*),ybfit(*),ynfit(*)

C   THIS ROUTINE COMPUTES THE LEAST SQUARES FIT FOR AN EXPONENTIAL
C   FUNCTION
C   USING THE COORDINATES FROM MINLOP TO MAXLOP OF THE X AND Y ARRAYS
C   THE LOG BASE 10 WILL BE TAKEN OF THE X VALUES

      sn     = 0.0
      sumx   = 0.0
      sumy   = 0.0
      sumxy  = 0.0
      sumsqx = 0.0
      sumsqy = 0.0

      DO 10 l = minl, maxl
        SN     = SN     + 1.
        SUMX   = SUMX   + XP(l)
```

```
          SUMY   = SUMY   + ALOG10(YBFIT(l))
          SUMXY  = SUMXY  + XP(l) * ( ALOG10(YBFIT(l)) )
          SUMSQX = SUMSQX + XP(l)**2.
          SUMSQY = SUMSQY + (ALOG10(YBFIT(l)) ** 2.)
   10   CONTINUE

      AONE = ((SN*SUMXY)-(SUMX*SUMY))/((SN*SUMSQX)-(SUMX**2))
      AZERO = 10**((SUMY-(AONE*SUMX))/SN)

        RN  =  (SN*SUMXY) - (SUMX*SUMY)
        RD  =  SQRT( ((SN*SUMSQX)-(SUMX**2)) * ((SN*SUMSQY)-(SUMY**2)) )
        RCC = RN/RD

C   CALCULATE NEW Y VALUES FROM EXPONENTIAL CURVE

C       DO 30 I = MINL, MAXL
C               YNFIT(I) = AZERO * ( 10.0**(XP(I) * AONE) )
C 30    CONTINUE

      RETURN
      END


      Subroutine Fit_lin(xp,ybfit,minl,maxl,aone,azero,rcc,ynfit,sn)
      dimension xp(*),ybfit(*),ynfit(*)

C   THIS ROUTINE COMPUTES THE LINEAR REGRESSION
C   THE COORDINATES FROM MINLOP TO MAXLOP

      SN     = 0.0
      SUMX   = 0.0
      SUMY   = 0.0
      SUMXY  = 0.0
      SUMSQX = 0.0
      SUMSQY = 0.0
        DO 10 l = minl, maxl
          SN     = SN     + 1.
          SUMX   = SUMX   + XP(l)
          SUMY   = SUMY   + YBFIT(l)
          SUMXY  = SUMXY  + (XP(l) * YBFIT(l))
          SUMSQX = SUMSQX + (XP(l)**2.)
          SUMSQY = SUMSQY + (YBFIT(l)**2.)
   10   CONTINUE

      AONE = ((SN*SUMXY) - (SUMX*SUMY)) / ((SN*SUMSQX)-(SUMX**2))
      AZERO = (SUMY- (AONE*SUMX)) / SN

        RN  =  (SN*SUMXY) - (SUMX*SUMY)
        RD = SQRT( ((SN*SUMSQX)-(SUMX**2)) * ((SN*SUMSQY)-(SUMY**2)) )
        RCC = RN/RD

C   CALCULATE NEW Y VALUES FROM LINEAR REGRESSION
C
C       DO 30 I = MINL, MAXL
C               YNFIT(I) = AZERO + ( AONE * XP(I) )
C 30    CONTINUE
```

```
      RETURN
      END


        Subroutine Fit_power(xp,ybfit,minl,maxl,aone,azero,rcc,ynfit,sn)
        dimension xp(*),ybfit(*),ynfit(*)

C   THIS ROUTINE COMPUTES THE LEAST SQUARES FIT
C   THE COORDINATES IN THE X,Y ARRAY BOUNDED THE MINLOP TO MAXLOP VALUES
C   USING THE POWER FIT REGRESSION
C   THE LOG BASE 10 WILL BE TAKEN OF ALL COORDINATES FOR THE POWER FIT

      SN=0.0
      SUMX=0.0
      SUMY=0.0
      SUMXY=0.0
      SUMSQX=0.0
      SUMSQY=0.0

        DO 10 l= minl, maxl
          SN=SN+1.
          SUMX=SUMX+ALOG10(XP(l))
          SUMY=SUMY+ALOG10(YBFIT(l))
          SUMXY=SUMXY+(ALOG10(XP(l))*(ALOG10(YBFIT(l))))
          SUMSQX=SUMSQX+(ALOG10(XP(l))**2)
          SUMSQY=SUMSQY+(ALOG10(YBFIT(l))**2)
   10   CONTINUE

      AONE=((SN*SUMXY)-(SUMX*SUMY))/((SN*SUMSQX)-(SUMX**2))
      AZERO=10**((SUMY-(AONE*SUMX))/SN)

        RN = (SN*SUMXY) - (SUMX*SUMY)
        RD = SQRT( ((SN*SUMSQX)-(SUMX**2)) * ((SN*SUMSQY)-(SUMY**2)) )
        RCC = RN/RD

C   CALCULATE NEW Y VALUES FROM POWER FIT REGRESSION
C
C       DO 30 I = minl, maxl
C               YNFIT(I) = AZERO * (XP(I) ** AONE)
C 30    CONTINUE

      RETURN
      END


        Subroutine Power_fit6(xp, y, y_bf, pfao, pfaz)
        dimension xp(*), y(*), y_bf(*),pfao(*), pfaz(*)

        yvalue(ao,az,xv) = az * (xv ** ao)

c Compute the best fit values using power fit procedure 6
c The y values for time periods 0.1667 to 1 hr are use as are (no fit)
c The    times    for y values are power fitted , y best values for times    found

c Procedure                     Interval time         TP peak exposure times
```

```
c
c    1                           Use actual values        0.1667 -    1 hr
c    2   Interval of fit          0.5 -   5hrs             2       -    3 hrs
c    3   Interval of fit          0.5 -   7hrs             4       -    5 hrs
c    4   Interval of fit          4    - 24hrs             6       -   10 hrs
c    5   Interval of fit          8    - 40hrs            12       -   20 hrs
c    6                           Use actual values        24       -  100 hrs

c procedure 1

        do 10 i = 1,5
              y_bf(i) = y(i)
   10   continue

c power fit for times  .1667 - .2, .2 - .25, .25 - .5, .5 - 1, 1 - 2, h+hrs
c correlation values computed
        j = 0
        do 25 i = 1, 5
              j = j + 1
              min = i
              max = i + 1
                  call fit_power(xp, y, min, max, aone, azero, rcc, y_bf, sn)
                  pfao(j) = aone
                  pfaz(j) = azero
   25   continue

        do 20 i = 6, 19
                                                    !procedure 2
              if(i .eq. 6) then                     !power fit times .5 to 5 hrs
                  min = 4
                  max = 9
                  call fit_power(xp, y, min, max, aone, azero, rcc, y_bf, sn)
                  pfao(6) = aone
                  pfaz(6) = azero
                                                    !procedure 3
              else if(i .eq. 8) then                !power fit times .5 to 7 hrs
                  max = 11
                  call fit_power(xp, y, min, max, aone, azero, rcc, y_bf, sn)
                  pfao(7) = aone
                  pfaz(7) = azero
                                                    !procedure 4
              else if(i .eq. 10) then               !power fit times 4 to 24 hrs
                  min =  8
                  max = 20
                  call fit_power(xp, y, min, max, aone, azero, rcc, y_bf, sn)
                  pfao(8) = aone
                  pfaz(8) = azero
                                                    !procedure 5
              else if(i .eq. 15) then               !power fit times 8 to 40 hrs
                  min = 12
                  max = 21
                  call fit_power(xp, y, min, max, aone, azero, rcc, y_bf, sn)
                  pfao(9) = aone
                  pfaz(9) = azero
              endif
```

```
            y_bf(i) = yvalue(aone,azero,xp(i))

   20   continue

c  procedure 6
        y_bf(20) = y(20)
        y_bf(21) = y(21)
        y_bf(22) = y(22)

c power fit for times 20-24,24-40,40-100 h+hrs
c correlation values computed
        j = 9
        do 30 i = 19, 21
              j = j + 1
              min = i
              max = i + 1
                  call fit_power(xp, y, min, max, aone, azero, rcc, y_bf, sn)
                  pfao(j) = aone
                  pfaz(j) = azero
   30   continue
        return
        end


      Subroutine Scaler_a(icyc)

        character*30 nfile, nfcom
        character*30 nblank/'                              '/
        character*1 ipnt, ixfind, itwo, icyc
        real mfl_erl(22), mf_tye, mf_cpe
        dimension ynfit(23)

        include 'plot_parameters'
        include 'scaler_params'
        logical yes

c Scaling computation for fallout values
c
c  multiplication factors for computing tyde
        data mfl_erl/4.363, 4.254, 4.11,  3.57,  2.904, 2.278, 1.99,  1.82,
     +1.707, 1.626,  1.562, 1.511, 1.467, 1.429, 1.364, 1.311, 1.265, 1.226,
     +1.191, 1.133,   .983,  .74/

c multiplication factors equations for computing tyde as a factor of x
c Equations for interval  1  if  x  <   1 mile
c               interval  2  if  x  >=  1 mile   and  <  8 miles
c               interval  3  if  x  >=  8 miles  and  < 37 miles
c               interval  4  if  x  >= 37 miles  and  < 90 miles
c               interval  5  if  x  >= 90 miles

        eqintv1(x) =    2.486e4  * ( x ** (-0.9808))
        eqintv2(x) =    2.486e4  * ( x ** (-1.8691))
        eqintv3(x) =    4.0069e4 * ( x ** (-2.0986))
        eqintv4(x) =    5.3117e5 * ( x ** (-2.8144))
        eqintv5(x) =    6.3545e6 * ( x ** (-3.3659))
```

```
c   id is output unit number
        id = 10
c   wind speed, height in thousands of feet, and wind shear for analog event
        v = 15.
        h =  5.
        a = 20.

        write (10, '("  <012>  !!! Values being computed !!!")' )

c  Prime values associated with new event
c  X Prime  centerline distance from ground zero new event
        DO 10 i = 1, 22
           if( i .le. 5) then                       !times less than eq 1hr
               xp(i) = vp(1) * tp(i)

             else if(i .le. 14) then                !times from 2 to 10 hrs
               xp(i) = vp(i-4) + xp(i-1)

           else                                     !vp hp greater 10hr unchanged
              xp(i) = ( (tp(i) - 10.) * vp(10) ) + xp(14)
           endif
   10   continue

C  Scaling factor for X Prime
        do 40 i = 1, 18                             !times ge to 1hr
              if(i .le. 10) then
                 sfxp(i) = 75.0 / ( vp(i) * hp(i) )    ! v * h = 75.0
              else
                 sfxp(i) = sfxp(10)             !values greater 10hr unchanged
              endif
   40   continue

c  X  centerline distance from ground zero analog event

        DO 50 i = 1, 22                               !distances less than eq 1hr
           if( i .le. 5) then
               x(i) = xp(i) * sfxp(1)
           else                                       !distances gt than 1hr
              x(i) = xp(i) * sfxp(i-4)
           endif
   50   continue

c  Erl  [ Exposure rate @ H+1 ] for analog event (interval multiplication
c     factor equations)
        do 80 i = 1, 22
             if(x(i) .ge. 90.) then
                   erl(i) = eqintv5( x(i) )

               else if(x(i) .ge. 37.) then
                   erl(i) = eqintv4( x(i) )

               else if(x(i) .ge.  8.) then
                   erl(i) = eqintv3( x(i) )

               else if(x(i) .ge.  1.) then
                   erl(i) = eqintv2( x(i) )
```

```
            else
                erl(i) = eqintvl( x(i) )
           endif
   80   continue

c  A is the exposure rate levels as a function of distance along the
c    centerline for the analog event
c  Scaling factor A

        do 90 i = 1, 18
           if(i .le. 10) then
             sfa(i) = (1.125e5 * r) / ( (vp(i)**2) * ( hp(i)**2) * alfa(i))
           else

             sfa(i) = sfa(10)          !vp hp alfa greater 10hr unchanged
           endif
   90   CONTINUE

c  ER1 Prime at H+1  for new event

        do 95 I = 1, 22
          if( i .le. 5) then
              erlp(i)    = sfa(1)     * erl(i)
          else
              erlp(i)    = sfa(i-4)   * erl(i)
          endif
   95   continue

c Erlp_bf, erlp fit using power_fit6  [ suffix bf for best fit ]
c     power_fit6 refers to 6 different intervals for applying a power_fit
c     regression

        call power_fit6(xp, erlp, erlp_bf, erlp_aone, erlp_azero)

c  Tyde_bf,Tye_bf,Cpe_bf,Dper_bf, and Ryde_bf values determined from Erlp_bf
c
c       Tyde_bf  Total first year deposition exposure
c       Tye_bf   Total first year year exposure
c       Cpe_bf   Cloud passage exposure
c       Dper_bf  Deposition peak exposure rate
c       Ryde_bf  Residual first year deposition exposure

c  Multiplication factors for computing TYE and CPE from TYDE
        do 100 I = 1, 22
           mf_tye = 1.1611   * ( tp(i) ** ( -0.02354 ) )
           mf_cpe = 0.28624 * ( tp(i) ** ( -0.49365 ) )

c  mf1_erl  multiplication factor for computing tyde_bf
           tyde_bf(i) = mf1_erl(i) * erlp_bf(i)
           tye_bf(i)  = mf_tye * tyde_bf(i)
           cpe_bf(i)  = mf_cpe * tyde_bf(i)

           dper_bf(i) = rdf(i) * erlp_bf(i)
           ryde_bf(i) = tye_bf(i) - cpe_bf(i)

  100   CONTINUE
```

```
      write (10, '("  <012>  !!! Writing data to disk files !!!")' )

c Write Dper_bf to disk
c Write Tye_bf, Cpe_bf and Dper_bf to disk

      nfcom = nblank
      nfile = nblank
      nfile = 'ns_a_tye_bf.dat'
      call dskw  (nfile, nblank, nfcom, xp, tye_bf)

      nfile = nblank
      nfile = 'ns_a_cpe_bf.dat'
      call dskw  (nfile, nblank, nfcom, xp, cpe_bf)

      nfile = nblank
      nfile = 'ns_a_dper_bf.dat'
      call dskw  (nfile, nblank, nfcom, xp, dper_bf)

c Infant Thyroid Dose for green(tdg_bf) and dry feed(tdd_bf)
c Best fit Tdg_bf and Tdd_bf
      do 105 i = 1, 22
             tdg_bf(i) = erlp_bf(i) * 0.21156
             tdd_bf(i) = erlp_bf(i) * 0.0423
 105  continue

c Write Tdg_bf and Tdd_bf to disk

      nfcom = nblank
      nfile = nblank
      nfile = 'ns_a_tdg_bf.dat'
      call dskw  (nfile, nblank, nfcom, xp, tdg_bf)

      nfile = nblank
      nfile = 'ns_a_tdd_bf.dat'
      call dskw  (nfile, nblank, nfcom, xp, tdd_bf)

c  Special Values for exposures and doses

      ixfind    = 'y'                !find x
      mina      =  1                 !beginning location of array
      maxa      = 22                 !last location of array
      itype_fit =  3                 !power_fit

c  compute special values
      call special_values(ixfind, itype_fit, mina, maxa, ynfit)

c Write special values for Tye_bf, and Tdg_bf to disk

      nfcom = nblank
      nfile = nblank
      nfile = 'ns_a_spl_tye_bf.dat'
      p_spl_tye_bf(1) = spl_tye_bf(2)
      p_spl_tye_bf(2) = spl_tye_bf(3)
      p_spl_tye_bf(3) = -9999.
```

```
        p_spl_mr(1)     = spl_mr(2)
        p_spl_mr(2)     = spl_mr(3)
        p_spl_mr(3)     = -9999.
        call dskw  (nfile, nblank, nfcom, p_spl_tye_bf, p_spl_mr)

        nfcom = nblank
        nfile = nblank
        nfile = 'ns_a_spl_tdg_bf.dat'
        p_spl_tdg_bf(1) = spl_tdg_bf(1)
        p_spl_tdg_bf(2) = -9999.
        p_spl_rad(1)    = spl_rad(1)
        p_spl_rad(2)    = -9999.
        call dskw  (nfile, nblank, nfcom, p_spl_tdg_bf, p_spl_rad)

c Combine xp and special distances for TYE in one array then

        call comb_bf(xp, tye_bf, spl_tye_bf, spl_mr, p_tye_xco, p_tye_yco)
        call smooth_xy_bf(xp, tye_bf, p_tye_xco, p_tye_yco, p_tye_xbf,
     +p_tye_ybf, ynfit)

c Write P_Tye to disk for semi_log plots
        nfile = nblank
        nfile = 'ns_a_tye_pbf.dat'
        call dskw  (nfile, nblank, nfcom, p_tye_xbf, p_tye_ybf)

c Combine xp and special distances for CPE in one array then

        call comb_bf(xp, cpe_bf, spl_cpe_bf, spl_mr, p_cpe_xco, p_cpe_yco)
        call smooth_xy_bf(xp, cpe_bf, p_cpe_xco, p_cpe_yco, p_cpe_xbf,
     +p_cpe_ybf, ynfit)

c Write P_Cpe to disk for semi_log plots
        nfile = nblank
        nfile = 'ns_a_cpe_pbf.dat'
        call dskw  (nfile, nblank, nfcom, p_cpe_xbf, p_cpe_ybf)

        write (10, '("  <007> <012>  If you do Not want a printout, ")' )
      write (10, '("     data will be displayed on YOUR terminal!  <012> ")')


c id is unit output device number 10 for input display device and
c                                 12 for output disk file
c
        if(yes (' <012>  Do you want a printout (y/n)? [n] ',ipnt) ) id = 12

        if(ipnt .eq. 'y') then
          if(yes (' <012>  Two copies of first part of printout (y/n)? [n] ',
     +itwo) ) then
                icopy = 2
            else
                icopy = 1
            endif
            open (1,status='old', file = ('='//'nolptfile'), iostat=ios)
            if(ios .eq. 0) then
                close (1,status='delete',err=140)
            else
```

```
             write (id, '(1h1)' )
          endif
        else
          id = 10
          icopy = 1
        endif

  140   continue

c  output
        call scaler_output_a(icopy, icyc)

        if( id .eq. 12) write (id, '(" ")' )

  500   RETURN

  888   write (10, '( " <012> Error when trying to open file! ")' )
        go to 500
  999   write (10, '( " <012> Error when closing file! ")' )
        go to 500

        END


        Subroutine Scaler_output_a(icopy, icyc)

        character*1 ixfind, icyc
        include 'scaler_params'

c  output text
        write (id, '(/, "  NSCALE ")' )
        write (id, '( /,"  R = ", f12.3)' ) r
        write (id, '("  TIME   SPEED   CLD. HGT. SHEAR")' )
        write (id, '(" (H+HRS) (MPH)  (*1000 FT) (DEG.) ")' )
        write (id, '( 1x, i4, f9.0, f9.1, f9.0)' ) (i, vp(i), hp(i), alfa(i),
     +  i = 1, 10 )

        if(id .eq. 10) pause
C All values are prime values, the label x is for xp values .... etc'

      do 50 k = 1, icopy

        if( k  .eq. 2 .and. id .eq. 12) write (id, '(1h1)' )

        write (id, "(/,'     TP            X            TYE           CPE ',
     +'       ITD_GF        ITD_DF ',
     +/,'   (H+HRS)      (MILES)        (mR)          (mR) ',
     +'        (RADS)        (RADS)')" )
        write (id, '( 0pF10.3, 0pf12.2, 1x, 1p4e13.3)' )
     +  (tp(i), xp(i), tye_bf(i), cpe_bf(i), tdg_bf(i), tdd_bf(i), i = 1,  4)

        write (id, '( 0pF7.0, 2x, 0pf12.1, 2x, 1p4e13.3)' )
     +  (tp(i), xp(i), tye_bf(i), cpe_bf(i), tdg_bf(i), tdd_bf(i), i = 5, 22)

          if(id .eq. 10) pause
c Print special exposure and dose values
```

```
      write (id, "(//,'  EXPOSURE       DISTANCES (MILES)           DOSE ',
     +'      DISTANCES (MILES)',
     +/,'   (mR)            TYE         CPE           (RADS)       ITD_GF   ',
     +'   ITD_DF')" )

    do 20 j = 1, 2
    write (id, '(0pf7.0, 3x, 0P2f12.2, 3x, 0pf13.3, 0p2f12.2)' ) spl_mr(j),
   +spl_tye_bf(j), spl_cpe_bf(j), spl_rad(j), spl_tdg_bf(j), spl_tdd_bf(j)
 20      continue

        do 30 j = 3, 6
           write (id, '(0pf7.0, 3x, 0P2f12.2)' )  spl_mr(j), spl_tye_bf(j),
   +          spl_cpe_bf(j)
 30      continue

c       if( k .eq. 2) go to 50

        if(id .eq. 10) pause
        if( id .eq. 12) write (id, '(1h1)' )

        write (id, "( /,'     TP             X            ER1          DPER ',
     +'       TYDE          RYDE     ',
     +/,'   (H+HRS)      (MILES)      (mR/HR)       (mR/HR)        (mR)   ',
     +'       (mR)                ')" )
        write (id, '( 0pF10.3, 0pf12.2, 1x, 1p4e13.3)' )
     +(tp(i), xp(i), er1p_bf(i), dper_bf(i), tyde_bf(i), ryde_bf(i), i = 1,  4)
        write (id, '( 0pF7.0, 2x, 0pf12.1, 2x, 1p4e13.3)' )
     +(tp(i), xp(i), er1p_bf(i), dper_bf(i), tyde_bf(i), ryde_bf(i), i = 5, 22)

        if(id .eq. 10) pause
        call define_data( id )
        if(id .eq. 10) pause

 50 continue

        return
        end


        Subroutine Scinp(tp, r, vp, hp, alfa, last_input, icnts)
        dimension tp(*), vp(*), hp(*), alfa(*)
        character*1 irest, ins, ls, lva
        logical yes

c  Manual input routine

        icnts = icnts + 1

        assign 5 to label_num
  5     write (10, '( "  <012>  <012>  R  =  ",$)' )
        read  (11, *, err = 888) r

        if(icnts.le.1) go to 30
        if(yes(' <012>  Use last scaling values (y/n)? [n] ',lva) ) then
           write (10, '(/, " Hour   Speed  Cld.Hgt Shear" )' )
```

```
           write (10, '("        (mph)  (k  ft) (deg) ",/)' )
        write (10, '(i4,3F7.1)' ) (i,vp(i),hp(i),alfa(i), i=1,10)
        go to 180
     endif
 30  write (10, '( " <012>  <012> Enter Speed, Cloud Hgt. and Shear",
    +"  <012> if the remaining data is the same...KEY:  0,0,0   (newline/cr)",
    +"  <012>  <012> ")' )

c  Input parameters for hours 1 to 10 hours

     assign 40 to label_num
     k = 0
     write (10, '( "    Hrs  Speed  Cld Hgt.  Shear ")' )
     write (10, '( "         (mph)  (k  ft)   (deg) ",/)' )
     do 90 i =  1, 10
         k = k + 1
 40      write (10, '("   ",i4,"  ",$)' ) i
         read  (11, *, err = 888) vp(i), hp(i), alfa(i)
           if(vp(i) .eq. 0.0) go to 120
 90  continue
     last_input = 10
     go to 180

120  last_input = k - 1
     do 150 i = k, 10
        vp(I) =   vp(last_input)
        hp(I) =   hp(last_input)
        alfa(I) = alfa(last_input)
150  continue
180  continue

   if( .not. yes('  <012>  Any corrections  (y/n )? [n]  ',ins) ) go to 330

C  CORRECTIONS

     IMORE = 0
210          write (10, '(/, " Hour  Speed  Cld.Hgt Shear")' )
             write (10,   '("        (mph)  (k  ft) (deg) ",/)' )
             write (10, '(i4,3F7.1)' ) (i,vp(I),hp(I),alfa(I), I=1,10)
                IF(IMORE.GT.0) GO TO 250
240          assign 245 to label_num
245          write (10, '("  <012>  Enter: Hour, Spd,Hgt,Shear... = ",$)')
             read  (11, *, err = 888) ich,cvp,chp,cal

             if(ich .gt. 10) then
                write (10, '( <012>  " Time greater then 10 hours!" )' )
                go to 210
             endif

             vp(ich)   = cvp
             hp(ich)   = chp
             alfa(ich) = cal

     if(.not. yes(' <012> Are the remaining sets the same (y/n )? [n] ',
    +irest) ) go to 250
                     last_input = ich
```

```
                        ich = ich + 1
                        do 270 i = ich, 10
                                vp(i)    = vp(last_input)
                                hp(i)    = hp(last_input)
                                alfa(i) = alfa(last_input)
270                     continue
                        imore = imore + 1
                        go to 300

250         if( yes(' <012>  Any more corrections (y/n)? [n] ',ins) ) go to 240
            imore = imore + 1

300         if( yes (' <012>  List  input data (y/n)? [n]  ',ls) ) go to 210

330      RETURN

888      write (10, '(/," <007>  <007>  !!!  Bad data reenter  !!!",/)' )
         go to label_num

         END


         Subroutine Smooth_XY_bf(xbf, ybf, xc, yc, xpb, ypb, ynfit)
         dimension xbf(*), ybf(*), xc(*), yc(*), xpb(*), ypb(*), ynfit(*)
         character*1 ixfind
         real increm
c
c  compute x,y values between calulated values using the power fit
c  regression so that when data is plotted on a semi_log graph the
c  curve will be smooth
c
         do 10 i = 1, 299
            xpb(i) = 0.0
            ypb(i) = 0.0
10       continue

         ixfind    = 'n'                      !find y
         mina      =  1                       !min for array
         maxa      = 22                       !max for array
         itype_fit =  3                       !power fit regression
         ico  = 1                             !counter for combine bf and spl array
         new  = 0                             !counter for new plot array
         increm = 5.                          !increment for multi of 5

         do 20 l = 1, 299
               new = new + 1
               if( xc(ico) .eq. -9999.) go to 50

               if(increm .lt. xc(1) ) then        !fist value
                  xpb(new) = xc(1)
                  ypb(new) = yc(1)
                  increm   = increm + 5

                 else if (increm .eq. xc(ico) )  then
                    xpb(new) = xc(ico)
                    ypb(new) = yc(ico)
```

```
                  ico      = ico + 1
                  increm   = increm + 5

               else if(increm .gt. xc(ico) ) then
                  xpb(new) = xc(ico)
                  ypb(new) = yc(ico)
                  ico      = ico + 1

            else                                ! fine y increm  lt xc(ico)
                xv  = increm
                call  Find_xy(itype_fit,ixfind,xbf,ybf,xv,yv,mina,maxa,ynfit)
                xpb(new) = increm
                ypb(new) = yv
                increm   = increm + 5

            endif

   20   continue
   50   new = 1 + 1
        xpb(new) = -9999.
        ypb(new) = -9999.
        if(new .ge. 300) then
          new = 300
          xpb(new) = -9999.
          ypb(new) = -9999.
        endif

        if( xpb(new - 1) .ne. xbf(22) ) then
              new = new - 1
              xpb(new) = xbf(22)
              ypb(new) = ybf(22)
        endif

        if( xpb(new - 1) .lt. xbf(21) ) then
              new = new - 1
              xpb(new) = xbf(21)
              ypb(new) = ybf(21)
        endif

        return
        end


        SUBROUTINE DSKR(NFILE,NBLANK,NFCOM,IRED,J,X,Y)
        character ired
        CHARACTER*30 NFILE, NBLANK,NFCOM
        DIMENSION X(12,300), Y(12,300)

c   read data from disk into a two dimension array

        OPEN (1, FILE=('='//NFILE),IOSTAT=IOS, ERR=999, STATUS='OLD',RECFM='DS')
           READ (1, '(a30)' ) NFCOM
           DO 20 I = 1,300
              READ  (1, '(1P2E13.5)',end=29 )  X(J,I),Y(J,I) !READ X,Y From DISK

                 IF(X(J,I).EQ.-9999. .OR. Y(J,I).EQ.-9999.) THEN
```

```
                  IF(X(J,I).NE.-9999.) X(J,I) = -9999.
                  IF(Y(J,I).NE.-9999.) Y(J,I) = -9999.
                  GO TO 30
              ENDIF

 20        CONTINUE
           go to 30

 29        x(j,i) = -9999.
           y(j,i) = -9999.


 30    CLOSE (1, IOSTAT= IOS, ERR=88)
       RETURN

C ERROR CHECKS

 999   CONTINUE
1020   FORMAT(/,1X,' <007> No file Named ',A30,/)
       RETURN

 88    WRITE (10, '(/,1X," Unable to close channel IOS ERR = ",I5)' ) IOS
       RETURN
       END


       Subroutine Special_values(ixfind, itype_fit, mina, maxa, ynfit)
       include 'scaler_params'
       character*30 nfile, nfcom
       character*30 nblank/'                              '/
       character*1 ixfind
       dimension ynfit(*)

c  Find x value using power fit regression when y values are known
c
c  ixfind    = 'y'        !find x
c  itype_fit = 3          !power_fit
c  mina      = 1          !beginning of arrary
c  maxa      = 22         !end of array

     do  10 l = 1, 6
c exposure
       yspecial = spl_mr(l)

c total first year
     call find_xy(itype_fit,ixfind,xp,tye_bf,xspecial,yspecial,mina,maxa,
    +ynfit)
                  spl_tye_bf(l) = xspecial

c cloud passage
     call find_xy(itype_fit,ixfind,xp,cpe_bf,xspecial,yspecial,mina,maxa,
    +ynfit)
                  spl_cpe_bf(l) = xspecial

  10 continue
```

```
c dose

        do 20 l = 1, 2
        yspecial = spl_rad(l)

c infant thyroid dose from green feed
      call find_xy(itype_fit,ixfind,xp,tdg_bf,xspecial,yspecial,mina,maxa,
     +ynfit)
                  spl_tdg_bf(l) = xspecial

c infant thyroid dose from dry  feed
      call find_xy(itype_fit,ixfind,xp,tdd_bf,xspecial,yspecial,mina,maxa,
     +ynfit)
                  spl_tdd_bf(l) = xspecial

   20   continue

        return
        end
```

```
c DATA_INT ..... Include file
c    This include statement mainly initializes data
c
c   tp is time of peak exposure rate

        data tp/0.166667, 0.2, 0.25, 0.5, 1., 2., 3., 4., 5., 6., 7., 8., 9.,
     +10., 12., 14., 16., 18., 20., 24., 40., 100., -9999./

c   special exposure rates mr/r
        data spl_mr/5000., 500., 170., 100., 10., 1.0/
c   special rad values
        data spl_rad/0.5, 0.05/

c  value indicates end of data for write disk file

        x(23)          = -9999.
        xp(23)         = -9999.

        erl(23)        = -9999.
        erlp(23)       = -9999.
        erlp_bf(23)    = -9999.

        tyde_bf(23)    = -9999.

        tye_bf(23)     = -9999.
        spl_tye_bf(7)  = -9999.
      p_spl_tye_bf(7)  = -9999.
        p_tye_xco(32)  = -9999.
        p_tye_yco(32)  = -9999.
        p_tye_xbf(300) = -9999.
        p_tye_ybf(300) = -9999.

        cpe_bf(23)     = -9999.
        spl_cpe_bf(7)  = -9999.
        p_cpe_xco(32)  = -9999.
        p_cpe_yco(32)  = -9999.
        p_cpe_xbf(300) = -9999.
        p_cpe_ybf(300) = -9999.

        tdg_bf(23)     = -9999.
        spl_tdg_bf(3)  = -9999.
      p_spl_tdg_bf(3)  = -9999.

        tdd_bf(23)     = -9999.
        spl_tdd_bf(3)  = -9999.

        dper_bf(23)    = -9999.
        cper_bf(23)    = -9999.
        ryde_bf(23)    = -9999.

        p_spl_mr(7)    = -9999.
        p_spl_rad(3)   = -9999.
```

```
cccccccccccccccccccccccccccccccccccccccccccccc

c Scaler_params .... Include file ....

        COMMON /SCAL/r, tp(23), vp(18), hp(18), alfa(18), sfxp(23), sfa(18),
     +x(23),  erl(23), erlp(23), erlp_bf(23), erlp_aone(12), erlp_azero(12),
     +xp(23),
     +    tye_bf(23),      cpe_bf(23), tyde_bf(23),  tdg_bf(23),     tdd_bf(23),
     +spl_tye_bf(7),   spl_cpe_bf(7),            spl_tdg_bf(3),  spl_tdd_bf(3),
     +p_spl_tye_bf(7),                          p_spl_tdg_bf(3),
     +  p_tye_xco(32),   p_cpe_xco(32),
     +  p_tye_yco(32),   p_cpe_yco(32),
     +  p_tye_xbf(301),  p_cpe_xbf(301),
     +  p_tye_ybf(301),  p_cpe_ybf(301),
     +    rdf(23),         dper_bf(23),    cper_bf(23),   ryde_bf(23),
     +spl_mr(6),  p_spl_mr(7),
     +spl_rad(2), p_spl_rad(3),
     +last_input, id,
     +DR(23), FD(23),   CPD(23),FTD(23), IDEV

        character*60 l_brief
        character*1  ians_brief_label

        data rdf/ 3.45,     3.093,     2.705,     1.785,     1.0,      3.94e-1,
     +2.13e-1,    1.354e-1, 9.458e-2, 7.099e-2, 5.651e-2, 4.71e-2,  4.061e-2,
     +3.586e-2,   2.923e-2, 2.462e-2, 2.114e-2,  1.839e-2, 1.618e-2, 1.29e-2,
     +6.954e-3,   2.526e-3, -9999./

c varible definition
c       r           = source factor
c
c       tp          = time after detonation in hours ( H+hour [time of
c                       peak exposure rate] )
c
c forecasted values ( prime values new event )
c       vp          = wind speed/mph
c       hp          = height above surface in thousand of feet
c       alfa        = wind shear in degrees
c
c       xp          = centerline distance from ground zero new event
c     sfxp          = scaling factor for xp
c
c       x           = centerline distance from ground zero analog event
c       erl         = exposure rate at H+1 hours analog event
c     sfa           = scaling factor for a
c
c       erlp        = exposure rate at H+1 hours new event
c       erlp_bf     = exposure rate at H+1 hours new event best fit
c       erlp_aone   = aone value from best fit for distance interval
c       erlp_azero  = azero value from best fit for distance interval
c
c       tye_bf      = total first year gamma exposures [total exposure
c                     from both suspended and deposited debris from
c                     arrival time out to 1 year]  best fit
c   spl_tye_bf      = special mr/hr values best fit
```

```
c p_spl_tye_bf     = special mr/hr values best fit for plotting
c     p_tye_xco     = total first year gamma exposures distances combined
c     p_tye_yco     = total first year gamma exposures and special
c                     exposures combined
c     p_tye_xbf     = total first year gamma exposures distances for plot
c     p_tye_ybf     = total first year gamma exposures for plot
c
c       cpe_bf      = cloud passage gamma exposure [total exposure during
c                     cloud passage...includes exposure due to early
c                     deposition] best fit
c   spl_cpe_bf      = special cloud passage gamma exposure
c p_spl_cpe_bf      = special cloud passage gamma esposures for plotting
c     p_cpe_xco     = cloud passage gamma exposures distances combined
c     p_cpe_yco     = cloud passage gamma exposures and special
c                     exposures combined
c     p_cpe_xbf     = cloud passage gamma exposures distances for plot
c     p_cpe_ybf     = cloud passage gamma exposures for plot
c
c       tyde_bf     = total first year gamma deposition exposure [exposure
c                     from deposition during and after cloud passage out to
c                     1 year]
c
c       tdg_bf      = infant thyroid dose (green feed)
c   spl_tdg_bf      = special rad values for infant thyroid dose (green feed)
c p_spl_tdg_bf      = plot values for infant thyroid dose (geen feed)
c
c       tdd_bf      = infant thyroid dose (dry feed)
c   spl_tdd_bf      = special rad values for infant thyroid dose (dry feed)
c
c       rdf         = new pike relative decay factor as a fuction of tp(h+hrs)
c       dper_bf     = deposition peak exposure rate [exposure rate at time tp]
c
c       ryde_bf     = first year residual deposition exposure [exposure
c                     from deposition after cloud passage out to 1 year]
c
c       spl_mr      = special mr/hr values
c     p_spl_mr      = special mr/hr values for plotting
c
c       spl_rad     = special rad values
c     p_spl_rad     = special rad values for plotting
c
c    last_input
c    id             = unit number for output device
c
c   l_brief  = label for plots
c   ians_brief_label = answer for entering a label
c
cccccccccccccccccccccccccccccccccccccccc
```

APPENDIX C

NSCALE INPUT EXAMPLE

This section will detail how to run NSCALE on one of the DG computers. The operation of NSCALE on a PC is essentially the same. In order to show how NSCALE operates, an example computation will be made. In this example, as many options as possible will be exercised. Prompts displayed on the screen will be shown in ***bold italic*** text. User responses (input into the computer) will be shown in normal text.

Once logged into the computer and in the proper directory, type NSCALE and strike the ENTER[1] key.

R = 1←

Enter Speed, Cloud Hgt. and Shear
if the remaining data is the same...KEY: 0,0,0 (newline/cr)

Hrs Speed Cld Hgt. Shear
(mph) (k ft) (deg)

1 15,5,20←
2 15,5,30←
3 0,0,0←

Any corrections (y/n)? [n] y←

Hour	***Speed (mph)***	***Cld.Hgt (k ft)***	***Shear (deg)***
1	***15.0***	***5.0***	***20.0***
2	***15.0***	***5.0***	***30.0***
3	***15.0***	***5.0***	***30.0***
4	***15.0***	***5.0***	***30.0***
5	***15.0***	***5.0***	***30.0***
6	***15.0***	***5.0***	***30.0***
7	***15.0***	***5.0***	***30.0***
8	***15.0***	***5.0***	***30.0***
9	***15.0***	***5.0***	***30.0***
10	***15.0***	***5.0***	***30.0***

Enter: Hour, Spd,Hgt,Shear... = 1,12,5,20←

Are the remaining sets the same (y/n)? [n] ←

---

[1]In the following example NSCALE run, whenever the ENTER key should be struck, the symbol, ←, will be used.

Any more corrections (y/n)? [n] y←

Enter: Hour, Spd,Hgt,Shear... = 8,20,5,30←

Are the remaining set the same (y/n)? [n] y←

List input data (y/n)? [n] y←

Hour	Speed (mph)	Cld.Hgt (k ft)	Shear (deg)
1	12.0	5.0	20.0
2	15.0	5.0	30.0
3	15.0	5.0	30.0
4	15.0	5.0	30.0
5	15.0	5.0	30.0
6	15.0	5.0	30.0
7	15.0	5.0	30.0
8	20.0	5.0	30.0
9	20.0	5.0	30.0
10	20.0	5.0	30.0

Any more corrections (y/n)? [n] ←

List input data (y/n)? [n] ←

!!! Values being computed !!!

!!!Writing data to disk files !!!

If you do Not want a printout,
data will be displayed on YOUR terminal!

Do you want a printout (y/n)? [n] ←

At this time, the NSCALE results will be displayed upon the screen. Figures 6.2 and 6.3 show what appears on the screen. When the screen becomes full, scrolling stops and the message:

****** PAUSE ******
Type NEW-LINE to continue.

appears at the bottom of the screen. Strike ENTER when ready to view the next screen.

If you had answered "y" to "Do you want a printout (y/n)?," no results would be displayed on the screen but the following question would be presented:

Two copies of first part of printout (y/n)? [n] ←

```
 Create plot files (y/n)? [n] y←

When sending plots to AFOS the semi_log plot will be sent to the HP plotter!

   Send plots to AFOS (y/n)? [n] y←
   Using line to DOE (y/n)? [n] ←

 Enter Locations  (y/n)? [n] y←


Text may be placed within the plotting area,
A maximum of 6 names of 27 characters each can be entered
Names can be in upper and/or lower case
Name or location ID = Rachel←
  Distance      = 40←

Enter another location (y/n)? [n] ←

Enter Briefing and Event Time and Date (y/n)? [n] y←

Briefing time and date [e.g. 1430 PDT 04/12/86] = 0600 PDT 05/31/89←

Event time and date [e.g. 0830 PDT 04/13/86] = 0800 PDT 05/31/89←

Generating plots
tye_cpe.spl
NMCGPH2PL (NTS) on 2PL is on its way to AFOS at CP1.
NMCGPH2PN (NTS) on 2PN is on its way to AFOS at CP1.
NMCGPH2PB (NTS) on 2PB is on its way to AFOS at CP1.
tye_cpe_sl.spl
NMCGPH2TL (NTS) on 2TL is on its way to AFOS at CP1.
NMCGPH2TN (NTS) on 2TN is on its way to AFOS at CP1.
NMCGPH2TB (NTS) on 2TB is on its way to AFOS at CP1.
tdg_tdd.spl
NMCGPH2GL (NTS) on 2GL is on its way to AFOS at CP1.
NMCGPH2GN (NTS) on 2GN is on its way to AFOS at CP1.
NMCGPH2GB (NTS) on 2GB is on its way to AFOS at CP1.
dper.spl
NMCGPH2DL (NTS) on 2DL is on its way to AFOS at CP1.
NMCGPH2DB (NTS) on 2DB is on its way to AFOS at CP1.

 AFOS PLOTS sent .... Plot sent to HP when program exited..last plot saved

 New data or change parameters (y/n)? [n] ←

  Send PRINT file to AFOS (y/n)? [n] y←

 Send PRINT file to decwriter (y/n)? [n] y←

STOP
It's on its way!
Sent Doelscale toafos 07-MAY-89 00:25:44
```

Plots sent by 07-MAY-89 00:25:46

Plot on it's way to HP_plotter NTS ......Transparency!!!

Graphics Spooler Version 3.73 05/07/89 00:25:50
-- Processing 3.70 binary spool file generated on 05/07/89 at 00:22:53

Graphics Spooler Version 3.73 05/07/89 00:26:16
-- Processing 3.70 binary spool file generated on 05/07/89 at 00:22:53

typ_cpe_sl.spl sent 2 copies to HP plotter at NTS

Graphics Spooler Version 3.73 05/07/89 00:26:42
-- Processing 3.70 binary spool file generated on 05/07/89 at 00:23:14

tdg_tdd.spl sent to HP plotter at NTS
Afos plots should be in data base !!!

QLISTER Version 1.1 - formatting for DECwriter III (LA120)

NSCALE.PRINT (2 pages)

Your listing should be on the DECWRITER III!

APPENDIX D

THE EFFECTS OF PARAMETER CHANGES

In Chapter 7, it was pointed out that the radiation briefer is sometimes asked to comment about the effects upon a certain set of exposure estimates if one of the parameters were changed. This appendix discusses such changes in association with both the radiological and meteorological parameters.

FISSION YIELD AND FALLOUT FRACTION

The radiological source term, RST, in equation 4.1 (page 41) is represented by (f_p Y_p / f Y). From this equation, it can be seen that the H+1 hr exposure rate, $ER1_p$, at a particular downwind distance, X_p, in association with a new event, is directly proportional to both the new event's fallout fraction and fission+ yield. Thus, if the yield was increased by a factor of two, the exposure rate would be increased by a factor of two at X_p, or if the fallout fraction was reduced by half, the exposure rate would be reduced by half.

In readiness briefings prior to detonations, the fission+ yield estimate that is supplied by the national laboratory is not normally questioned. That is, safety officials realize that the estimate will probably verify. Thus, it is quite doubtful that the radiation briefer has ever been asked to comment on the effect to the predicted exposures if the fission+ yield was assumed to be greater than expected.

As pointed out earlier, the assumption is used that the new-event fallout fraction will be the same as the PIKE-event fallout fraction. At a readiness briefing, the radiation briefer is rarely asked about what would be the effect on the fallout estimates if a different fallout-fraction assumption was used. However, such fallout-fraction questions are occasionally asked when radiation briefers are explaining the PIKE Model to interested organizations.

Figure D.1 exemplifies the effects upon the predicted centerline position of the 170 mR TYE exposure estimate when the source term is changed. The same four meteorological cases used in deriving values for the Circle Chart (Figure 7.1 - page 107) are used in this example. Recall that case 1 is a typical light-wind situation and case 4 is a typical strong-wind situation.

Consider the example where a small population is located 25 miles downwind from a new-event GZ. If the centerline is projected directly over these people, the meteorological parameters are characterized by a case-1 situation, and the RST is 10, then, from Figure D.1, it can be seen that the centerline distance to the 170 mR position would be at 25 miles, the distance to the population in question.

What would happen according the PIKE model if ten times more debris came out in association with the new event than with PIKE? The most obvious change would be that instead of having 170 mR at 25 miles downwind, there would be 1700

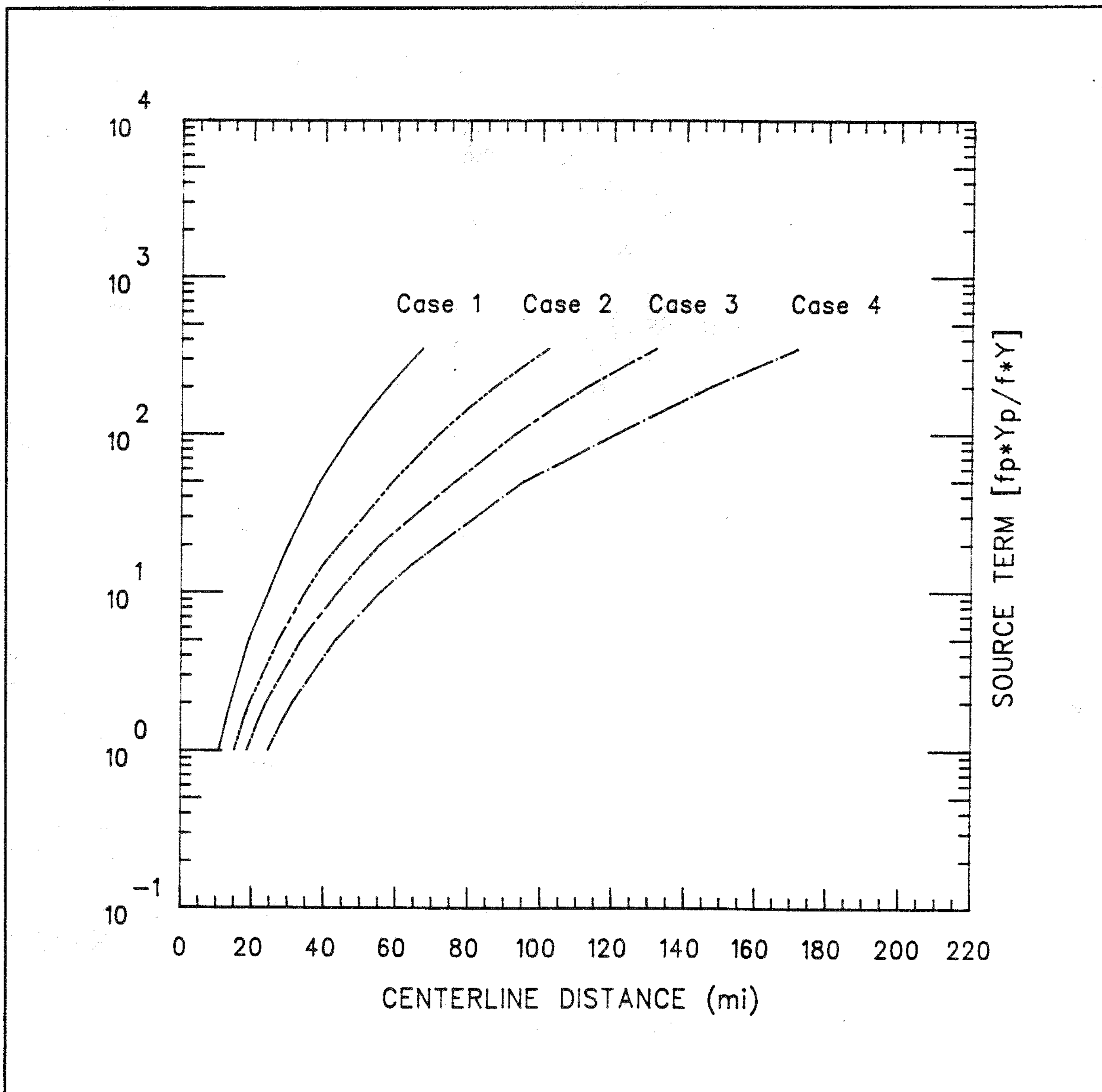

Figure D.1 Source Term Versus 170 mR Centerline Distance

mR. And, according to Figure D.1, the 170 mR position would move from 25 miles to 47 miles downwind, a change of a factor of 1.9.

If this ten-times scenario had occurred under case-4 conditions, the 170 mR position would have moved from 56 miles to 121 miles downwind, a change of a factor of 2.2. Thus, in general, it can be seen that under similar circumstances, a ten-times increase in the source term only moves the 170 mR position out by a factor of two, though it increases the exposure at any one location by a factor of ten.

WIND SHEAR

As indicated by equation 4.1, the change in the H+1 hr exposure rate, $ER1_p$, would be inversely proportional to the change in the wind shear, α_p. For example, if TYE at 25 miles downwind was forecast to be 170 mR based upon a forecast wind shear of 40°, it would increase to 340 mR if the wind-shear forecast was decreased to 20°.

Figure D.2 exemplifies the effects upon the predicted centerline position of the 170 mR TYE exposure estimate when the wind-shear term is changed. The

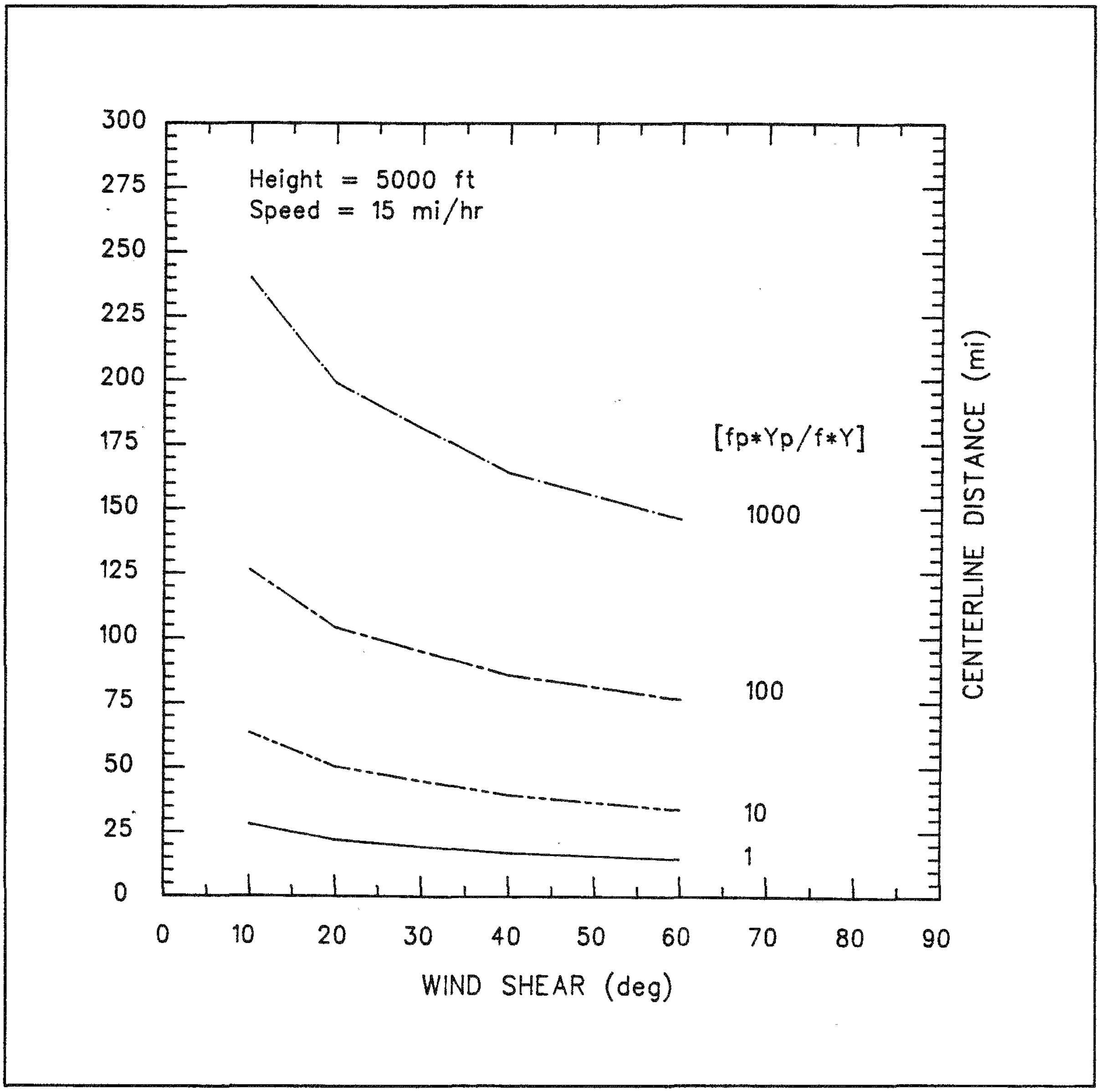

Figure D.2 170 mR Centerline Position Versus Wind Shear change in the 170 mR centerline position with a change in the wind shear is shown as a function of the RST, assuming a cloud height of 5000 ft and a wind speed of 15 mi/hr.

For example, if 40° of shear were forecast with an RST of 10, then the 170 mR position would be 39 miles downwind. However, if that shear angle were reduced to 20°, then the 170 mR position would move out to 50 miles. This would be an increase in distance of about a factor of 1.3. If the RST had been 100 instead of 10, the 170 mR position would have moved from 86 miles to 104 miles downwind, a change of a factor of 1.2. Thus, it can be seen that under similar circumstances, the 170 mR position only increases by a factor of about 1.25 when the shear angle decreases by a factor of 2.

WIND SPEED

A relatively frequent question asked the radiation briefer is what effect a change in the forecast wind speeds would have upon the forecast exposures. A quantitative answer is not easy to arrive without running NSCALE.

As pointed out earlier, $ER1_p$ is not inversely proportional to V_p as indicated solely by equation 4.1, since ER1 is determined by X and X is inversely proportional to V_p. This complex relationship is exemplified in Figure D.3, which shows values of TYE versus centerline distance as a function of wind speed, with the assumptions that the cloud height is 5000 feet, the shear is 20°, and the RST is 1.

At 10 mi downwind, this chart gives a TYE of 630 mR with a wind speed of 5 mi/hr. If the wind should triple to 15 mi/hr, TYE increases to 1300 mR, an increase of a factor of 2.1. At 40 mi downwind, the exposure increases from 9.2 mR to 33 mR (an increase of a factor of 3.6) with the same increase in wind speed. Finally, at 100 mi downwind, the exposure increases from 0.34 to 2.0 mR (an increase of a factor of 5.9) with the same increase in wind speed.

For similar situations, a simple rule-of-thumb would be that the increase in exposures due to increased winds is larger at greater distances.

Figure D.4 exemplifies the effects upon the predicted centerline position of the 170 mR TYE exposure estimate when the wind-speed term is changed. The change in the 170 mR centerline position with a change in the wind speed is shown as a function of the RST, assuming a cloud height of 5000 ft and wind shear of 20°.

It can be seen from Figure D.4 that if the winds speed was 10 mi/hr and the RST was 10, then the centerline distance to the 170 mR position would be 44 mi. If the winds were increased to 20 mi/hr, the downwind distance to the 170 mR position would increase to 55 mi, an increase of a factor of 1.3. (NSCALE calculations show that the TYE at 44 mi would increase from 170 to 320 mR, an increase of a factor of 1.9.)

If the RST had been 100 instead of 10 in the above case, the distance to the 170 mR position with a 10 mi/hr wind would have increased from 87 mi to 118 mi when the wind speed was increased to 20 mi/hr. This change in downwind dis-

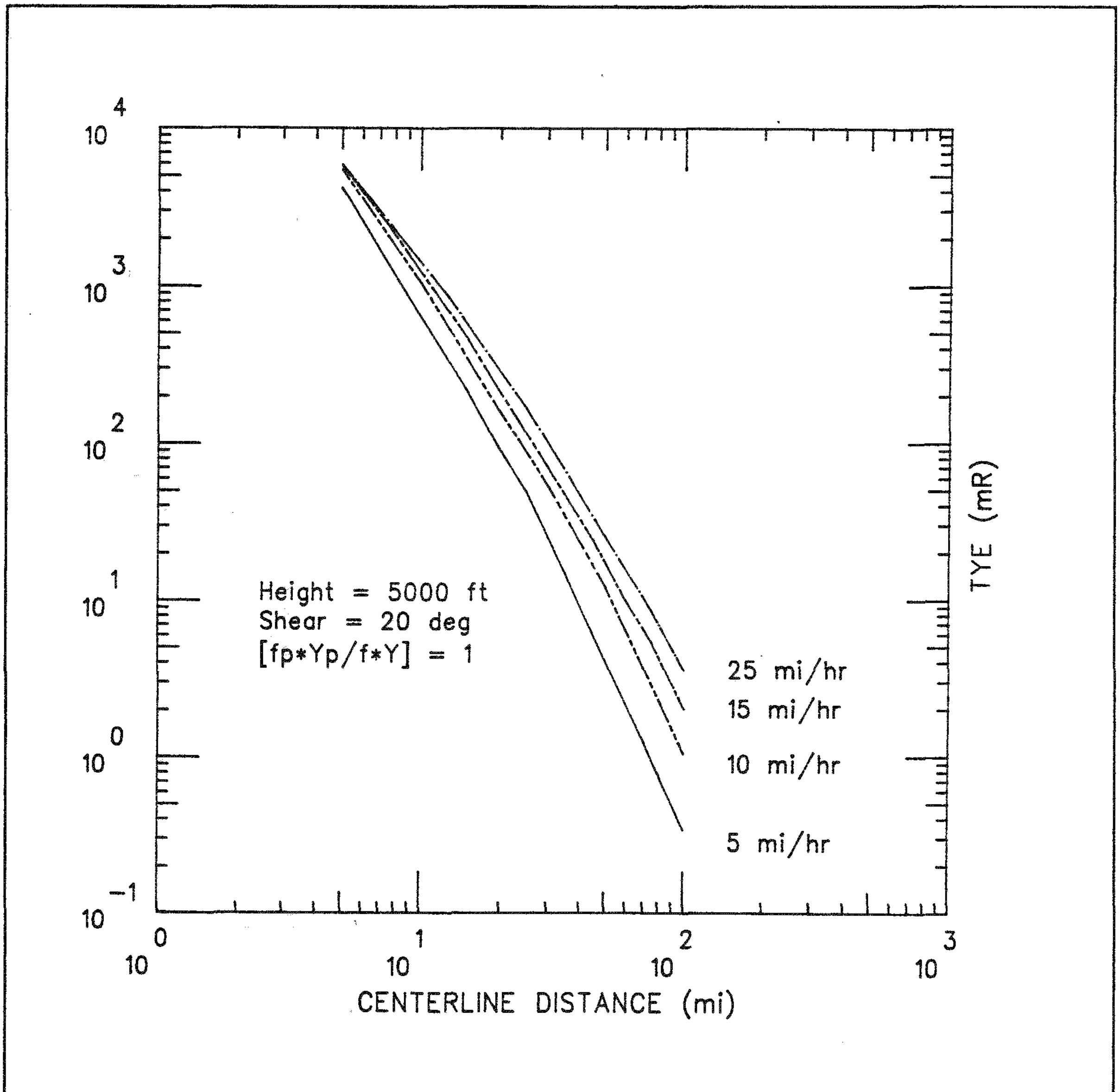

Figure D.3 An Example of Distance Versus TYE as a Function of Wind Speed

tance would be a factor of 1.4 higher. (NSCALE calculations show that the TYE at 87 mi would increase from 170 to 480 mR, an increase of a factor of 2.8.) Thus, it can be seen that in similar circumstances, with a doubling of the wind speed, the distance to the 170 mR position only increases by a factor near 1.35.

CLOUD HEIGHT

As discussed earlier, the predicted cloud height is one of the most uncertain terms that is input into NSCALE. Occasionally, the radiation briefer will be asked to comment on what would happen to the exposure estimates if the

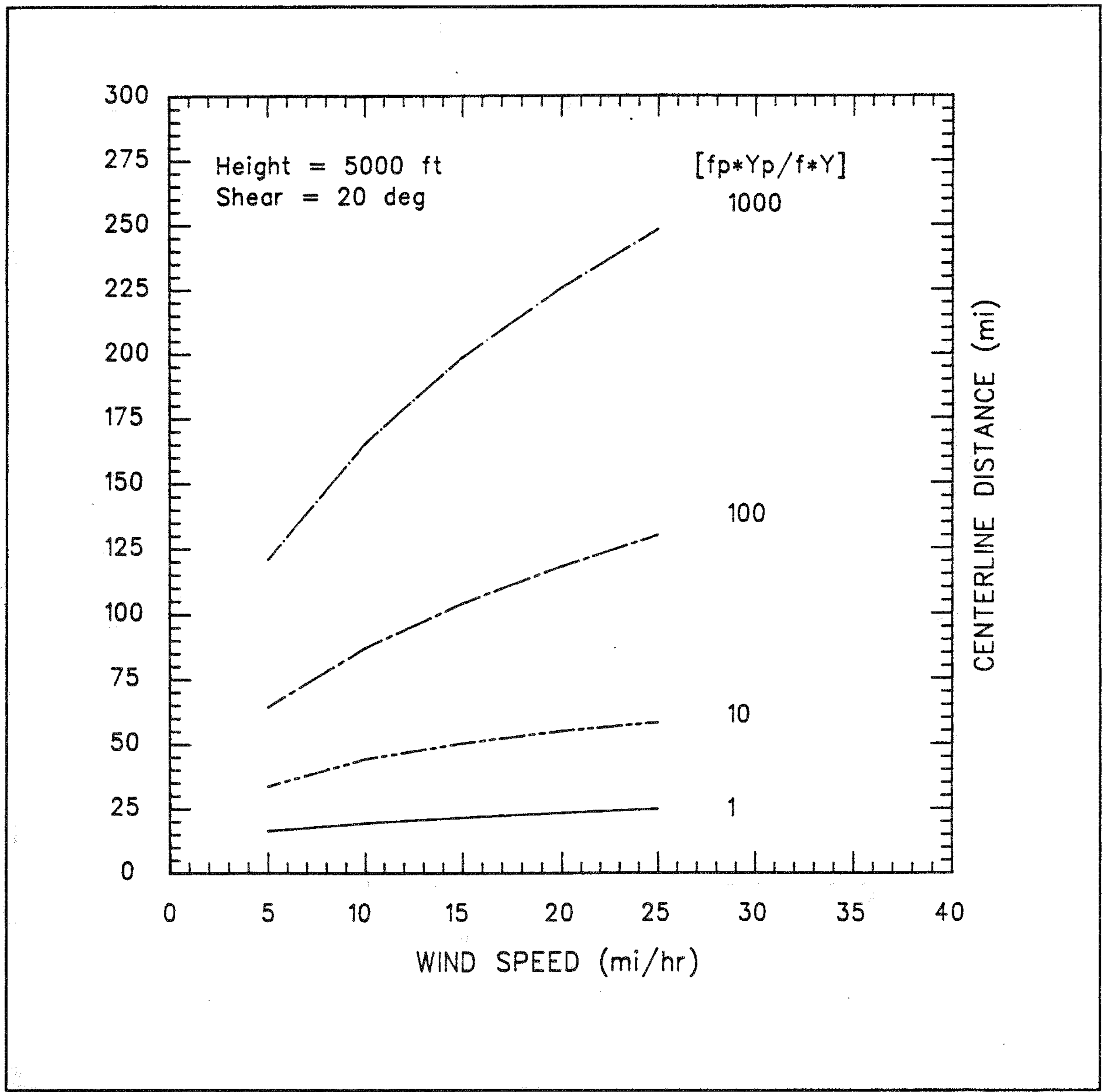

Figure D.4 170 mR Centerline Position Versus Wind Speed ·

cloud height was greater or less than indicated.

An inspection of equations 4.1 and 4.2 shows that the forecast cloud height, H_p, has a similar relationship to the predicted H+1 hr exposure rate, $ER1_p$, as does the forecast wind speed, V_p. This complex relationship is exemplified in Figure D.5, which shows values of TYE versus centerline distances as a function of cloud heights, with the assumptions that the wind speed is 5 mi/hr, the wind shear is 20°, and the RST is 1.

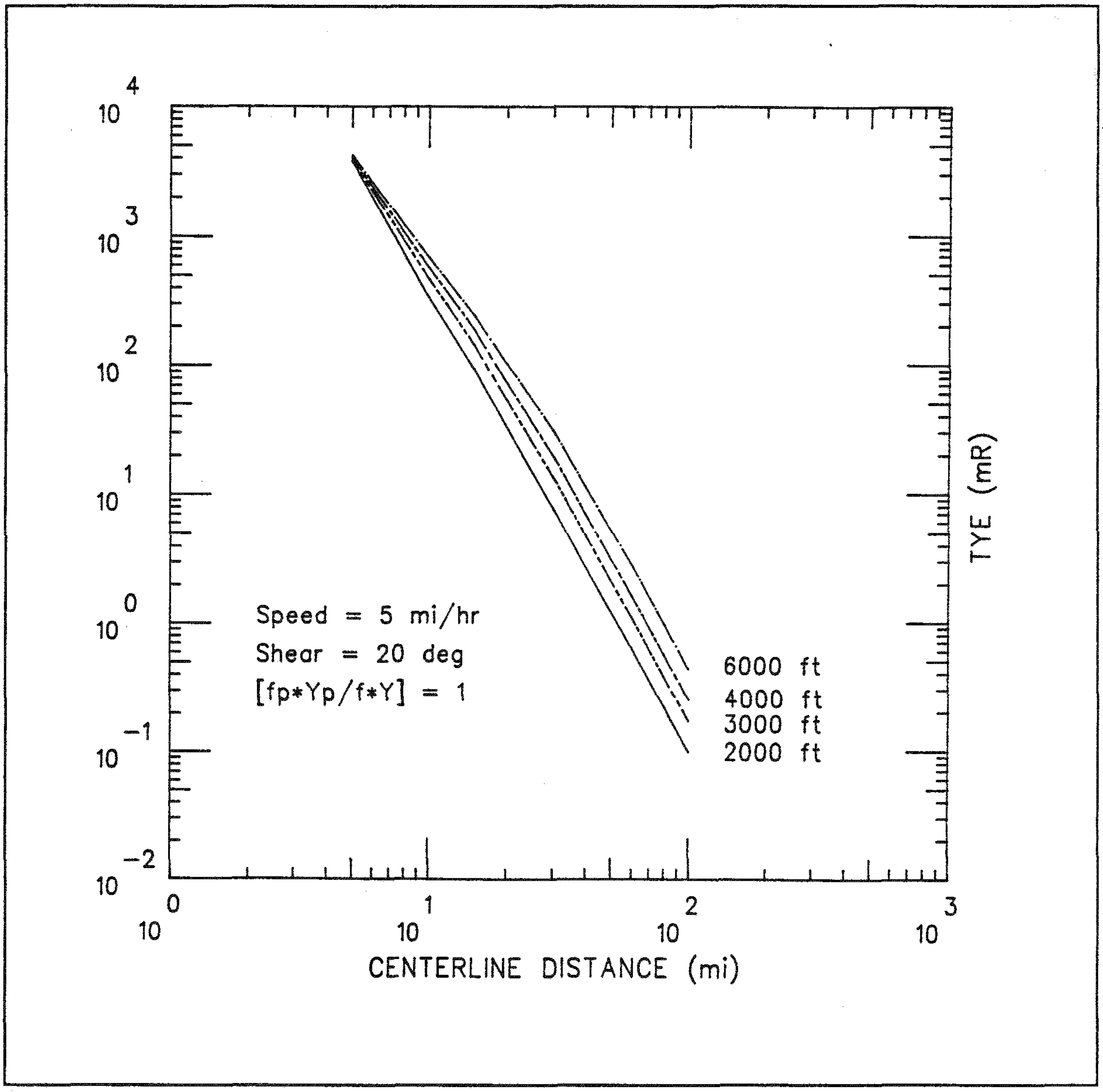

Figure D.5 An Example of Distance Versus TYE as a Function of Cloud Height

At 10 mi downwind, this chart gives a TYE of 460 mR with a cloud height of 3000 ft. If the cloud height should double to 6000 ft, TYE increases to 680 mR, an increase of a factor of 1.5. At 40 mi downwind, the exposure increases from 4.8 mR to 11 mR (an increase of a factor of 2.4) with the same increase in cloud height. Finally, at 100 mi downwind, the exposure increases from .17 mR to .43 mR (an increase of a factor of 2.6) with the same increase in cloud height.

For similar situations, a simple rule-of-thumb would be that the percentage increase in exposures due to an increased cloud height is larger at greater distances.

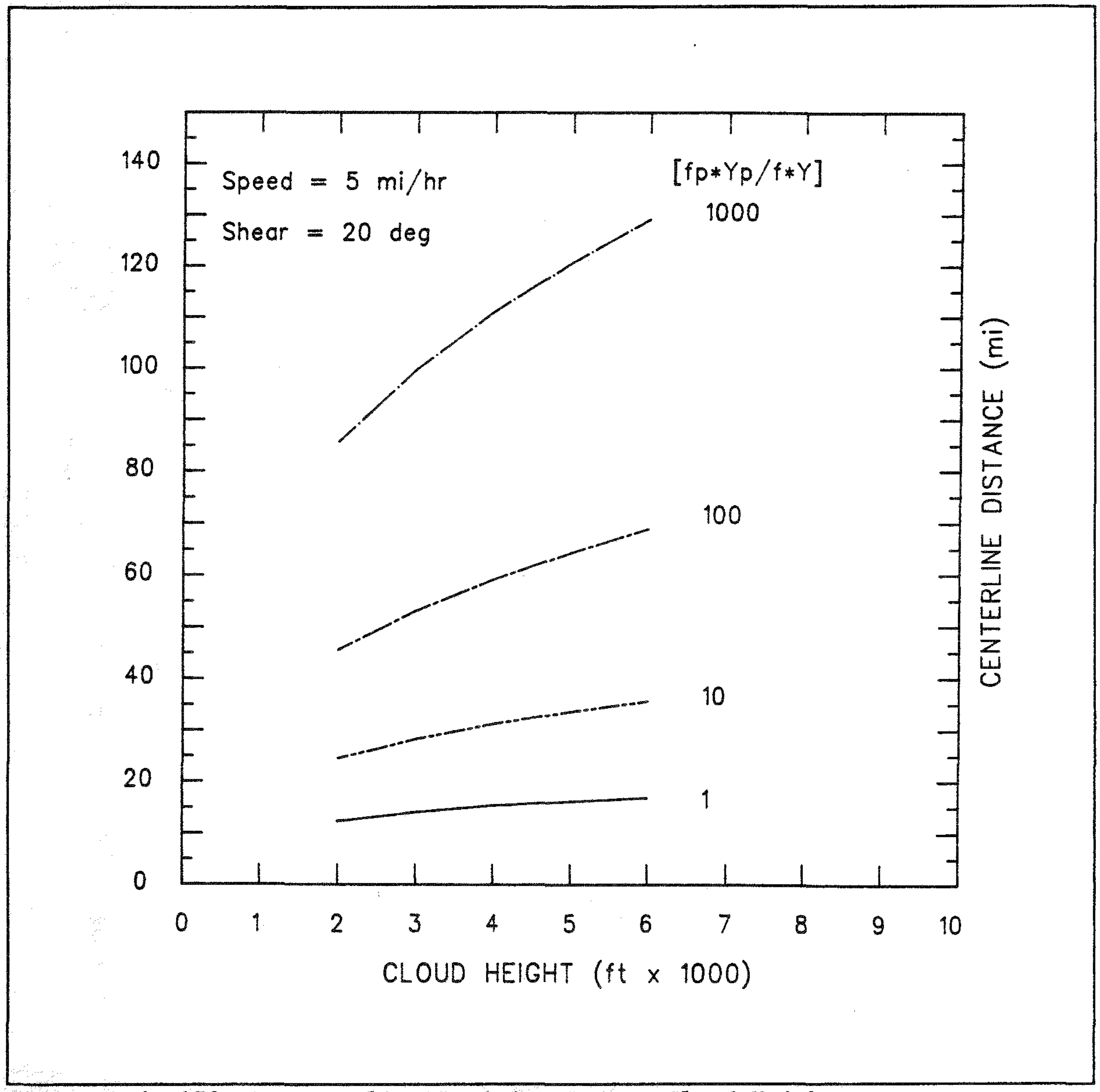

Figure D.6 170 mR Centerline Position Versus Cloud Height

Figure D.6 exemplifies the effects upon the predicted centerline position of the 170 mR TYE exposure estimate when the cloud-height term is changed. The change in the 170 mR centerline position with a change in the cloud height is shown as a function of the RST, assuming a wind speed of 5 mi/hr and wind shear of 20°.

It can be seen from Figure D.6 that if the cloud height was 3000 ft and the RST was 10, then the centerline distance to the 170 mR position would be 28 mi. If the cloud height was increased to 6000 ft, the downwind distance to the 170 mR position would increase to 36 mi, an increase of a factor of 1.3. (NSCALE calculations show that the TYE at 28 mi would increase from 170 to 380 mR, an increase of a factor of 2.2.)

If the RST had been 100 instead of 10 in the above case, the distance to the 170 mR position with a 3000 ft cloud height would have increased from 53 mi to 69 mi when the cloud height was increased to 6000 ft. This change in downwind distance would be a factor of 1.3 higher. (NSCALE calculations show that the TYE at 53 mi would increase from 170 to 400 mR, an increase of a factor of 2.4.) Thus, it can be seen that in similar circumstances, with a doubling of the wind speed, the distance to the 170 mR position only increases by a factor near 1.3.